

**UNIVERSITA' DI NAPOLI FEDERICO II**  
**Dipartimento di Biologia e Patologia Cellulare e**  
**Molecolare "L. Califano"**

**Doctorate School in Molecular Medicine**

**Doctorate Program in**  
**Genetics and Molecular Medicine**  
**Coordinator: Prof. Lucio Nitsch**  
**XXIII Cycle**

**"The zebrafish model to identify new genes involved in**  
**thyroid development"**

**Immacolata Porreca**

**Tutor: Prof. Roberto Di Lauro**

**Co-Tutor: Dott. Paolo Sordino**



**Napoli 2010**

## Table of contents

ABSTRACT.....	4
1. Introduction .....	5
Organogenesis: the thyroid model .....	5
Thyroid gland in mammals .....	5
General aspects .....	5
Embryonic thyroid gland development in mammals: morphology and genetics .....	7
The hallmark of the thyroid cells.....	10
Genes involved in thyroid morphogenesis .....	11
Congenital hypothyroidism with thyroid dysgenesis .....	15
Description and genetics.....	15
Zebrafish advantages to study vertebrate organogenesis .....	16
Zebrafish embryology .....	17
Thyroid gland in zebrafish .....	19
General aspects .....	19
Embryonic thyroid development in zebrafish .....	20
2. Aim of the present project .....	23
3. Material and methods .....	25
Zebrafish care and preparation of specimens.....	25
Embryonic manipulation.....	25
Probes preparation and Whole Mount In Situ Hybridization (WMISH) .....	25
Double staining (WMISH + WMIHC) .....	26
RNA extraction, cDNA synthesis and cloning procedures .....	27
Identification of zebrafish orthologs in Ensembl and NCBI databases .....	28

4. Results and discussion .....	29
Zebrafish analysis of mouse thyroid enriched genes .....	29
Identification of the zebrafish orthologs of the murine thyroid enriched genes.....	29
Expression patterns analysis of the putative zebrafish orthologs .....	29
Expression analysis of the zebrafish putative thyroid genes .....	31
Analysis of zebrafish bcl2 and bcl2l expression patterns during morphogenesis .....	34
The role of bcl2l on zebrafish thyroid development .....	35
Thyroid-specific transcription factors role on bcl2l expression .....	35
<i>Bcl2l</i> functional analysis.....	38
Analysis of apoptosis during thyroid degeneration in manipulated embryos .....	42
5. Conclusions .....	45
6. Acknowledgements .....	46
7. References .....	47
8. Appendix .....	56

## ABSTRACT

Thyroid organogenesis is a very complex developmental process that leads to the formation of an organ able to produce specific hormones through specification, migration, structural organization and functional differentiation of thyroid precursor cells. In mammals, alteration of these mechanisms might be responsible for congenital hypothyroidism (CH), the most frequent inherited endocrine disease.

Thyroid development in fish is comparable to mammals at both ontogenetic and molecular levels: the thyroid develops from the endodermal tissue, at the midline of the pharyngeal floor, and its formation is subdivided into main successive steps shared with mammals. The genetic program involved in fish thyroid differentiation, including the activity of transcription factors such as *Nkx2.1a*, *Pax8* and *Hhex*, is conserved with respect to expression patterns and functions.

To gain further insights on the genetic machinery implicated in normal thyroid development, and therefore in CH disease, an oligonucleotide microarray analysis was performed in mouse with the aim to identify genes differentially expressed during gland organogenesis. This approach highlighted a list of genes enriched in embryonic mouse thyroid. In the present work, the zebrafish model was used to perform functional analysis on fish counterparts of the murine thyroid enriched genes. Looking at the expression territories of the zebrafish orthologs, a very low correlation in thyroid expression profile between mouse and zebrafish was found: indeed, very few mouse thyroid expressed genes have their zebrafish ortholog being expressed in thyroid primordium. This observation strongly suggests that some changes concerning thyroid development occurred from lower to higher vertebrates; during evolution, the thyroid of higher vertebrates probably recruited new genetic pathways/functions by means of mutations occurred in *cis*-regulatory elements. Despite the low correlation in expression profiles, a new conserved function relevant for thyroid development was identified with this comparative approach; an anti-apoptotic function, represented by Bcl2 in mouse and *bcl2l* in zebrafish, was conserved during thyroid evolution. Knock-down experiments conducted by means of morpholinos injection, have revealed that *bcl2l* is regulated by the thyroid transcription factors and plays a relevant role in normal thyroid development. Indeed, *bcl2l* thyroid expression was lost in embryos deprived of the thyroid transcription factors, leading to thyroid degeneration via apoptosis. It is feasible to hypothesize that a conserved antiapoptotic function during thyroid evolution could counteract a putative proapoptotic function, ready to intervene if something fails during normal gland morphogenesis.

# 1. Introduction

## ***Organogenesis: the thyroid model***

The development of an embryo is a very complex process that leads to the formation of structures, the adult body organs, enormously complicated, and that brings together vast numbers of components organized in exactly the right position, assembled in a logistically correct time sequence, and connected with the other components to make a functional whole.

In particular, organogenesis in the vertebrate embryos involves 2 processes: morphogenesis, which is the shaping of an organ, and cytodifferentiation, which is the acquisition and expression of specialized cellular functions within that organ. Both these processes require a detailed schedule of cell induction, migration, proliferation, differentiation, communication and cell death and are the result of an accurate reading of the genetic program. Of course, these steps must be tightly controlled; indeed, an alteration at any level of the organogenesis process can lead to a severe impairment of organ function and so to an invalidating clinical disorder.

In line with this, many efforts are being devoted to understand the mechanisms involved in organogenesis and therefore in disease, primarily thanks to the study of a few model organisms, among which mice and zebrafish. Furthermore, comparative approaches are applied to understand how developmental mechanisms have evolved to bring about the formation of organs of different shape and function during evolution.

To study organogenesis the thyroid is a very interesting experimental model. It is an endocrine gland present in all vertebrates. It is a rather simple organ, with one main cell type, the thyroid follicular cell (TFC) (Gorbman and Bern, 1962); its embryology, physiology and pathology are, at least in part, sufficiently known; it is affected by frequent diseases, among which congenital hypothyroidism (CH) is the most common congenital disorder (1/4000 newborns).

Thyroid development can be divided into 3 phases in which it is possible to recognize the features of organogenetic mechanisms: a)thyroid precursor cell specification, b)budding and migration of the thyroid primordium, c)functional differentiation of TFCs.

The genes and pathways involved in normal thyroid development and function and so in disease are at least in part known and this is primarily due to the study of the two most used model organisms in developmental biology of vertebrates, mouse and zebrafish. A huge amount of knowledge about thyroid development comes from murine models; thanks to the researchers ability to generate genetically modified mice, many mouse models for thyroid disease are available to the scientific community. In the last years, thanks to the studies on the zebrafish thyroid, several novel mechanisms concerning thyroid development have been discovered. Moreover the zebrafish has introduced new techniques and new strategies to investigate thyroid organogenesis.

## ***Thyroid gland in mammals***

### **General aspects**

Thyroid gland in all vertebrates is responsible for producing thyroid hormones (THs).

In humans, the thyroid gland is located in front of the trachea and it consists of two lobes (**Figure 1 A**) connected by a central isthmus. It is enveloped by a thin, fibrous capsule of connective tissue that sends septa into the gland forming a framework for the entire organ. The thyroid parenchyma is composed of various cells. The TFCs, or thyrocytes, designed to produce thyroid hormones, are most abundant and are organized in spheroid structures known as follicles, each composed of a cell layer surrounding a closed cavity containing the colloid, a mixture of proteins, principally thyroglobulin (Tg) (**Figure 1 B**). The follicle may be considered the secretory unit of the organ. In addition to TFCs, individual cells or small groups of cells, the C-cells, are distributed among the follicles (**Figure 1 B**). These cells produce calcitonin and derive from the neural crest *via* the ultimobranchial body (UB). In adult human thyroid, they represent 1% of the cell population (Wolfe et al., 1974). Outside the follicles two other types of cells populate the thyroid, the endothelial cells and fibroblasts. In normal dog thyroid, the relative proportions of follicular, endothelial cells and fibroblasts are 70%, 6% and 24% (Dow et al., 1986).

TFCs are highly differentiated cells and express all the proteins required for the synthesis and the release of THs, such as Tg (the substrate for synthesis of THs by iodination), thyroperoxidase (TPO; the enzyme responsible for Tg iodination), the Sodium/Iodide symporter (NIS; that transports iodine into the thyroid cells) (Damante and Di Lauro, 1994) and pendrin (PDS; that is responsible for the efflux of iodide from the thyroid cell to the follicle's cavity) (Royaux et al., 2000).

The main THs are the tetra-iodothyronine (T<sub>4</sub>) or thyroxine, and the triiodothyronine (T<sub>3</sub>). THs production starts with the synthesis of Tg, that is secreted into the colloidal lumen of the follicle where it is iodinated on tyrosine residues. After a variable period of storage in thyroid follicles, iodinated Tg is subjected to proteolysis and the released hormones are secreted into the circulation, where specific binding proteins carry them to target tissues (Kirsten, 2000).

The amounts of T<sub>3</sub> and T<sub>4</sub> secreted by the thyroid are controlled by the thyroid-stimulating hormone (TSH) produced by the pituitary gland and the amount of TSH, in turn, is regulated by thyroid-stimulating hormone releasing factor (TRF), secreted by the hypothalamus.

The THs are critical in regulating the growth and differentiation of many tissues and organs, as well as energy homeostasis and numerous key metabolic pathways. THs are known to play an important role in the perinatal development especially of the central nervous system (Bernal, 2007).

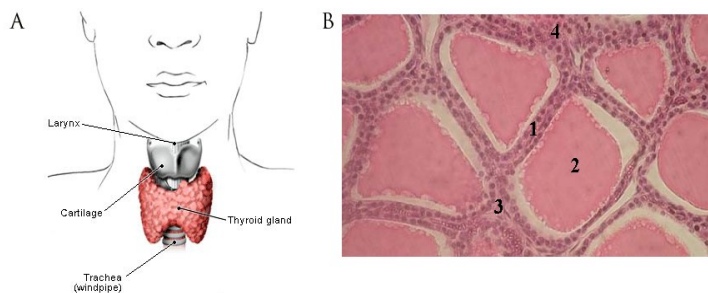


**Figure 1 Human thyroid gland. (A) Representation of thyroid position and related structures in neck region. (B) Cross section of the thyroid tissue showing the wall of the thyroid follicle, built from thyrocytes (1), the cavity of the thyroid follicle, filled with colloid (2), the blood vessels (3) and parafollicular cells (C-cells) (4).**

## Embryonic thyroid gland development in mammals: morphology and genetics

The thyroid gland development has been exhaustively studied in rodents and, because of the high conservation of this process in mammals, it is possible to extend data from animal models to humans (see **Figure 2** for a timing correlation of relevant events during thyroid development in humans and mouse). Indeed, studies on patients affected by congenital hypothyroidism with thyroid dysgenesis have confirmed that identical genetic mechanisms are involved in thyroid organogenesis both in humans and mice.

The thyroid gland development in mammals can be subdivided in few main phases characterized by proper morphological and molecular aspects:

1. Specification of TFC progenitors
2. Budding of thyroid anlage
3. Migration of thyroid primordium
4. Late thyroid morphogenesis and functional differentiation

These steps are schematized in **Figure 2** and the morphology of thyroid during the different steps is reported in **Figure 4**.

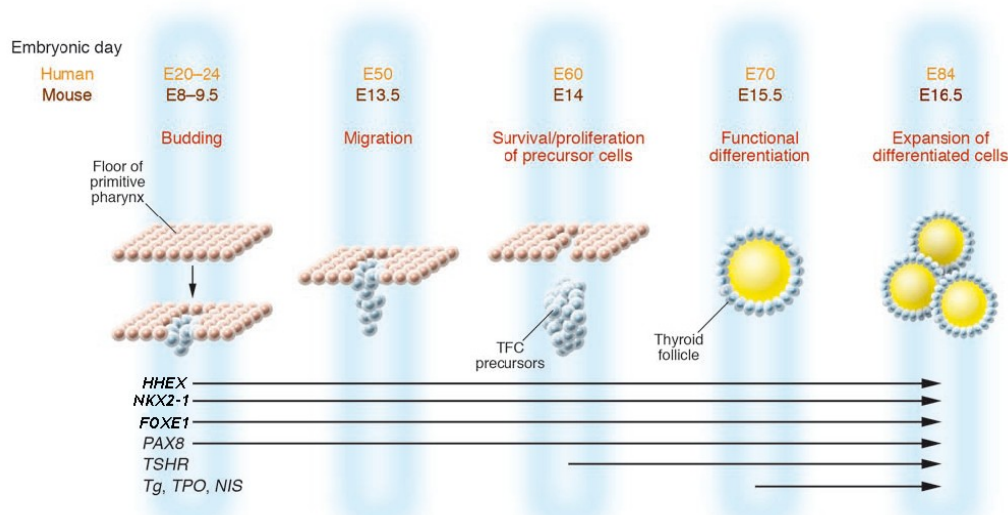


**Figure 2** Schematic representation of the stages of thyroid gland development and the expression of relevant genes (Davies et al., 2005).

### *Specification of TFC progenitors*

After the morphogenetic movement taking place during gastrulation, the definitive endoderm is transformed in the primitive gut tube, a cylindrical cavity running along the antero-posterior (A-P) axis of the embryo and surrounded by mesoderm. During this period, the gut tube regionalizes along the A-P axis into the foregut, midgut and hindgut domains. This sub-regionalization is driven by specific networks of signaling molecules and transcription factors and is controlled by interactions with nearby mesodermal tissues. Specific molecular mechanisms, selectively working in limited domains of the gut tube, are responsible also for the specification of the organs precursors (Shivdasani, 2002; Zorn and Wells, 2009).

The thyroid morphogenesis starts with the recruitment of a group of cells at the foregut level that enter a “thyroid fate” by means of a definite molecular program. The mechanisms responsible for the recruitment and the specification of thyroid precursor cells in mouse are largely unknown. Some research papers have reported that mutations of genes

expressed in the surrounding tissues and not in thyroid bud itself impair the correct organogenesis of the gland (Kameda et al., 2009; Lania et al., 2009; Xu et al., 2002). In particular, when *Tbx1*, an FGF signaling regulator expressed in the nearby thyroid mesoderm, is depleted, a smaller number of thyroid precursor cells than normal is observed, suggesting a role for this factor in precursors recruitment (Lania et al., 2009).

In mouse embryo, the thyroid anlage is first visible as a thickening in the primitive pharynx at embryonic day (E) 8-8.5 (E20-22 in human) (Kaufman and Bard, 1999). Starting from its first appearance, the thyroid anlage is in close spatial relationship with the heart primordium. It is reasonable that relevant inductive signals for thyroid specification originate from the heart mesoderm. This concept is supported by the findings that: a) cardiac malformations represent the most frequent congenital defect associated with thyroid dysgenesis (Olivieri et al., 2002); b) concomitant cardiac and thyroid defects have been observed in experimental studies (Dentice et al., 2006; Westerlund et al., 2008).

The precursors of TCFs, since their first appearance in the primitive pharyngeal floor, are characterized by the co-expression of four transcription factors: *Hhex* (Thomas et al., 1998), *Nkx2-1* (Lazzaro et al., 1991), *Pax8* (Plachov et al., 1990), and *Foxe1* (Zannini et al., 1997). Each of these transcription factors is expressed also in other tissues but their concomitant expression is a unique hallmark of both differentiated TFCs and their precursors (Damante et al., 2001). In **Figure 4 A** is reported the *Nkx2-1* expression in thyroid anlage. By means of gene targeting experiments, it was demonstrated that in absence of either *Nkx2-1*, *Hhex*, *Pax8*, or *Foxe1*, thyroid morphogenesis is severely impaired, suggesting that each of them plays an essential individual role in gland organogenesis. The specific role of these factors in thyroid formation is discussed below.

#### Budding of thyroid anlage

At E8.5-9 (E24 in human), the thickening deepens forming a small pit and then a hollow evagination in the endoderm, called thyroid bud (Romert and Gauguin, 1973) **Figure 3**). During the budding, the thyroid primordium approximates to the distal part of the outflow tract of the developing heart (Fagman et al., 2006).

The molecular mechanisms that regulate thyroid budding are largely unknown. A feature of several budding organs is the locally enhanced proliferation of progenitor cells

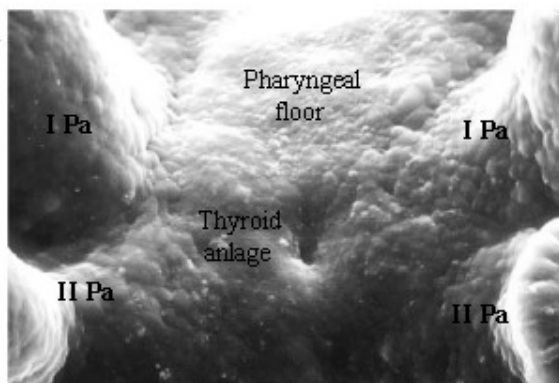


**Figure 3** The thyroid anlage (A) Scanning electron micrograph of the ventral wall of the pharynx of an E9 mouse embryo showing the area where the thyroid bud just invaginated, leaving behind the foramen cecum. Pa, Pharyngeal arch (De Felice and Di Lauro, 2004).

(Michael and Davies, 2004). This is not true for thyroid primordium in which an unexpected low proliferation rate was found (Fagman et al., 2006). Lung budding is regulated by several factors among which *Fgf10*, secreted by the surrounding mesenchyme (Kimura and Deutsch, 2007; Lu et al., 2005). It was found that *Fgf10* null mutant mouse embryos lack both lung and thyroid indicating that this secreted protein is required for thyroid morphogenesis (Ohuchi et al., 2000). However, in this study, only late embryos (E18.5) or newborns were analyzed precluding any conclusions on the early role of *Fgf10* in thyroid development.

### Migration of thyroid primordium

The detached bud migrates caudally to reach its final destination at the base of the neck, at E13.5 (E50 in human).

At E10, the migrating thyroid primordium is still connected to the pharyngeal floor by a thin channel, the thyroglossal duct (**Figure 4 B**); a small hole visible at the site of origin in the pharyngeal floor (the foramen cecum) is the remnant of the anlage (**Figure 3**). At E11.5 the thyroglossal duct disappears, and the thyroid primordium loses all connections with the floor of the pharynx and starts to expand laterally. Two days later the thyroid primordium reaches the trachea.

The molecular mechanisms involved in thyroid migration are not completely understood. Experiments on mouse models demonstrate that *Foxe1* has an important role in the migratory process. Indeed, in *Foxe1* mutant mouse embryos the thyroid is either absent or attached to the pharyngeal endoderm (De Felice et al., 1998).

A still open debate is whether embryonic thyroid migration is an active process due to a cell-autonomous mechanism or it is a passive process consequent to other morphogenetic events occurring in the neck region (Fagman and Nilsson). A characteristic of active migrating cells is the epithelial-mesenchymal transition (EMT): the migrating cells lose their epithelial phenotype and acquire mesenchymal features; they also acquire a spindle-shaped morphology (Thiery and Sleeman, 2006). However, TFC precursors seem to use a different and yet unidentified pathway to move, because the EMT is not observed and the cells retain their epithelial phenotype (Fagman et al., 2003). One recent finding, the so called collective cell migration, implicates that firm cell-to-cell adhesion, as it is observed in migrating thyroid, is a prerequisite for the movement of groups of cells (Friedl and Gilmour, 2009). This new mechanism could fit with thyroid translocation, considering also that the thyroid primordium has a leading edge that points toward the migration direction (Fagman et al., 2006), another feature observed in the collective migration.

### Late thyroid morphogenesis and functional differentiation

When the thyroid primordium reaches its final position, in front of trachea (E13-5,

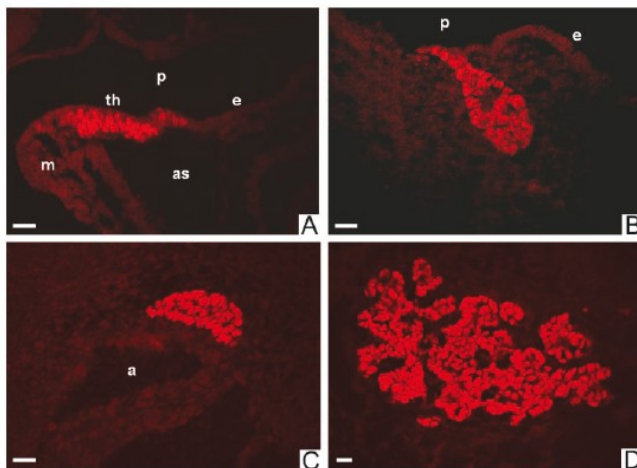


**Figure 4** Thyroid morphology in mouse embryo (A-E) Cross sections stained for Nkx2.1 antibody. (A) Thyroid anlage at E9.5. (B) Thyroid primordium at E10.5. (C) Thyroid primordium at E12.5. (D) Thyroid at E15.5. a, Aorta; as, aortic sac; e, foregut endoderm; m, mandibular component of first branchial arch; p, pharynx; th, thyroid primordium (Fagman et al., 2003).

E14), also the fusion with the UB occurs (Cordier and Haumont, 1980). At this point, the gland acquires its final shape and the lobes expand considerably (E15-16). The mechanisms underlying the proliferation of the precursors and the formation of the lobes are unknown. Surprisingly, while TSH is an important growth stimulus for adult thyroid cells, it is not relevant for the proliferation of the fetal thyroid cells (Marians et al., 2002; Postiglione et al., 2002). Genetic studies in mouse support a morphogenetic role for the embryonic vascular anatomy in late thyroid development; when either *Sonic hedgehog* (*Shh*) (Fagman et al., 2004) or *Tbx1* (Fagman et al., 2007)

activity is disrupted, correct patterning of the vessels is disturbed. In these conditions also the lobulation process is impaired and the thyroid assumes the shape of a midline mass located lateral to the trachea.

In the mouse, the first small thyroid follicles begin to appear by E15.5 (**Figure 4 D**) (E70 in human) and a day later the gland displays the typical follicular organization. At this point, the thyroid primordium is a functional gland able to produce and release hormones, by means of the expression of genes required for thyroid function.

### The hallmark of the thyroid cells

The small number of cells in the pharyngeal floor which are fated to become TFCs are univocally characterized by the co-expression of *Nkx2-1*, *Foxe1*, *Hhex* and *Pax8* already at E8.5. The simultaneous expression of these factors is a hallmark of the thyrocyte during its embryonic and adult life; although each of these proteins are also present in other embryonic tissues, where they exert distinct roles, only in thyroid they work together to drive organogenesis. These transcription factors were identified by virtue of their binding to the promoter of genes whose products are markers of terminal differentiation of thyroid follicular cells. It is worth noting that, in thyroid cells, they form a network of reciprocal cross-interactions (**Figure 5**).

From *in vitro* studies we know that *Pax8* and *Nkx2-1* interact physically (Di Palma et al., 2003); binding sites for *Nkx2-1* and *Pax8* were found in the *Hhex* promoter and it was demonstrated that these two factors are able to regulate the transcriptional activity of *Hhex* promoter (Puppini et al., 2003; Puppini et al., 2004); *Pax8* activates the transcription of *Foxe1* (D'Andrea et al., 2006); in addition, *Hhex* and *Nkx2-1* autoregulate their own promoters (D'Andrea et al., 2006; Puppini et al., 2003). *In vivo* studies have confirmed these findings even if the transcriptional regulation appears to change as the primordium progresses from one to the following developmental stage (Parlato et al., 2004). Indeed, at E8.5, when either one of *Nkx2-1*, *Pax8* or *Hhex* is deleted, the expression of the other two transcription factors remains unaltered; only *Foxe1* is under the control of *Pax8* already at this stage (Parlato et al., 2004). However, in the successive developmental steps the expression of *Pax8* and *Foxe1* is lost in *Hhex* null embryos and both *Foxe1* and *Hhex* are down-regulated in *Nkx2-1* or *Pax8* deficient embryos (Parlato et al., 2004). *Foxe1* probably holds a lower position in this network since the expression of the other transcription factors is maintained in *Foxe1*-deficient progenitors (De Felice et al., 1998; Parlato et al., 2004).

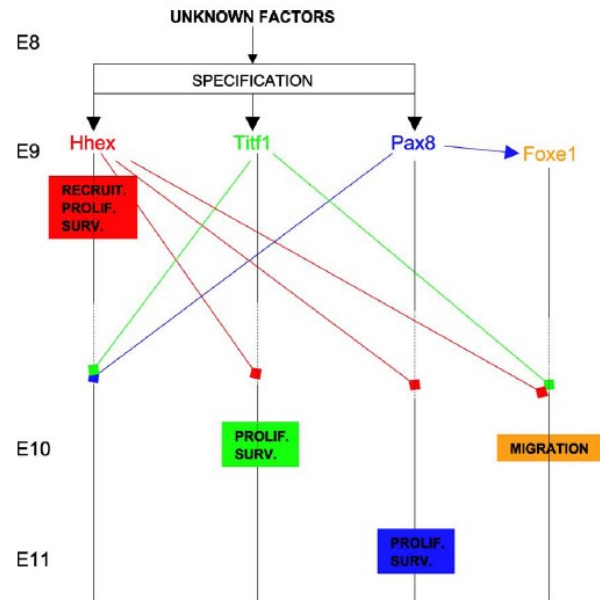


**Figure 5** Functional interaction among *Hhex*, *Nkx2-1*, *Pax8* and *Foxe1* in developing thyroid. The transcription factor and the functions controlled by it are indicated in different colors. Each factor regulates other transcription factors controlling the onset (arrow) or the maintenance (square) of their expression (Parlato et al., 2004).

## Genes involved in thyroid morphogenesis

The expression of the four transcription factors at the very beginning of thyroid morphogenesis suggested that these genes might play an important role in the process. This hypothesis has been confirmed by studies on animal models. Mice deficient for *Nkx2.1* (Kimura et al., 1996; Kimura et al., 1999), *Hhex* (Martinez Barbera et al., 2000), *Pax8* (Mansouri et al., 1998) or *Foxe1* (De Felice et al., 1998) are well-studied models of athyreosis (absence of thyroid gland). In these embryos the thyroid bud is correctly formed but eventually disappears leading to lack of thyroid tissue in late developmental stages. These findings indicate that *Nkx2.1a*, *Hhex*, *Pax8* and *Foxe1* are required for the survival and growth of thyroid progenitors but are not necessary for thyroid specification and early bud formation. However, the presence of these genes is not sufficient to guarantee a correct organogenesis of the gland. Mutations in other genes too, both thyroid-enriched and ubiquitous, have been demonstrated to impair the thyroid development.

### *Nkx2.1a*

*Nkx2.1a* is a 42 kDa homeodomain-containing transcription factor (Guazzi et al., 1990) expressed in both differentiated TFCs and in their precursors; in the thyroid primordium it is detected as soon as the thyroid anlage is visible. *Nkx2-1* was found also in the trachea and lung epithelium and in some areas of forebrain, including the posterior pituitary (Lazzaro et al., 1991). In thyroid gland, *Nkx2-1* expression is not restricted to the follicular cells; it is also present in parafollicular C-cells (Suzuki et al., 1998) and it was found in the epithelial cells of the UB (Mansouri et al., 1998).

In absence of *Nkx2-1*, mice die at birth because of pulmonary dysplasia. The thyroid defect is also severe; the anlage forms in its correct position but by E10.5 it appears smaller in size in comparison to wild type and subsequently undergoes degeneration (**Figure 6**). In these mutants also the pituitary is absent and severe alterations in the ventral region of the forebrain are observed (Kimura et al., 1996; Kimura et al., 1999).

The presence of the thyroid bud in mutant mouse embryos has demonstrated that *Nkx2-1* is dispensable for the initial commitment of thyroid cells, but the late thyroid phenotype has established that this transcription factor is required for the survival and differentiation of the cells. The mechanism by which the thyroid primordium degenerates in the absence of *Nkx2-1* has not been investigated in detail. The presence of fragmented nuclei in *Nkx2-1* deficient progenitor cells suggests involvement of an apoptotic process (Kimura et al., 1999). In support of this possibility an increased number of TUNEL positive cells is observed in the *Nkx2-1*-deficient UB (Kusakabe et al., 2006).

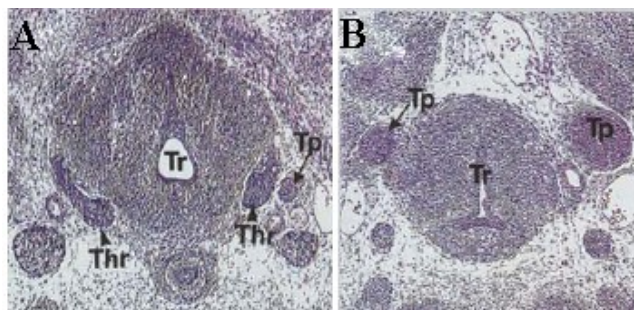


**Figure 6** *Nkx2.1* is responsible for thyroid development. Cross sections of wild-type (A) and *Nkx2-1*<sup>-/-</sup> (B) E12-13 mouse embryos. The thyroid is absent in the mutant embryo. (Thr) Thyroid; (Tp) thymic primordium; (Tr) trachea (Kimura et al., 1996).

The mechanisms responsible for the thyroid expression of *Nkx2-1* are not clear. The expression of *Nkx2-1* in the forebrain is *Shh*-dependent: indeed, in *Shh*-deficient mouse no *Nkx2-1* is observed in the brain, whereas normal levels of the protein are detected in the thyroid and lung anlage (Pabst et al., 2000). *In vitro* studies have proposed that the *Gata6* factor regulates the transcription of *Nkx2-1* (Shaw-White et al., 1999). However, analysis of *Gata6*<sup>-/-</sup>lungs has demonstrated that

Nkx2-1 is normally localized in epithelial cells of both wild-type and mutated lung (Keijzer et al., 2001).

Another issue that remains to be explored is the identification of the genes controlled by this transcription factor in the thyroid primordium. A detailed analysis of the phenotype of the affected tissue reveals that in absence of Nkx2-1, the expression of *Bmp4* (Minoo et al., 1999) and *Fgf8* (Takuma et al., 1998) is abolished in the developing lung and in the posterior pituitary, respectively. These data indicate that signaling molecules relevant for the morphogenesis of embryonic structures are controlled by this transcription factor. The finding that *Fgfr2* is expressed in the thyroid bud, suggests that Nkx2-1 could regulate the survival of TFCs through an Fgf-dependent mechanism (Parlato et al., 1999).

In differentiated thyroid cells, Nkx2-1 controls the expression of thyroid-specific genes, *Tg* and *Tpo* (De Felice et al., 1995), *Nis* (Endo et al., 1997) and *Tshr* (Civitareale et al., 1993).

Orthologs of *Nkx2-1* have been found in chicken (Pera and Kessel, 1998), frog (Small et al., 2000) and zebrafish (Rohr and Concha, 2000), where the distribution of Nkx2-1 is similar to that of mouse. The expression of *Nkx2-1* in the ascidian *Ciona intestinalis* (Urochordata, Chordata) (Ristoratore et al., 1999) is really interesting: *Nkx2-1* mRNA is present in some areas of the adult endostyle, the homolog of the vertebrate thyroid gland, but not in the same cells that concentrate iodine and express a peroxidase similar to Tpo. Hence, it could be speculated that the primordial function of Nkx2-1 was to specify the most anterior part of the gut and not to control the expression of genes involved in thyroid function. Nkx2-1 could have acquired this function later during the chordate evolution (De Felice and Di Lauro, 2004).

### *Pax8*

Pax8 is a transcription factor containing a paired domain acting as a DNA binding domain. Within the *Pax* gene family, *Pax8* forms a subfamily with *Pax2* and *Pax5* on the basis of sequence similarity. *Pax8*, like *Nkx2-1*, is expressed in adult and developing thyroid since the early stages of gland morphogenesis but it is not expressed in the UB. In addition, *Pax8* is transiently expressed in the early developing myelencephalon and throughout the embryonic life of the neural tube; it is also present in the developing kidney, where it is expressed throughout adult life (Plachov et al., 1990).

*Pax8*<sup>-/-</sup> mice which are born at the expected Mendelian ratio but with a low body weight, die within three weeks because of hypothyroidism (Friedrichsen et al., 2003; Mansouri et al., 1998). In contrast to the previously described knock-out mouse, *Pax8*<sup>-/-</sup> newborns have a restricted phenotype: TFCs are completely absent, but C-cells are normal (**Figure 7**). The animals present a rudimental gland composed almost completely of calcitonin-producing C cells and there is no other malformation. Moreover, the thyroid anlage forms, evaginates from the endoderm and begins to migrate. However by E11 the thyroid bud is smaller in comparison to that of wild type (Mansouri et al., 1998). Finally by E12.5 TFCs are not detectable (Mansouri et al., 1998). Thus, like Nkx2-1, Pax8 seems to be involved in TFC survival rather than in specification. The precise mechanism leading to the thyroid phenotype in these animals is unknown but it may involve loss of cells by apoptosis. A protective role of *Pax* genes against apoptosis has been suggested by *in vitro* studies on tumour cells (Bernasconi et al., 1996; Muratovska et al., 2003) and confirmed by *in vivo* studies on *C.elegans* in which the two *Pax2/5/8* genes act promoting cell survival (Park et al., 2006).

It is worth noting that other transcription factors, such as Foxe1 and Hhex, are down-regulated in the precursors of thyroid cells in the absence of Pax8 (Parlato et al., 2004). This observation demonstrated that Pax8 is not only required for the survival of thyroid precursor cells, but also holds an upper role in the genetic regulatory cascade controlling thyroid development.

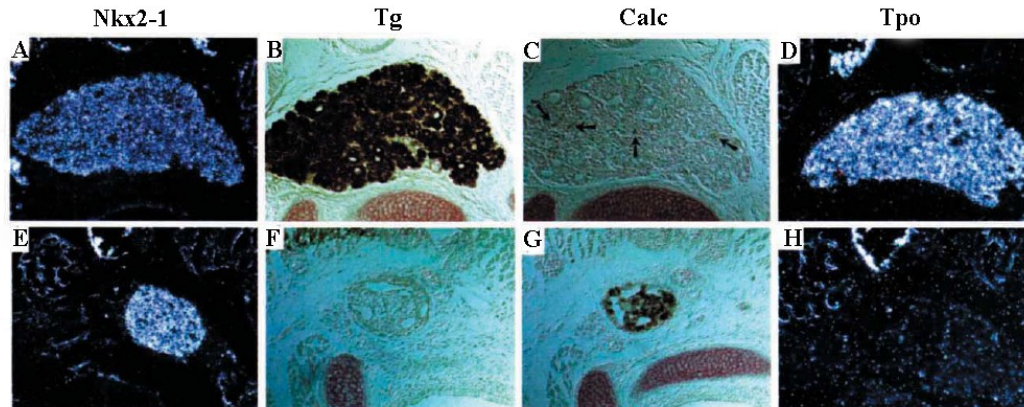


**Figure 7** Pax8 is responsible for TCFs survival. Cross sections of wild-type (A, B, C, D) and Pax8<sup>-/-</sup> (E, F, G, H) E18.5 mouse embryos stained with an Nkx2-1 (A, E) or Tpo (D, H) probe by in situ hybridization and with Tg (B, F) or calcitonin (C, G) antibody by immunohistochemistry. The small thyroid observed in the mutant mice is composed exclusively by C-cells as demonstrated by the positivity of these cells for Nkx2-1 and Calc and not for Tg and TPO that are absolutely TCFs markers. Black arrows in (E) indicate calcitonin positive cells (Mansouri et al., 1998).

It has been demonstrated that *Pax8* is the master gene for the regulation of thyroid-differentiated phenotype (Pasca di Magliano et al., 2000). It is able to bind and to activate the promoters of *Tg* and *Tpo* (Pasca di Magliano et al., 2000; Zannini et al., 1992) and an enhancer of *Nis* (Ohno et al., 1999). Using de-differentiated tumour thyroid cells, it was shown that Pax8 is able to induce a re-differentiation of these cells (Presta et al., 2005).

Very little is known about the transcriptional regulation of *Pax8*. The first thyroid-transcriptional regulatory element of the *Pax8* gene has been only recently identified; this element has the features of an enhancer and contains two binding sites for Nkx2-1, suggesting that this transcription factor participates to *Pax8* expression (Nitsch et al.). This finding is supported also by the slightly reduced expression of *Pax8* observed in *Nkx2-1*<sup>-/-</sup> mice (Parlato et al., 2004).

### *Foxe1*

Foxe1 is a 42 kDa winged helix/forkhead transcription factor. Like Nkx2-1 and Pax8, Foxe1 is detected in the thyroid primordium since E8.5 but its expression is extended to all endodermal cells of the foregut floor. The thyroid-specific expression is maintained during all developmental stages and in adulthood. During early embryonic life, Foxe1 is detected also in the pharyngeal arches and transiently in the Rathke's pouch. Subsequently, it is expressed in the tongue, palate, epiglottis, esophagus, and in the whiskers and hair follicles (Dathan et al., 2002).

Foxe1 deficient mice are born at the expected Mendelian ratio but die within 48 hours, probably due to the severe cleft palate observed. The thyroid phenotype is rather complex: the formation of thyroid bud occurs normally but its fate is variable (**Figure 8**). Indeed, at E10 the thyroid is no more present in 50% of the embryos (**Figure 8 C**), whereas TFCs are observed but they are still on the floor of the pharynx in the remainder cases (**Figure 8 B**). At the later stages of development, mutant mice continue to exhibit either a small thyroid remnant, still attached to the pharyngeal floor, or no thyroid gland at all (De Felice et al.,

1998; Parlato et al., 2004). These data indicate that *Foxe1* has an essential role in promoting thyroid bud migration but it is not involved in thyroid specification and budding. The mutant mice that completely lose the thyroid tissue indicate that *Foxe1* is also involved in thyroid cells survival. In any case, it is not involved in TFCs differentiation because the non-migrating thyroid cells are able to produce Tg. At the moment, the genes that execute the migration program controlled by *Foxe1* are still unknown. In addition, the variable phenotype observed in *Foxe1*<sup>-/-</sup> mice illustrates that, from a common genetic lesion, additional genetic or stochastic events can modulate thyroid development.

Little is known about the regulation of *Foxe1*. In absence of *Pax8*, *Foxe1* is not detected in TFC precursors (Parlato et al., 2004) consistent with the presence of *Pax8* binding sites in the *Foxe1* 5' UTR (D'Andrea et al., 2006).

In the adult gland, the role of *Foxe1* is not yet clear. *In vitro* functional studies in rat thyroid cells have shown that *Foxe1* can act as a promoter-specific transcriptional repressor (Perrone et al., 2000).

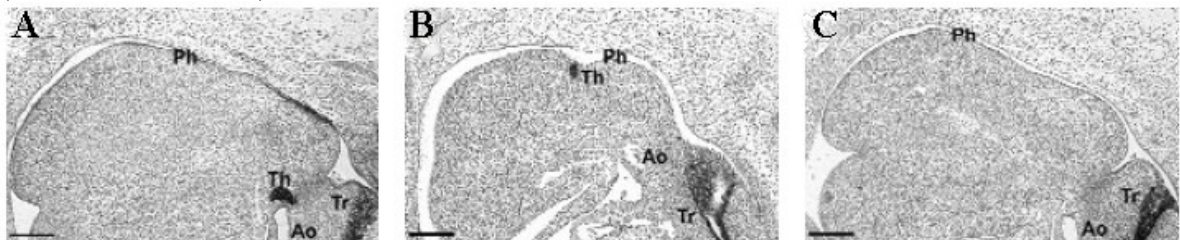


**Figure 8** *Foxe1* is important for thyroid bud migration. Sagittal sections of E11.5 *Foxe1*<sup>+/-</sup> (A) and *Foxe1*<sup>-/-</sup> (B-C) mouse embryos stained with an anti-Nkx2-1 antibody. In mutant embryos, the thyroid primordium is either present but still attached to the pharyngeal floor as shown in B, or absent as shown in C. Ph, pharynx; Th, thyroid bud; Ao, aorta; Tr, trachea (De Felice et al., 1998).

Until now, *Foxe1* homologous genes have been identified in a few species. Phylogenetic analysis suggests that the ancestral precursor of the vertebrate thyroid-specific *Foxe1* is a *FoxE4-like* gene expressed in lens and pharynx. In the urochordate *C. intestinalis*, *Ci-FoxE* is expressed in the adult endostyle and is detected in the same cells that express *Ciona TPO* (Ogasawara and Satou, 2003). Interestingly, a gene homologous of *FoxE4*, *AmphiFoxE4*, was isolated from the amphioxus (Cephalochordata, Chordata) (Yu et al., 2002); the expression of *AmphiFoxE4* does not occur in the endostyle but in the club-shaped gland, a pharyngeal-derived structure located near the endostyle that has no obvious homology with any vertebrate structures. It was proposed that the expression of *FoxE4* was transferred from the homolog of the club-shaped gland to the endostyle during the rise of vertebrates (Mazet, 2002).

### *Hhex*

*Hhex* is a transcription factor characterized by a homeodomain as a DNA binding domain (Bedford et al., 1993; Crompton et al., 1992). During mouse development, it is expressed in the primitive endoderm and then in the definitive endoderm. At later stage, *Hhex* mRNA can be detected in the ventral gut and finally, from E8.5, in the primordium of many organs derived from the foregut, such as thyroid, thymus, liver, pancreas and lungs. Thyroid expression of *Hhex* is maintained until adulthood (Bogue et al., 2000; Thomas et al., 1998).

The analysis of *Hhex*<sup>-/-</sup> embryos has revealed that this factor is absolutely necessary for thyroid morphogenesis (Martinez Barbera et al., 2000). *Hhex* null mice show multiple

malformations and are no more viable after E15.5. Thyroid specification occurs in *Hhex* mutants where the thyroid anlage is normally present at E9 but becomes absent or severely hypoplastic one day later, suggesting that *Hhex*, as well as *Nkx2-1*, *Pax8* and *Foxe1*, is not required for thyroid specification (Parlato et al., 2004). Concurring with the morphological alteration is the strong reduction in *Nkx2.1*, *Pax8* and *Foxe1* levels in the mutant mice (**Figure 9**); the role of *Hhex* could then be to maintain the expression of these transcription factors in thyroid cells (Parlato et al., 2004).

Some reports have indicated that *Hhex* can work as a transcriptional repressor (Brickman et al., 2000; Ho et al., 1999; Noy et al.) and that in thyroid cell lines it is able to inhibit *Tg* promoter activity (Pellizzari et al., 2000).

About *Hhex* regulation, cell culture studies have demonstrated that both *Nkx2-1* and *Hhex* itself (Puppini et al., 2003), as well as *Pax8* (Puppini et al., 2004), are able to activate the *Hhex* promoter.

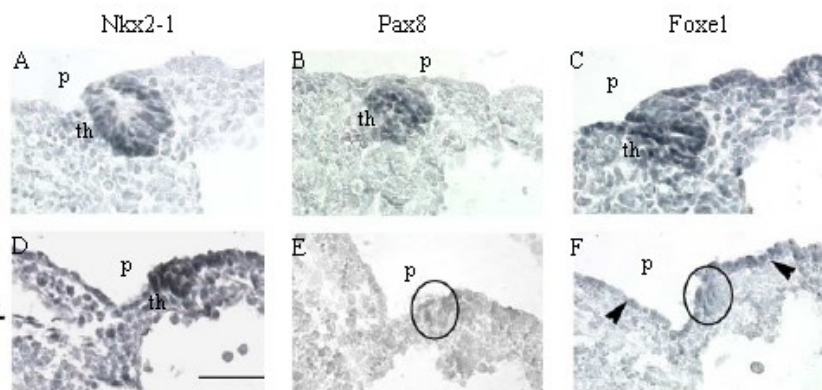


**Figure 9** *Hhex* is important for thyroid development. Cross sections of wild- type (A,B,C) and *Hhex*<sup>-/-</sup> (D,E,F) E10 mouse embryo stained with anti-*Nkx2-1* (A,D), anti-*Pax8* (B,E) and anti-*Foxe1* (C,F) specific antibodies. At E10 the thyroid primordium is hypoplastic (D) and both *Pax8* (E) and *Foxe1* (F) are strongly downregulated in the thyroid rudiment (encircled); *Foxe1* expression in the endodermal cells of the pharynx is preserved (L, arrowheads). p, pharynx; th, thyroid (Parlato et al., 2004).

## ***Congenital hypothyroidism with thyroid dysgenesis***

### **Description and genetics**

Congenital hypothyroidism (CH) is defined as thyroid hormone deficiency present at birth; it is the most common congenital endocrine disorder (Toublanc, 1992) with the incidence varying considerably with geographic location (Rastogi and LaFranchi).

Patients with CH can be divided mainly into two groups: those with inborn errors of thyroid hormone biosynthesis (dyshormonogenesis, TDH) (15% of cases) and those with thyroid developmental defects (dysgenesis, TD) (85% of the cases) (Grant et al., 1992). Mutations associated with TDH have been found in almost all the genes coding for the proteins responsible for THs synthesis (Abramowicz et al., 1992; Everett et al., 1997; Medeiros-Neto et al., 1993; Moreno et al., 2002; Moreno et al., 2008; Pohlenz et al., 1997). TD constitutes a heterogeneous group of affections due to disturbances in the gland organogenesis. It presents three major forms: thyroid ectopy, athyreosis or agenesis, and thyroid hypoplasia.

Ectopic thyroid means that the thyroid gland is not located in the right position and probably it is a consequence of thyroid migration defects. More than 50% of patients affected by CH shows an ectopic thyroid (Castanet et al., 2001), but, up to now, no

mutations in known genes has been associated to this dysgenesis, including *FOXE1* whose murine ortholog is known to control thyroid migration.

Thyroid agenesis or athyreosis account for 20-40% of CH cases. Both athyreosis and agenesis indicate the complete lack of thyroid tissue. However, agenesis means a total absence of the gland due to a defective initiation of thyroid morphogenesis. The term athyreosis indicates a dysgenesis characterized by the disappearance of the thyroid due to alterations in any step following the specification of the thyroid anlage. Up to now, there are no mouse model for thyroid agenesis because the initial specification always occurs in the models studied. Genes involved in early regionalization of the endoderm as well as genes responsible for the expression of *NKX2-1*, *FOXE1*, *PAX8* and *HHEX* in the thyroid bud could be affected in the cases of thyroid agenesis. On the contrary, all knock-out mice described in the previous section seem good models of athyreosis. Up to now, *FOXE1* is the only gene in which mutations associated with athyreosis have been identified (Bamforth et al., 1989; Castanet et al., 2002; Clifton-Bligh et al., 1998).

Hypoplastic thyroid means a gland smaller than normal. Hypoplastic thyroid is reported in 5% of CH cases. It could be a consequence of alterations in any of the steps controlling the number of thyroid cells during organogenesis. The best candidate gene for the control of adult thyroid growth is *TSHR*; indeed, loss-of-function mutations in this gene have been reported in patients with thyroid hypoplasia (Alberti et al., 2002; Cangul et al., ; Castanet et al., 2002; Clifton-Bligh et al., 1998; Jeziorowska et al., 2006; Nagashima et al., 2001; Park et al., 2004; Sunthornthepvarakui et al., 1995; Tonacchera et al., 2001). Heterozygous mutations in *NKX2-1* and *PAX8* have been reported in patients with variable grade of CH ranging from mild to severe hypoplasia, also in the presence of the same mutation, suggesting that the genetic background plays an important role in the appearance of *NKX2-1* or *PAX8* defects (Carre et al., 2009; Congdon et al., 2001; de Sanctis et al., 2004; Doyle et al., 2004; Grasberger et al., 2005; Krude et al., 2002; Macchia et al., 1998; Moya et al., 2006; Nagasaki et al., 2008).

Thyroid hemiagenesis has been included in the group of TD (Maiorana et al., 2003). This term is referred to the condition in which only one lobe is present. Thyroid hemiagenesis has a prevalence of 0.2-0.05% in normal population (Maiorana et al., 2003). The exact genetic mechanisms that are impaired in thyroid hemiagenesis are still unknown. Interestingly, it has been reported that adult double-heterozygous for both *Nkx2-1* and *Pax8*-null mutations mice show a high incidence of thyroid hemiagenesis, suggesting the genetic origin of this condition (Amendola et al., 2005).

The finding that TD is, at least in a subset of the patients (so far in less than 5%), caused by molecular genetic defects, which in principle are inheritable and that take place in genes accountable for TD also in animal models is the strongest argument supporting the notion of TD as a genetic and heritable disease. Of course the report of different thyroid phenotypes associated with the same genetic defect or the discordance for TD observed in monozygotic twins (Perry et al., 2002) are index that TD can range from monogenic to multifactorial genetic etiologies and that environmental and epigenetic modifiers are likely to be contributing factors.

### ***Zebrafish advantages to study vertebrate organogenesis***

The zebrafish (*Danio rerio*), a member of the Cyprinidae group of teleosts, is a tropical freshwater fish, native of India and Burma. It is one of the most important

vertebrate model organisms for biological research because of a combination of excellent embryology and powerful genetic manipulation. The excellent embryology is due to different aspects: a) fertilization and embryonic development are external and occur in large clutches; b) developing embryo is transparent, aiding observation of organogenic processes in live as well as embryonic manipulations, such as single cell injection with tracer dyes in intact developing embryos to track emerging cell lineages, the ablation of specific cells, the individual cell transplantation; c) embryonic development is very rapid, at 24 hours post fertilization (hpf) all the vertebrate body features can be seen, all organ primordia are in place and start to mature. Furthermore, despite an evolutionary distance of about 370 M years between mammals and teleosts, the molecular mechanisms underlying organs development are highly conserved giving the opportunity to use the zebrafish as a model to study organogenesis and as a complementary tool for the investigation of human diseases (this fish is able to phenocopy many genetic syndromes). The zebrafish organs can be considered as a minimalistic version of those of higher vertebrates, allowing also easier studies: indeed, using a much lower number of cells they execute the equivalent function in the organism.

The powers of genetic manipulation in this model are associated with the zebrafish genome-sequencing project started in 2001 at the Wellcome Trust Sanger Institute ([http://www.sanger.ac.uk/Projects/D\\_rerio/](http://www.sanger.ac.uk/Projects/D_rerio/)) and, to date, almost completed. The analysis of the zebrafish genome has revealed an extensive coding sequence conservation with higher vertebrates that enables relatively efficient delineation of the cognate orthologs for comparative biology (Postlethwait et al., 2000). The first crucial advantage of zebrafish associated to genome sequencing was the possibility to identify gene functions by means of mutagenesis screenings. Other techniques largely used for gene manipulation are a) the generation of transgenic fish lines that allow the stable expression of specific gene product, b) RNA injection to study gene's gain-of-function activity and c) gene knockdown by morpholino (MO) injection to study gene's loss-of-function.

A feature of the zebrafish genome is the presence of many duplicate copies, or co-orthologs, of single copy human genes. Many observations suggest that the mechanism underlying zebrafish duplicated genes is a whole genome duplication happened during the early evolution of the teleost fish lineage (Taylor et al., 2001). After genome duplication, the duplicated chromosomes began to rearrange and to lose duplicate genes, possibly due to functional redundancy. However, there are also retained duplicate genes (the rate of duplicated genes retentions is estimated in the realm of 20-30%) (Woods et al., 2005), some of which have the ancestral function divided between the two copies (subfunctionalisation) and some with new functions (neofunctionalisation) (Wagner, 1998).

## Zebrafish embryology

A complete and detailed description of zebrafish embryonic development is reported in (Kimmel et al., 1995). Embryonic staging of zebrafish is based upon morphological criteria. Each stage corresponds to a specific time of incubation at 28.5°C (the zebrafish optimal temperature of development) after eggs fertilization. Zebrafish development is divided in successive periods. The **zygote period** starts with the egg fertilization and lasts for around 40 minutes. The zygote is subdivided into two visibly different parts: a clear blastodisc at the animal pole and a yolky cytoplasm at the vegetal pole (**Figure 10 A**). The blastodisc undergoes cleavage and gives rise to blastomeres, the cells that later form the

embryo during the **cleavage period** ( $3/4 - 2\ 1/4$  hpf). At the end of the cleavage period, the 64-cell blastomeres form a mound of cells on top of the large yolk ( **Figure 10 B**). In the following period, the **blastula period** ( $2\ 1/4 - 5\ 1/4$  hpf) ( **Figure 10 C-D**), epiboly begins. Epiboly describes the thinning and spreading of the cellular blastodisc over the yolk. The blastula period ends at the 30% epiboly (30% epi) stage, when all blastomeres cover 30% of yolk surface ( **Figure 10 D**). Epiboly continues during the **gastrula period** ( $5\ 1/4 - 10$  h) ( **Figure 10 E**), when also the morphogenetic cell movements of involution, convergence and extension occur, producing the primary germ layers (ectoderm, mesoderm and endoderm) and the embryonic axes. Thus, the anterior head of the embryo is clearly distinguished from the posterior tail bud, dorsal tissues are distinct from ventral ones and medial tissues are easily discernible from lateral ones ( **Figure 10 F**). Finally, near the end of the gastrula period, the neural plate is formed, which is the first morphological sign of the development of central nervous system.

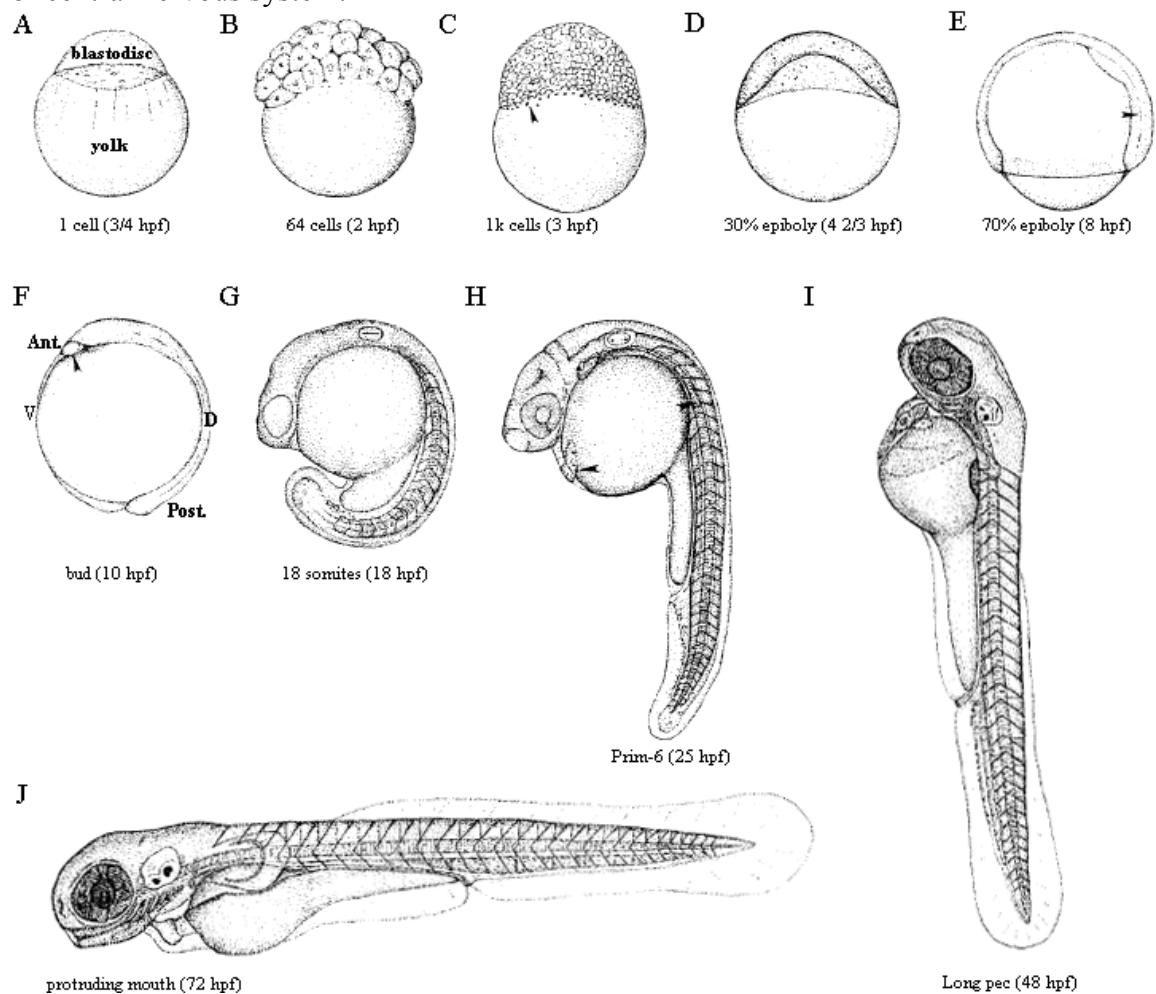


**Figure 10** Zebrafish developmental stages. The animal pole is to the top for the early stages (A-E), anterior is up (F) or to the left (G-L) at later stages (Modified from Kimmel et al., 1995).

The embryo elongates considerably during the **segmentation period** (10 - 24 hpf) when a variety of morphogenetic events occur ( **Figure 10 F-G**). A full complement of about 30 bilateral somite pairs forms in an anterior to posterior sequence. The rudiments of primary organs, become visible. The neural tube is formed and the brain becomes regionalized, with the forebrain, midbrain and hindbrain becoming distinct from one

another. The first weak muscular contractions happen. At 24 hpf, somitogenesis is complete and the embryo possesses a beating heart and circulating blood.

During the **pharyngula period** (24-48 hpf) (**Figure 10 H-I**), the seven pharyngeal arches are rapidly formed, the head straightens, pectoral fins appear, pigment cells differentiate, the circulatory system is formed, and coordinated swimming movements begin. By the end of this period, morphogenesis of many organ rudiments is rather complete, except for the gut and its associated organs.

During the **hatching period** (48-72 h), embryos develop branchial arches, mouth and they complete development of most organs (**Figure 10 L**). Embryogenesis ends at 72 hpf with the formation of the first fish bone, the cleithrum. After the hatching period, animals are called larvae. After the hatching period juvenile zebrafish starts swimming and feeding. The zebrafish embryo rapidly becomes a small version of the adult.

## Thyroid gland in zebrafish

### General aspects

As in other vertebrates, the functional unit of the teleost thyroid is the follicle, which is composed of endoderm-derived thyrocytes, it is filled with colloid, and seems to produce thyroid hormones in the same way. Follicular cells in zebrafish thyroid resemble thyrocytes of higher vertebrates in all aspects: they express the orthologous transcription factors *nk2-1a* (Rohr and Concha, 2000), *pax2.1*, *pax8* and *hhx* (Wendl et al., 2002) necessary for thyroid differentiation, the orthologous proteins involved in thyroid hormone synthesis such as *slc5a5* (also known as *Nis*) and *cathepsin b* (a protease involved in the proteolytic cleavage of iodinated TG) (Alt et al., 2006b); they produce TG (Alt et al., 2006b), accumulate iodine (Elsalini et al., 2003) and synthesise T4 (Wendl et al., 2002). It is interesting to observe that, in zebrafish, another Pax family gene, *pax2a*, is expressed in thyroid, besides *pax8*.

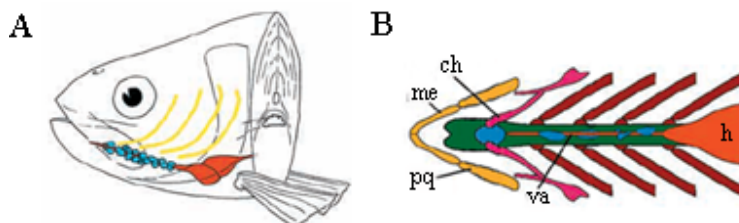


**Figure 11 (A)** Reconstruction of the distribution of thyroid follicles in the adult zebrafish head. Thyroid follicles in blue, heart and ventral aorta in red, gill arches in yellow. **(B)** Schematic drawing of a zebrafish larval head of 4.5 to 6 days post fertilization (dpf), ventral view, showing the skeleton, parts of the circulatory system and the thyroid. Blue, thyroid; brown, third to sixth branchial arches; green, basibranchial cartilage; magenta, second branchial arch; orange, heart and ventral aorta; yellow, first branchial arch. ch, ceratohyal cartilages; h, heart; me, Meckel's cartilage; pq, palatoquadrate; va, ventral aorta.

In contrast to higher vertebrate, however, the gross thyroid morphology of many teleosts is really different; in particular, the adult zebrafish thyroid consists of follicles that are not encapsulated by connective tissue to form a compact single gland, but that lie individually between the first gill arch and the bulbus arteriosus along the ventral aorta, within the mesenchyme of the ventral head region (**Figure 11**) (Wendl et al.,

2002). Another difference with mammals concerns C-cells localization. In zebrafish larvae, calcitonin-producing cells were found adjacent to the muscle surrounding the gut, far away from the thyroid follicles (Alt et al., 2006b).

## Embryonic thyroid development in zebrafish

Despite some morphological differences, the mechanisms underlying thyroid development are conserved between mouse and zebrafish. The studies carried out on zebrafish have confirmed for the most part what had already been found in mammals and have given new insights about thyroid gland development. In the following description I will focus on the knowledge about thyroid development acquired working with zebrafish as a model system.

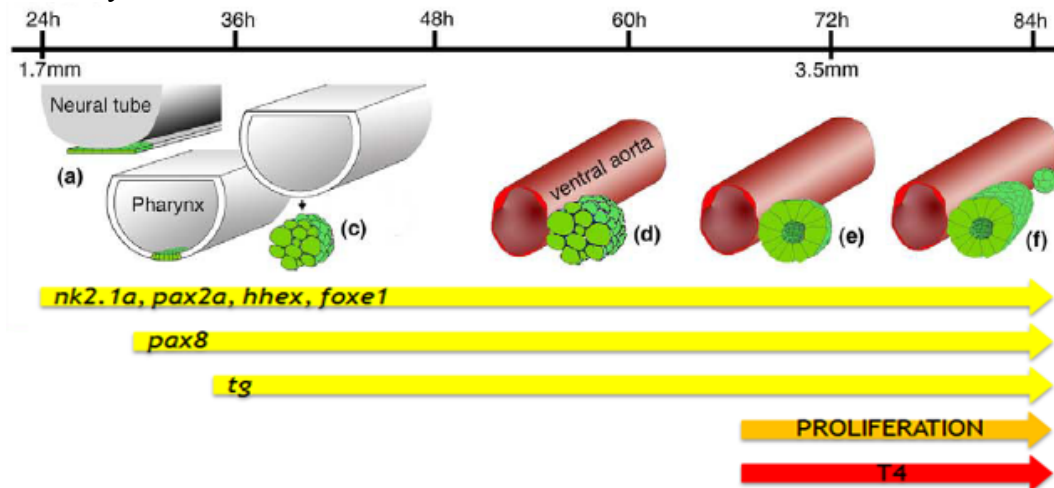


**Figure 12** Schematic illustration of thyroid development in zebrafish. The scale bar shows time of development (h, hpf). (a) Early marker gene expression in endoderm; (b) primordium budding at ventral midline of pharynx; (c, d) evagination and migration; (e) differentiation into one first follicle; (f) growth of follicles. Yellow arrows indicate the timing of thyroid genes expression; orange arrow the growth phase of thyroid development; red arrow onset of thyroid function as judged by T<sub>4</sub> production (Elsalini et al., 2003).

Also in zebrafish the thyroid development is classically subdivided into few distinguishable steps (**Figure 12**), shared with mammals: a) specification of TFC progenitors; b) budding of thyroid anlage; c) migration of thyroid primordium; d) late thyroid morphogenesis and functional differentiation of thyroid follicles.

Like in mammals, the zebrafish thyroid develops from the endodermal tissue at the level of the pharyngeal floor. The first direct proof that thyroid embryonic progenitor cells are completely derived from the definitive endoderm was obtained by means of a fate-mapping experiment conducted in zebrafish embryo, the first one for thyroid in any species (Alt et al., 2006b). In this study, to test whether the thyroid derives from Nodal-dependent endoderm, ectopic *Tar\** expression was used. Injection of *Tar\** mRNA causes activation of Nodal/activin pathway and induces zebrafish injected blastomeres to become endoderm in a cell-autonomous manner (David and Rosa, 2001). Alt and colleagues observed that injecting *Tar\** mRNA together with a lineage tracer, all thyroid primordium cells expressed this tracer indicating that they derived from the injected cell. These data confirmed that the midline primordium of the thyroid derives from Nodal-dependent endoderm. The endodermal origin of thyroid is also confirmed by its absence in zebrafish mutants of the Nodal cofactor *one-eyed-pinhead* (*oep*) in which the endoderm is not specified and the gut tube fails to form (Elsalini et al., 2003). The thyroid anlage is also completely absent in *cas*<sup>-/-</sup> and *bon*<sup>-/-</sup> mutants (Elsalini et al., 2003), in which activation of Sox17, a downstream effector of Nodal crucial for the expression of endoderm specific genes, is disrupted. The demonstration that this phenotype, in addition to be secondary to the global disturbance of endoderm formation, is also thyroid-specific, come from the finding that in zebrafish mutants of the GATA homologue *faust* (*fau*), a downstream target of Nodal that activates

Sox17, thyroid primordium is lost (Elsalini et al., 2003) whereas at the same time early gut tube formation is only mildly affected (Reiter et al., 2001).

In zebrafish, the specified thyroid precursor cells appear at 24 hpf, characterized by co-expression of key transcription factors such as *hhex*, *nk2.1a*, *pax2a* and *pax8* ( **Figure 13 A**). Elsalini and colleagues have demonstrated that during differentiation of the thyroid gland, zebrafish *hhex*, *nk2.1a*, and *pax2a* act presumably in the same manner as mouse *Hhex*, *Nkx2.1* and *Pax8*, respectively. Knock-down experiments have demonstrated that in zebrafish these genes have a late role in thyroid development and are not involved in early thyroid specification; when one of these transcription factors is absent, the expression of molecular markers is lost and the thyroid primordium disappears (in **Figure 13 B** is reported the downregulation of *nk2.1a* using a specific morpholino) (Elsalini et al., 2003).

The zebrafish genome contains a high number of duplicated genes that derive from teleost-specific genome duplication. In the case of these three transcription factors, it was found that duplicated paralogous genes have not maintained a redundant role in thyroid development. For *hhex*, only this single gene can be found in the zebrafish genome (Elsalini et al., 2003). The *Nkx2.1* gene is duplicated in zebrafish, but only *nk2.1a* is expressed in thyroid (Rohr and Concha, 2000). In the case of *pax2.1/pax8*, it was shown that both are expressed in zebrafish thyroid with *pax8* acting downstream of *pax2.1*, and that *pax2.2* is not expressed in thyroid (Wendl et al., 2002). Concerning *Foxe1*, only one ortholog, *foxe1*, was found in the zebrafish genome, which is expressed in thyroid primordium. However, this gene is not functionally involved in thyroid development, in contrast to its role in mouse and human. However, it cannot be excluded the possibility that an unknown *foxe1* paralog and/or other *foxe* gene(s) may compensate for the loss of *foxe1* activity in zebrafish thyroid (Nakada et al., 2009).

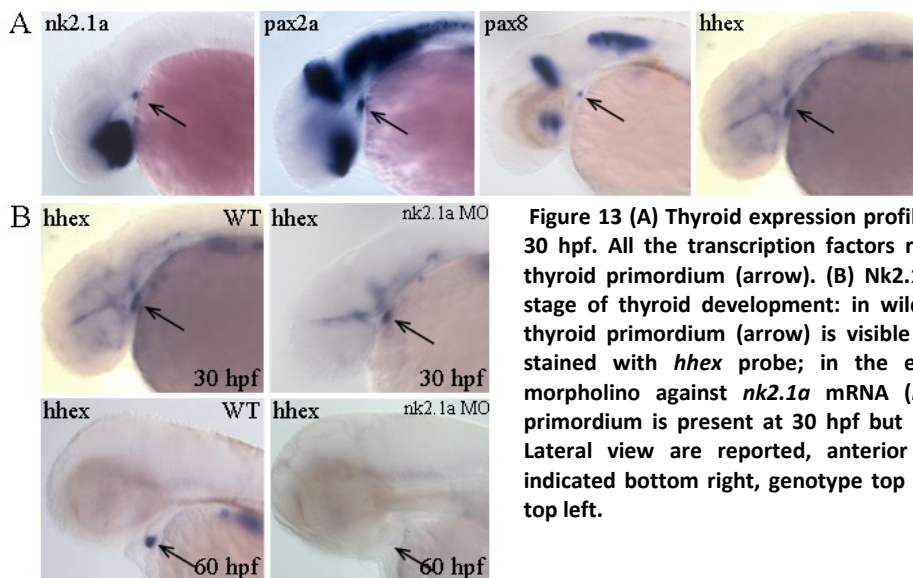


**Figure 13 (A)** Thyroid expression profile of zebrafish embryos at 30 hpf. All the transcription factors reported are expressed in thyroid primordium (arrow). **(B)** *Nk2.1a* is required in the late stage of thyroid development: in wild-type (WT) embryos the thyroid primordium (arrow) is visible at 30 hpf and at 60 hpf stained with *hhex* probe; in the embryos injected with a morpholino against *nk2.1a* mRNA (*nk2.1a* MO) the thyroid primordium is present at 30 hpf but disappears at later stage. Lateral view are reported, anterior to the left. Stages are indicated bottom right, genotype top right and staining/marker top left.

Thanks to the zebrafish studies, new knowledge about the induction of thyroid fate was obtained. In particular, the first direct evidence for a role of FGF in the induction of thyroid fate comes from studies in zebrafish (Wendl et al., 2007). Exposure of early embryos to an inhibitor of FGF at a stage prior to specification leads to lack of thyroid primordium without global defects in endoderm patterning. A similar phenotype is found in embryos mutant for the transcription factor *hand2* that has been suggested to be

upstream of *FGF* (Abe et al., 2002). This effect is most likely due to *hand2* activity in the cardiac lateral plate mesoderm, where this gene is expressed, juxtaposed to the thyroid anlage. It is conceivable that *hand2* is necessary for the development of certain tissues (most probably lateral plate mesoderm or heart) in the vicinity of the endoderm. Thyroid development, in turn, depends on the proper development of these surrounding structures because if the development of adjacent tissue is impaired also local sources of signaling molecules, such as FGFs, could be deficient. Hence, these findings elucidate also how the interaction between mesoderm and endoderm is fundamental for proper thyroid specification and development in zebrafish. As reported above, recent work in mouse models has confirmed and further elaborated these findings (Kameda et al., 2009; Lania et al., 2009).

In addition to the surrounding mesoderm, much attention has been paid to the possible involvement of embryonic vessels and endothelial cells as a source of inductive signals for endoderm derived organs. Like in mammals, the zebrafish thyroid primordium starts to develop near the outflow tract of the heart; from about 40 hpf, the globular primordium expands along the A-P axis into a strand of follicular tissue, thereby always remaining restricted to the midline. During the expansion phase, the thyroid tissue is in close contact with the growing ventral aorta that connects the heart to the branchial arteries. Considering that this aspect, is conserved in mammals and zebrafish, it was raised the question whether factors generated by the vessel wall or provided by the local circulation may influence early thyroid development. Works in zebrafish have clearly demonstrated that thyroid specification does not require a vascular signal. Specifically, in zebrafish lacking *Scl*, *vegf* or *Kdr* functions, in which the vascular patterning of the thyroid specification zone of the endoderm is severely disturbed, thyroid progenitors are readily specified (Alt et al., 2006a). Likewise, in *cloche* mutants lacking all vascular progenitors of the anterior trunk, the thyroid primordium is present (Alt et al., 2006a). Even if normally differentiated, the thyroid follicles in these mutants were mislocalized and irregularly distributed around the cardiac outflow tract, indicating that vascular cells influence thyroid morphology rather than thyroid induction (Alt et al., 2006a).

## 2. Aim of the present project

As described in the introduction section, there is a series of aspects concerning the thyroid development that remain unknown. The necessity to elucidate this missing information is by no means solely academic, since identification of the molecular mechanisms involved in any steps of thyroid development will likely provide clues to novel pathogenetic mechanisms of thyroid dysgenesis. To date, only in 5% of the patients with TD examined it was found a mutation in the known thyroid genes. This number could be an underestimate because the mutation analysis was limited to the coding regions of the genes examined, excluding potential disease-causing mutations in non-coding regions of the same genes. Still, the low frequency of mutation in the genes studied thus far suggests that other genes and/or mechanisms could be involved in the pathogenesis of TD.

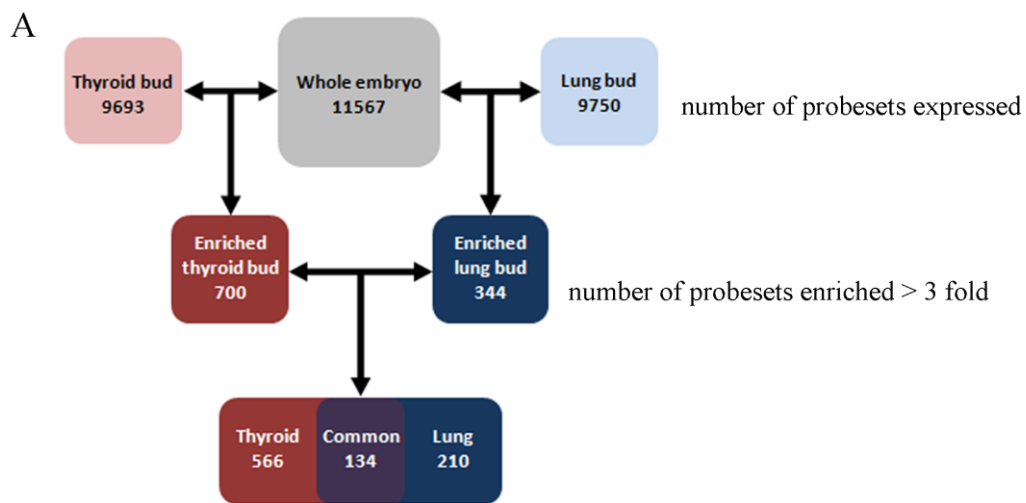
Many efforts are being devoted to understand the mechanisms by which thyroid precursors cell specification, thyroid primordium migration and final organ shaping occur. In particular, the genes involved in the transcriptional regulation of the thyroid transcription factors Nkx2.1, Hhex, Pax8, Foxe1, as well as their downstream genes that ultimately actuate the specific thyroid developmental program are still unknown. Different experimental strategies are currently used from different research groups to investigate these aspects.

In the case of my PhD project, it was decided to use a comparative approach to contribute to the elucidation of the genetic mechanisms underlying the early steps of thyroid development. In particular, my objective was to use the zebrafish as a model for validating genetic information preliminarily gained in the mouse model system, taking in mind that comparison between related species may be a successful approach to uncover conserved and divergent principles of development.

Embryonic thyroid-enriched gene lists obtained combining Laser Capture Microdissection (LCM) and microarray technology in mouse model were the starting point of my PhD project. Three mouse transcriptomes, from thyroid bud, lung bud and whole embryo, have been compared and two different gene lists, thyroid enriched and enriched in both thyroid and lung were generated (**Figure 14 A**). Significantly enriched GO categories in which these thyroid enriched genes are classified are reported in **Figure 14 B**.

The main aim of the present work was to identify new genes involved in thyroid development, by functional analysis in the zebrafish system of the mouse thyroid enriched genes.

It was decided to conduct this work proceeding through three steps/objectives that have been approached in a chronological order. The first point was the identification of the zebrafish orthologs of the murine thyroid enriched genes by searching in publicly available genomic databases; the orthologs identified were either cloned from zebrafish embryo cDNA or purchased from a distributor of clones generated by the I.M.A.G.E. *Consortium*. The second point was the expression profile analysis of the zebrafish orthologs in order to verify their transcription in the developing thyroid; this step was performed with the application of whole-mount in situ hybridization (WMISH) technique. The last point was the functional analysis of the genes whose expression was found to be conserved in zebrafish thyroid, with the aim to characterize the thyroid phenotype.



B

GOID	GO term	Thyroid	Lung
560	cell morphogenesis	●	
4902	nervous system development	●	
4909	axonogenesis	●	
13004	neurite development	●	
14805	cellular structure morphogenesis	●	
14806	cell part morphogenesis	●	
22082	cell development	●	
22273	neuron morphogenesis during differentiation	●	
22414	neurite morphogenesis	●	
22459	cell projection morphogenesis	●	
562	cell morphogenesis during differentiation	●	●
880	morphogenesis of a branching structure	●	●
4699	cell adhesion	●	●
6464	anatomical structure morphogenesis	●	●
11867	biological adhesion	●	●
22337	system development	●	●
22457	anatomical structure development	●	●

Figure 14 (A) Scheme describing mouse thyroid enriched genes lists generation: thyroid bud transcriptome and lung bud transcriptome were compared to whole embryo transcriptome to highlight thyroid bud enriched and lung bud enriched genes lists; comparing the thyroid enriched genes with the lung enriched genes, the genes enriched only in thyroid bud and the genes enriched in both tissues were selected. (B) Significantly enriched Gene Ontology categories in which the thyroid enriched genes are classified.

### 3. Material and methods

#### ***Zebrafish care and preparation of specimens***

The work on zebrafish *Danio rerio*, was carried out essentially according to standard procedures (Westerfield, 2000) and staging refers to the development at 28.5-29°C. The *noi<sup>tu29</sup>* mutant fish lines was used (Lun and Brand, 1998).

To perform WMISH and whole mount immunohistochemistry (WMIHC) experiments, embryos were dechorionated manually and anaesthetized in tricaine before fixed over night using 4% Paraformaldehyde (PFA) in PBS. Then they were washed in PBS containing 0.1% Tween 20 (PBT) and stored in methanol at -20°C.

#### ***Embryonic manipulation***

Morpholinos were acquired from Gene Tools (Corvallis, OR) and dissolved as recommended by the provider. Morpholino sequences are: *hhx*: 5'-gctgctgggtgctggaattgcatga-3'; *nk2.1a*: 5'-gctcaaggacatggttcagccgc-3'; *bcl2l*: 5'-aggtgttgctcgttctccgatgc-3'; *pax8-1*: 5'-gttcacaaacatgcctcctagtga-3'; *pax8-2*: 5'-gacctgcccagtgctgttgacat-3'; control: 5'-cctcttacctcagttacaattata-3'. The *bcl2l* full-length mRNA was synthesized by *in vitro* transcription reaction from the pCS2+ *bcl2l* construct (see below for the construction of the plasmid) using the SP6 polymerase (Ambion kit). Microinjection setup and embryos were prepared and injected according to Rembold et al., 2006. Morpholinos and mRNA were always injected into one-cell-stage embryos.

#### ***Probes preparation and Whole Mount In Situ Hybridization (WMISH)***

The template to synthesize the probe was prepared by either linearizing a plasmid or by PCR on plasmid. The plasmid, containing the template to be transcribed, has been digested with the appropriate restriction endonucleases, following the manufacturer's instructions, and purified with a classical phenol:chloroform:isoamyl alcohol extraction. 1 µg of purified, linearized DNA has been used as template for ribonucleic probe synthesis labeled with digoxigenin (DIG) or fluorescein (Fluo). When the plasmid containing the template to be transcribed was not provided of RNA polymerase binding site, the template was amplified by PCR using a reverse primer that introduce at 3' end of the fragment the T3 binding site. The amplified product was then purified by agarose gel extraction. The *in vitro* transcription reactions were performed using the appropriate RNA polymerase, Sp6, T7 or T3 (Roche) following the manufacturer's instructions. The synthesized ribonucleic probes have been purified with the mini Quick Spin RNA Columns G-50 Sephadex (Roche), following manufacturer instructions and their quality has been checked by gel electrophoresis. The recovered samples have been immediately stored at -80°C till the use.

Embryos stored in 100% methanol at -20°C were washed twice with PBT, digested with 10 mg/ml proteinase-K in PBT for several minutes depending on the stage, washed further and fixed again in 4% PFA for 20 min. After additional washes, the embryos were prehybridized in hybridization mix (HM) (50% formamide, 1.33X SSC, 0.2% Tween20, 100 µg/ml Heparin, 50 µg/ml yeast or torula RNA, 5 mM EDTA pH8, 0.5% chaps) for 2-4 h at 63°C and then DIG-labelled RNA probe or Fluo-labelled RNA probe was added (1µl for 300µl of hybridization mix). The embryos were then submitted to several washing treatments at 63°C: 5 min in HM/2XSSC (75:25); 5 min in HM/2XSSC (50:50), 5 min in HM2XSSC (25:75), 10 min in 2XSSC, 30 min in 0,2XSSC. Then they were rinsed once with warm 0.2SSC and let them cold to RT. Once reached room temperature (RT),

embryos were washed with MBT for 5 minutes and then incubated in 2% blocking reagent (Roche) for at least 2 hrs at RT. The antibody incubation step is usually performed ON at 4°C, diluting the appropriate antibody in 2% blocking reagent with the following proportions: 1:5000 for Fab-AP  $\alpha$ -DIG and 1:2000 for Fab-AP  $\alpha$ -Fluo (Roche). The following day, the antibody was removed and embryos washed four times in MBT for 15 min each and with MAB with 0,1% Tween 20 for 30 min. Then, for staining reactions with BMpurple (Roche) that gives the blue precipitate, it was performed an incubation in a solution containing Tris-HCl 0.1M pH 9.5 and 0.1% Tween 20 for 30 min followed by a wash in NTMT (0.1 M Tris pH 9.5, 0.05 M MgCl<sub>2</sub>, 0.1 M NaCl, 1% Tween 20) for 30 min, before the staining reaction. For staining reactions with Fast Red tablets reagent (Roche) that gives the red precipitate, samples were incubated in a solution containing Tris-HCl 0.1 M pH 8.2 and 0.1% Tween 20 for 30 min, followed by the staining reaction with Fast Red (1 tablet/ml in Tris-HCl 0.1 M pH 8.2). The staining reaction was stopped by the addition Stop solution (1X PBT, 1mM EDTA pH 8.0), followed by the fixation in 4% PFA. The stained embryos were then washed in PBT, gradually transferred to 90% glycerol and studied for detailed analysis.

In double *in situ* experiments, embryos were hybridized with two different probes: the strongest one labeled with Fluo and the weaker with DIG. The first detection was usually performed for the DIG-labeled probe with BMpurple and the second for the Fluo-labeled probe with Fast Red. After the first detection, embryos were washed with Stop Solution and the Fab-AP  $\alpha$ -DIG was inactivated with a 10' wash in 0.1 M Glycine pH 2.2 with 0.1% Tween 20. Then, embryos were rinsed in MABT for few minutes, incubated in Block and finally with the second antibody.

### **Double staining (WMISH + WMIHC)**

For tg immunodetection, the ISH was stopped with PBT and the *in situ* hybridized zebrafish embryos were washed further 5 times in PBT. Then, they were treated in dark with 10% H<sub>2</sub>O<sub>2</sub> in PBS for 15 min to block endogenous peroxidases, rinsed twice with PBT, post-fixed in 4% PFA for 15 min and washed 5 times in PBT for 5 min each. They were then incubated with 3% normal goat serum (NGS) for 2 h, then with polyclonal anti-human thyroglobulin antibody (Dako) (dilution 1:6000 in 3% NGS) for 2 h and washed several times in PBT for 3 h or ON. They were then incubated with anti-rabbit biotinylated secondary antibody (Vectastain) (dilution 1:200 in 3% NGS) for 2 h, washed several times in PBT for 3 h or ON and further incubated with the ABC reagent (Vectastain) for 2 h (1 ml PBT + 20  $\mu$ l A + 20  $\mu$ l B). After several washes in PBT for 3 h, the embryos were stained with DAB (1: 5) in PBS with 0.3% H<sub>2</sub>O<sub>2</sub> for 30 min and observed while staining. All the incubations with 10% H<sub>2</sub>O<sub>2</sub> in PBS, 4% PFA, NGS, primary antibody, secondary antibody and DAB were carried out at RT.

For active-caspase-3 immunodetection, the ISH was stopped with PBT and the *in situ* hybridized zebrafish embryos were washed further 5 times in PBS+TritonX (0,1%). Then, they were treated with pre-cooled acetone for 20 min at -20°C, washed in PBS+TritonX (0.1%), treated in dark with 10% H<sub>2</sub>O<sub>2</sub> in PBS+TritonX (0.1%) for 30 min to block endogenous peroxidases and washed again in PBS+TritonX (0.1%). They were incubated in blocking solution (5% NGS + 2mg/ml BSA) for 2 h at RT and then with the anti-human active-caspase-3 antibody (BD Biosciences) (dilution 1:500 in blocking solution) ON. They were then washed 3 times in PBS+TritonX (0.1%) for 20 min each and incubated for 2h in anti-rabbit biotinylated secondary antibody (Vectastain) (dilution 1:1000 in blocking solution). After 3 washes in PBS+TritonX (0.1%) for 20 min each, the embryos

were incubated with the ABC reagent (Vectastain) for 45 min (1 ml PBT + 5  $\mu$ l A + 5  $\mu$ l B). The staining was performed with DAB as reported above.

### **RNA extraction, cDNA synthesis and cloning procedures**

Total RNA was extracted from whole zebrafish embryos at 24, 48 and 72 hpf using TRIzol Reagent (Invitrogen), according to the manufacturer's instructions. Residual DNA was digested with DNase I using a DNA-free kit (Ambion, Austin, TX). The concentration of RNA was estimated using a NanoDrop ND-1000 spectrophotometer and its integrity by gel electrophoresis.

4  $\mu$ gs of total RNA were used as template for the synthesis of the first cDNA strand starting reverse from oligo dT primers, using the Superscript II Reverse Transcriptase kit (Invitrogen) according to the manufacturer's instructions.

Gene fragments to use as templates for probe preparation and WMISH experiments have been amplified by PCR using gene-specific oligonucleotides (Table 1) and cloned by TOPO-TA cloning (Invitrogen), according to manufacturer instructions.

**Table 1 Oligonucleotide list used for cloning**

Zebrafish gene symbol	Primer forward sequence	Primer reverse sequence
irgf3 - LOC797731	AACTCAGAATGACTTGGAGG	CTAGACTTCAGTCTCCAGTG
LOC565002	CCAAACGTTCAAACATAATGTC	AGGTTATCTTCTTTGTGAGGG
LOC100007513	CTGATGGTGTATAAACATGAACTG	TGAAAGCCTCGCCAGTGATCC
Prlra	TGCAGATTTAATATCGCAAGCAGC	GGAAGAAGCCCAGCTTGTTT
Prlrb	GTCATTCTCCACCAGGGAGG	TGATGGTCCGTGCTCTGGGATA
si:dkey-5n4.1	GGAATGGTCATTCTTACCCTGTGC	GACTCATAGTCTGACAGGCCTTTG
NP_001038642.1	GATCATCCCATATGACTTCAACAG	CATATATCCATCTATGTGTGAGAGC
LOC567443	GATCATCCCATATGACTTCAACAG	GACGCGGTCCAGCGGAGCATTG
lypd6b	GTGTCCTAACAGCGTCTCAAAC	GTGGCATGAGTCCAGACAGAGCGG
A2CE94_DANRE	ACCCTCAGCATTGTGCGCAAAG	GGCGATGGGGATCTAAATGATGGC
LOC10000503	GAGCAGGGAGGGCAAGATTCCG	AATGGAGGTGAGGTGTACTGCTGT
LOC794722	CCCAGTCCACAGCGACTCTGC	CAGTGATGGGCGCTGTTATATGGC
clstn2	GCATGAAGATGCGCGGATAAC	TGCCGTCCAATTGGTGGATGTGCT
LOC569664	GGTTTCCACGTGCAGGGCCTCAG	GAGAGTCACCGTCCAGTTACATAC
CHDH	CAGCAGGCTGGATACCCCTACAC	TAATGGCGTCCGCCGCTTCTCTG
LOC562973	CAAAATATGTGTCTTCTGCT	TGCTCCCACTTCTGAATC
ENSDARG00000073889	CGTTCCTCCATCGGAAACCA	GCAATGTACTTCTCTCATCCC
LOC562570	ACTGCTGGCTCATAGAAGGT	GCCACACAGTAGGTGTAATC
sich211-210c8.8	GGTTGTCGATCCAGGGCAA	CGTGGAGAGATGCTGAAGAG
socs2	ATGACCTGTCACTCATCCGA	TATAAGTGTAGTCTGTCAAGTA
SORL1	CAATGAGAGCAGCTCAGTTTAAACA	CCATTAAAGCAGGTGGCGTGAGGA
zgc:101788	CTGCTAGCAAACAGAGGGAC	TAAGTGGCACAACGCTGTTT
B8A438_DANRE	TCAAGACACTGCAAGAAGGAGAGA	AGCATATATGCCATTGTCCGAAAC
Q32PL4_DANRE	ATCCGGTCTTCAATAATGGC	CAGTGATAAATCACAGGTGTC
cdh1	ATGGCTTGTGTAACAACACTGTGGG	TCTGGATCAATGGCTGTAAGAGGG
si:ch211-81i17.1	GAGGAGTTTCAGTTCCTTCAGGC	CAGGAAGTGAGGAGGACAGCC
cadherin 16	GAGTATAGTCTTGAGGGAGAGTT	GCTGTGGATGCAGGTCCGTAT
bmf1	ACGAGGATGATGTGTTTCAGGA	ACCTGCGGTTCTCTCTGGC

To produce the pCS2+ bcl2l construct, the *bcl2l* cDNA was amplified from the clone IRBOP991H0214D from the IMAGE Consortium using the following primers: forward primer 5'- ATCCGGAATTCAATTATGTCTTACTATAACCGA-3' containing a EcoRI restriction site in 5' tail; reverse primer 5'-

TTGCTCTCGAGTTATCCTCATCTTCACAG-3' containing a XhoI restriction site in 5' tail. Then, the amplified *bcl2l* cDNA was digested with EcoRI and XhoI and cloned in EcoRI and XhoI sites in pCS2+.

All the standard molecular biology techniques were carried out according to Sambrook et al., 2001; plasmids were transformed into the E. Coli k12 strain and cultured in 5 ml LB medium containing appropriate antibiotics; the DNA was then purified using Qiagen Mini prep kits (Qiagen).

#### ***Identification of zebrafish orthologs in Ensembl and NCBI databases***

Zebrafish orthologs have been identified by means of successive steps: first of all Ensembl databases were checked looking for the zebrafish genes already annotated as orthologs of the mouse thyroid enriched genes; the orthologs identification was then confirmed and completed by browsing Ensembl (<http://www.ensembl.org/index.html>) and NCBI (<http://www.ncbi.nlm.nih.gov/blast/Blast.cgi>) peptide databases, using mouse protein sequence as query and BLATP as search tool. The criteria adopted for a likely ortholog was > 40% amino acid identity over the entire length of the protein. When more than two sequences showed a good identity percentage to the query, they were align with the mouse protein sequence using an *online* available multialignment tool (<http://multalin.toulouse.inra.fr/multalin/multalin.html>). Analyzing the multialignment the proteins, that showed the higher identity to the mouse protein in the domains relevant for the protein function, were selected as zebrafish ortholog proteins.

## 4. Results and discussion

### ***Zebrafish analysis of mouse thyroid enriched genes***

#### **Identification of the zebrafish orthologs of the murine thyroid enriched genes**

We decided to focus our study on the genes enriched in mouse thyroid bud and on that enriched in both mouse thyroid bud and lung bud, overcoming a fold change 10.

These two gene lists consist of a total of 92 genes (excluding the already known thyroid genes). Furthermore, other 11 thyroid-enriched mouse genes with a fold change lower than 10 were selected, for the study, because of their implication in molecular processes candidate to be relevant for thyroid development.

To find the putative zebrafish orthologs of the mouse thyroid-enriched genes, the last version of the ongoing zebrafish genome sequencing project (Zv8, June 2008) was analyzed by performing BLAST alignments against the zebrafish Ensembl databases. The obtained results were confirmed and sometimes completed performing the BLAST search in the zebrafish NCBI databases. For 90 mouse genes (88% of investigated genes) a total of 167 putative zebrafish orthologs were identified; in particular, for each of 40 mouse genes two zebrafish orthologs were found, in line with the whole genome duplication event occurred during the early evolution of teleost fishes (e.g., *prlra* and *prlr*b are the two zebrafish orthologs of the mouse *Prlr*); for each of 37 mouse genes only one zebrafish ortholog was found, in line with the gene loss events occurred after the zebrafish whole genome duplication (e.g., *zgc:158317* is the only zebrafish ortholog of the mouse *Zbtb20*); for each of 13 genes more than two zebrafish orthologs were found (e.g., *tcfcp2l1*, *si:ch211-207c15.3* and *sich211-210c8.8* are the three putative zebrafish orthologs of the mouse *Tcfcp2l1*). This latter aspect could be due to single gene duplication events occurred in addition to the whole genome duplication or could be a consequence of large gene family in which it is difficult to identify the “true” orthologous genes (e.g., 10 putative zebrafish orthologs were found for the mouse gene *ligp*). Finally, zebrafish orthologous matches were not found for 13 mouse genes probably because the zebrafish genome is not fully completed or because of genes loss during the genome evolution (e.g., 4930426D05Rik, *Cd44*).

The gene lists, with the zebrafish orthologs identified are reported in Appendix (**Table 5, Table 6 and Table 7**).

#### **Expression patterns analysis of the putative zebrafish orthologs**

After the identification of the zebrafish orthologs of the mouse thyroid-enriched genes, their expression profile was investigated, during zebrafish embryonic development, to evaluate the conserved expression in thyroid primordium. The spatiotemporal expression pattern of these orthologs was analyzed by means of WMISH. With this purpose, gene fragments to use as templates for the synthesis of digoxigenin-conjugated riboprobes have been gained following two main approaches: EST databases have been screened for clones of genes of interest, which have been commercially acquired from the I.M.A.G.E. Consortium; otherwise, gene-specific PCR primers have been used for amplification from total cDNA. Through these two approaches, acquisition and cloning, 104 clones resulted available for the expression profiles analysis (~62% of the orthologs). The expression pattern was studied at different developmental stages starting from the first appearance of

thyroid primordium in zebrafish embryo (24 hpf) until the distribution of the functional thyroid follicle in their final position along the ventral aorta (96 hpf). The embryonic territories in which these genes were found expressed are reported in Appendix (**Table 5**, **Table 6** and **Table 7**).

On the basis of the expression profiles observed, it is possible to cluster the genes analyzed in three groups: a) the genes that are expressed neither in thyroid region nor in surrounding tissues; b) the genes expressed in surrounding tissues but not in thyroid region; c) the genes expressed in thyroid region. The majority of the genes studied are included in the first group: despite their unquestionable expression in other embryonic tissues, they resulted clearly not expressed in zebrafish thyroid in any embryonic stages analyzed. The second group includes 37 zebrafish orthologs, corresponding to 32 mouse genes, expressed in the tissue surrounding the area of thyroid primordium development, such as the pharyngeal endoderm, pharyngeal arches, heart field, but clearly not expressed in thyroid. In **Figure 15** there are reported the *nk2.1a* expression profile as an example of thyroid staining (**Figure 15 A-B-C**) and some examples of genes expressed in adjacent tissues (**Figure 15 D-O**).

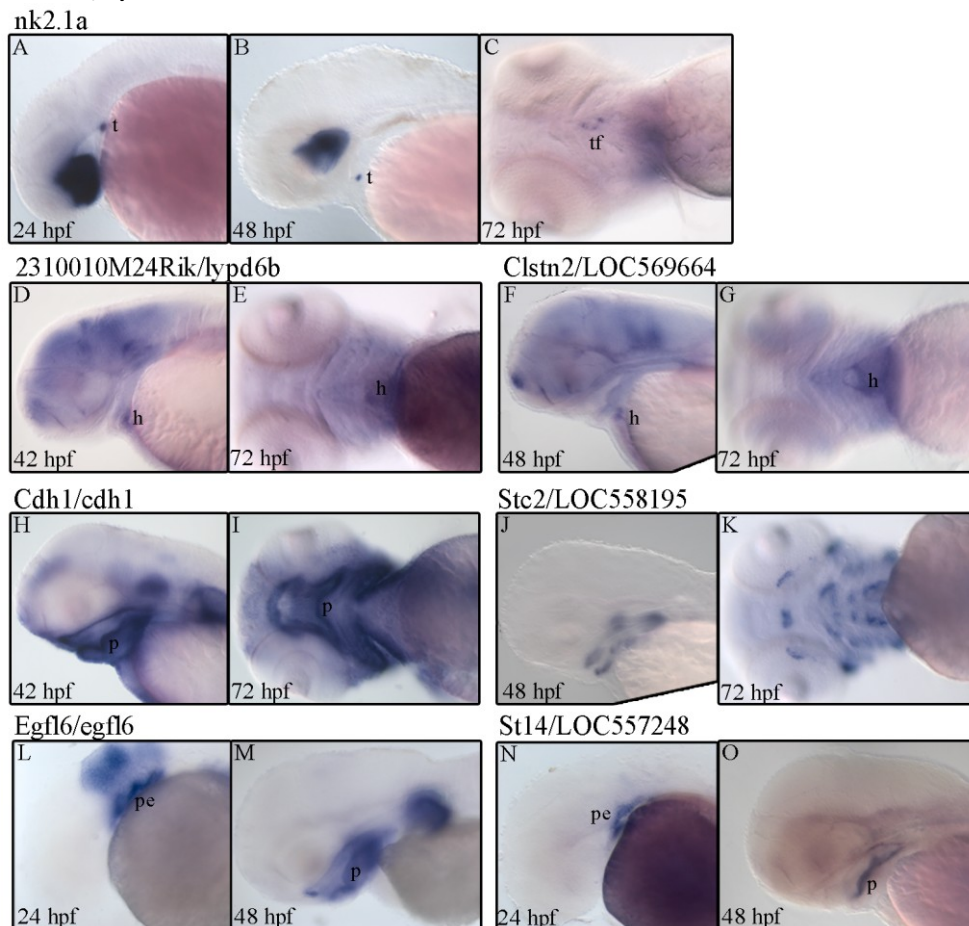


**Figure 15** Example of WMISH of genes expressed in tissues nearby the thyroid primordium. Stages are indicated bottom left, staining/marker top left. Lateral (A-B-D-F-H-J-L-M-N-O) and ventral (C-E-G-I-K) views are shown with anterior to the left. (A-B-C) *nk2.1a* expression profile showing the thyroid primordium position at 24, 48 and 72 hpf. t, thyroid; tf, thyroid follicles; h, heart; p, pharynx; pe, pharyngeal endoderm.

In zebrafish, *lypd6b* (**Figure 15 D-E**), the ortholog of the mouse gene identified as 2310010M24Rik, and LOC569664 (**Figure 15 F-G**), the *Clstn2* ortholog, are expressed in the

heart at 48 and 72 hpf. It is worth noting that the heart field and the thyroid primordium are in contact in zebrafish embryo especially from 24 to 48 hpf, making it difficult to discern a thyroid signal from a cardiac one. *Cdh1*, also known as E-cadherin, a well known thyroid epithelial marker (Fagman et al., 2003), is present in our lists; four putative orthologs were identified for this gene but only two, *cdh1* (**Figure 15 H-I**) and LOC567602, could be ISH assayed, both showing a strong expression in the pharynx, according to mouse *Cdh1* expression in the foregut endoderm, but clearly not in thyroid primordium. According to the gene chip analysis, *Stc2* was 30 times overexpressed in thyroid tissue; the mouse E10 thyroid expression of this gene was also confirmed by *in vivo* experiments. *Stc2* zebrafish ortholog, LOC558195, was expressed in cartilaginous segments of the pharyngeal region but not in thyroid primordium (**Figure 15 J-K**). The *Egfl6* ortholog, *egfl6* (**Figure 15 L-M**) and the *St14* ortholog, LOC557248 (**Figure 15 N-O**) were both expressed in pharyngeal tissues at 24 and 48 hpf.

From the current analysis, the only genes found to be expressed in thyroid primordium are: 1) *htra1*, ortholog of *Htra1*; 2) A2BFE2\_DANRE, ortholog of *Ltbp3*; 3) Q06Z31\_DANRE, ortholog of *Zbtb4*; 4) LOC100151488, ortholog of *Dock9*; 5) *bmfl*, ortholog of *Bmfl*; 6) *chdh*, ortholog of *Chdh*.

The divergence observed in thyroid expression profile between zebrafish and mouse was not expected in consideration of the high conservation of the molecular mechanisms responsible for thyroid primordium differentiation, and of the homology in thyroid function.

This divergence could be explain taking into account the different morphology of the differentiated gland. In zebrafish, as well as in the adult lamprey and the other bony fishes, the thyroid is not encapsulated and the follicles are widely scattered along the ventral aorta, either single or in small clusters. During this morphological transformation from lower to higher vertebrates, occurred after that the biochemical evolution of the gland had ceased, the thyroid of the higher vertebrate have acquired the function to group the follicles and to become encapsulated, probably through adaptive mutations in *cis*-regulatory regions, bringing new functions under the control of a thyroid expressed transcription factor. So the high number of genes enriched in mouse thyroid and not expressed in zebrafish thyroid could be explain considering this aspect.

In the current analysis, a good percentage of mouse thyroid enriched gene orthologs was found to be expressed in tissues near the zebrafish thyroid instead of the thyroid itself. It has been hypothesised a mechanism of homeogenetic transfer during thyroid evolution (Yu et al., 2002): *FoxE4*, the ancestral precursor of the vertebrate thyroid-specific *Foxe1*, was likely recruited in the endostyle, the invertebrate chordate thyroid homolog, from an adjacent region of the pharynx. A similar mechanism could have occurred during the evolution of one or more of the zebrafish genes expressed in surrounding tissues.

In addition, it cannot be excluded the possibility that unidentified or unchecked zebrafish orthologs/paralogs still retain the thyroid function.

### **Expression analysis of the zebrafish putative thyroid genes**

*Htra1* is a serine protease belonging to the high-temperature requirement factor A protein family with the ability to regulate TGF- $\beta$  (transforming growth factor- $\beta$ )/BMP (bone morphogenetic protein) signaling (Canfield et al., 2007). Two *Htra1* orthologs were found in zebrafish genome: *htra1* and *zgc:172061*. *Htra1* was found to be specifically expressed in the heart field, probably the bulbus arteriosus, and in the thyroid region, starting from 48 hpf (**Figure 16**). Actually, *htra1* expression domain appears much more

extended than the typical thyroid signal; the double staining for *htra1* mRNA and tg protein shows that the thyroid follicles are surrounded by the *htra1*-positive cells (**Figure 16D**).

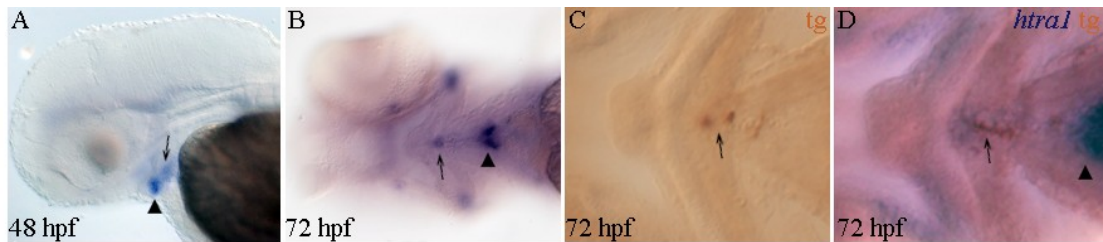


**Figure 16** Expression profile of *htra1*, zebrafish ortholog of murine *Htra1*, by *in situ* hybridization assay. Stages are indicated bottom left, staining/marker top left (when it is different from *htra1*). Lateral view (A) and ventral view (B-C-D) with anterior to the left are shown. At 48 and 72 hpf *htra1* is expressed in thyroid region (arrow) and in the bulbus arteriosus (arrowhead). In (C), a ventral view of 72 hpf embryo stained with the tg antibody, a marker of thyroid follicles. In (E) is reported the co-staining with *htra1* probe (blue) and tg antibody (brown).

The latent transforming growth factor beta binding protein 3 (Ltbp3) is an extracellular matrix protein able to modulate the TGF  $\beta$  bioavailability (Chen et al., 2003). Starting from 24 hpf, the zebrafish ortholog of *Ltbp3*, A2BFE2\_DANRE, is expressed in the heart field, probably in the bulbus arteriosus, and in the region where the thyroid primordium is located (**Figure 17**). Actually, A2BFE2\_DANRE is expressed in a wider region that includes the thyroid primordium; in particular, the double staining for A2BFE2\_DANRE mRNA and tg protein at 72 hpf shows that the thyroid follicles are located in the A2BFE2\_DANRE positive region (**Figure 17D**).

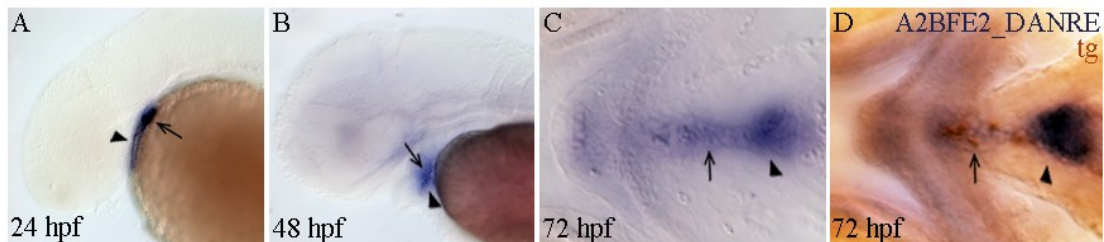


**Figure 17** Expression profile of A2BFE2\_DANRE, zebrafish ortholog of murine *Ltbp3*, by *in situ* hybridization assay. Stages are indicated bottom left, staining/marker top left (when it is different from A2BFE2\_DANRE). Lateral view (A-B) and ventral view (C-D) with anterior to the left are shown. Starting from 24 hpf A2BFE2\_DANRE is expressed in thyroid (arrow) and heart region (arrowhead). In (D) is reported the co-staining with the A2BFE2\_DANRE probe (blue) and the tg antibody (brown).

Zbtb4 is a transcriptional repressor able to recognize methylated DNA through a Kaiso-like zinc finger domain (Filion et al., 2006). It is involved in the cell cycle regulation by transcriptional repressing *P21CIP1*, an inhibitor of the Cdk2 kinase (Weber et al., 2008). The zebrafish genome contains Q06Z31\_DANRE, the only *Zbtb4* ortholog, whose expression profile was analyzed (**Figure 18**). This gene seems to be expressed in thyroid primordium starting from 30 hpf. A double staining for *zbtb4* mRNA and tg protein shows a colocalization of the two signals (**Figure 18 E**).

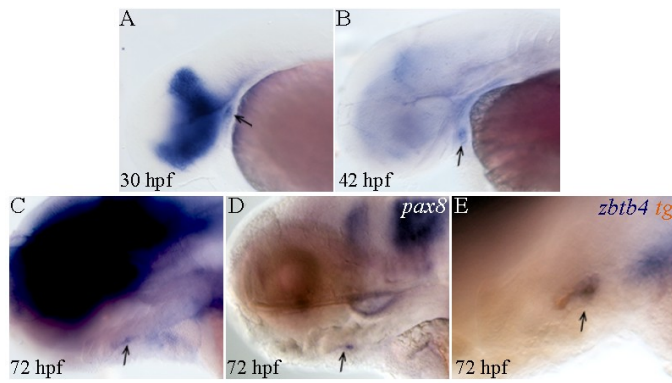


**Figure 18** Expression profile of Q06Z31\_DANRE, zebrafish ortholog of murine *Zbtb4*, by *in situ* hybridization assay. Stages are indicated bottom left, staining/marker top left (when it is different from Q06Z31\_DANRE). Lateral view with anterior to the left are shown. Starting from 35 hpf, Q06Z31\_DANRE is likely expressed in thyroid (arrow). In (D) is reported a 72 hpf *pax8*-stained embryo to show the thyroid primordium in a lateral view at this stage. In (E) is reported the co-staining with Q06Z31\_DANRE probe (blue) and tg antibody (brown).

*Dock9*, *dedicator of cytokinesis 9*, is a guanine nucleotide exchange factor able to activate the small G-protein Cdc42. The only known physiological function of this protein is the involvement in the dendrite growth in hippocampal neurons (Kuramoto et al., 2009). Two orthologs for *Dock9* were found in the zebrafish genome, *dock9* and LOC100151488, both expressed in pharyngeal region. Starting from 35 hpf, LOC100151488 shows a typical thyroid expression profile (**Figure 19**). Double in situ hybridization shows that this gene is expressed in a territory that partially overlaps with *tg*-positive cells (**Figure 19 E**).

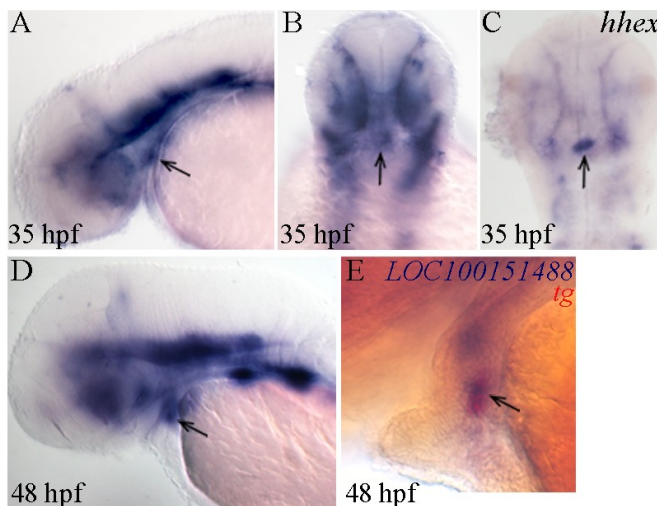


**Figure 19** Expression profile of LOC100151488, zebrafish ortholog of murine *Dock9*, by *in situ* hybridization assay. Stages are indicated bottom left, staining/marker top left (when different from LOC100151488). Lateral with anterior to the left (A-D-E) and dorsal with anterior to the top (B-C) views are shown. At 35 and 48 hpf, LOC100151488 is expressed in a region corresponding to the thyroid primordium position (arrow) (A-B-D). In (C) is reported ventral view of *hhx*-stained embryo to show the thyroid primordium in a ventral view. (E) shows a double in situ hybridization for LOC100151488 (blue) and *tg* (red).

Bcl2-modifying factor (*Bmf*) is a member of the BH3-only group of proapoptotic proteins that is implicated in cell death caused by anoikis, histone deacetylase inhibitors, transforming growth factor  $\beta$ , and tumor necrosis factor  $\alpha$  (Hubner et al.). Of the two zebrafish orthologs, *bmf1* and *bmf2*, *bmf1* expression profile was analyzed, finding that, at 48 hpf, the gene is expressed in thyroid region (**Figure 20**). Double in situ hybridization shows that the *bmf1* signal is partially overlapping with *tg* signal (**Figure 20 B**) and it is localized in the posterior part of thyroid primordium.

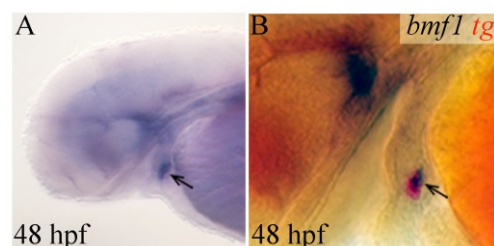


**Figure 20** Expression profile of *bmf1*, zebrafish ortholog of murine *Bmf*, by *in situ* hybridization assay. Stage is indicated bottom left, staining/marker top left (when it is different from *bmf1*). Lateral view with anterior to the left are shown. At 48 hpf *bmf1* is expressed in thyroid region (arrow). In (B) is reported a double in situ hybridization for *bmf1* (blue) and *tg* (red).

*Choline dehydrogenase (Chdh)* encodes an enzyme involved in choline metabolism. It has been demonstrated that high level of choline in mother diet has a protective role against nonsyndromic cleft lip with or without cleft palate at birth (Shaw et al., 2006), and that specific polymorphisms in genes involved in choline metabolisms can influence the risk of this malformation (Mostowska et al.). The zebrafish genome contains one ortholog of *Chdh*, *chdh*. This gene was found to be expressed in thyroid region at 48 hpf (**Figure 21**). Double in situ hybridization shows a colocalization between *chdh* positive cells and *tg* positive cells (**Figure 21B**).

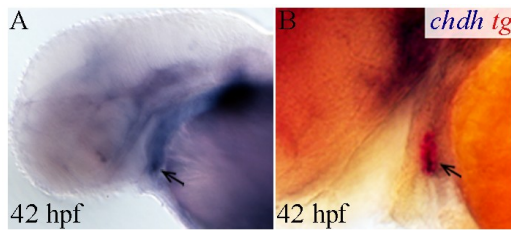


**Figure 21** Expression profile of *chdh*, zebrafish ortholog of murine *Chdh*, by in situ hybridization assay. Stage is indicated bottom left, staining/marker top left (when it is different from *chdh*). Lateral view with anterior to the left are shown. At 48 hpf *chdh* is expressed in thyroid region (arrow). In (B) is reported a double in situ hybridization for *chdh* (blue) and *tg* (red).

### Analysis of zebrafish *bcl2* and *bcl2l* expression patterns during morphogenesis

Experimental data, in both mouse and zebrafish, have demonstrated that in absence of the thyroid transcription factors, *Nkx2-1/nk2.1a*, *Hhex/hhex* or *Pax8/pax2a*, the thyroid primordium is specified but then disappears (Elsalini et al., 2003; Parlato et al., 2004). To date, no evidence is available about the fate of the thyroid cells deficient of their transcription factors; one possibility is that they undergo a degenerative process through an apoptotic program.

In support of this hypothesis, the antiapoptotic factor *Bcl2* was found 82 times overexpressed in thyroid tissue in the differential microarray analysis; the mouse E10 thyroid expression of this gene was also confirmed by *in vivo* experiments (unpublished data). Analyzing the zebrafish genome, only one ortholog of this gene was found, *bcl2*, whose expression pattern was investigated during zebrafish development. WMISH clearly shows that *bcl2* is expressed in otic vesicles, pectoral fin buds and pronephric ducts starting from 24 hpf but not in thyroid primordium in all the developmental stage studied. This expression pattern is maintained during later developmental stages (**Figure 22**).

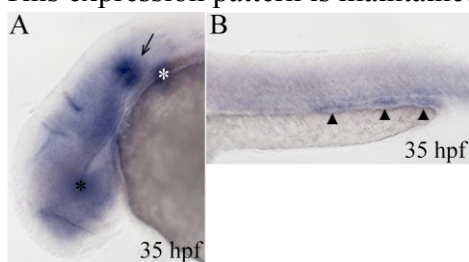


**Figure 22** *Bcl2* expression pattern in zebrafish embryo at 35 hpf, by *in situ* hybridization assay. Lateral views with anterior to the top are shown. In (A) arrow indicates otic vesicle, white asterisk pectoral fin bud, black asterisk lens. In (B) arrowheads indicates the pronephric ducts.

Considering the relevance that the presence of a survival mechanism could have in thyroid development, the expression pattern of *bcl2l*, another antiapoptotic factor of *Bcl2* family, paralog of zebrafish *bcl2* and ortholog of mouse *Bcl-XL*, was investigated in zebrafish embryos. This gene is expressed in thyroid primordium starting from 30 hpf (**Figure 23 A**) throughout embryonic development (**Figure 23D-E**). The expression in the developing thyroid was confirmed by a double WMISH showing colocalization of *bcl2l* positive cells with *tg* positive cells (**Figure 23H**). Besides thyroid expression, *bcl2l* is transcribed also in some areas of the central nervous system (hindbrain, telencephalon

and diencephalon), in lens and in yolk extension. At 96 hpf, no *bcl2l* expression was detected in thyroid follicles suggesting that this gene is dispensable during late thyroid development.

These data demonstrate the presence of an antiapoptotic function in thyroid that could be relevant for its development. This function is conserved during evolution: it is represented by Bcl2 in mouse thyroid (at date, there are no information about *Bcl-XL* expression in mouse thyroid) and by *bcl2l* in zebrafish. Furthermore, the presence of an antiapoptotic function in developing thyroid primordium suggests the idea that its role consists into suppress an hypothetical proapoptotic factor able to induce cell death against developmental defects. This idea is supported by the finding, exposed in the previous section, that the proapoptotic factor *bmf1* is transiently expressed in a region overlapping with thyroid primordium (Figure 20).

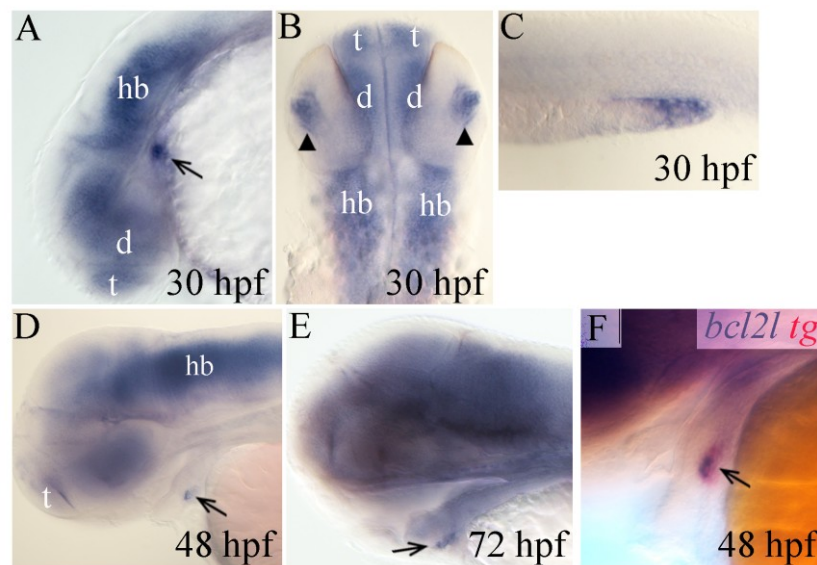
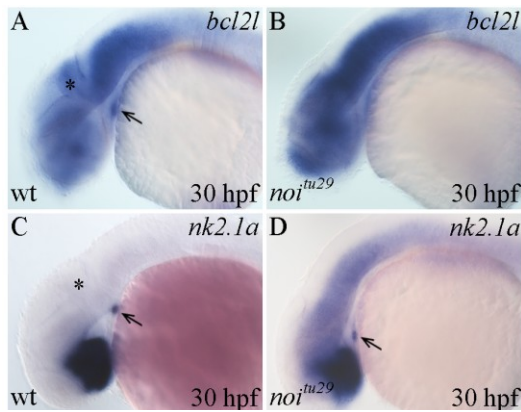


Figure 23 Bcl2l expression pattern in zebrafish embryo, by *in situ* hybridization assay. Lateral views with anterior to the left (A-C-D-E-F) and dorsal view with anterior to the top (B) are shown. Stages are indicated bottom left. (A-B-D-E) Bcl2l is expressed in thyroid (arrow), hindbrain, telencephalon, diencephalon and lens. (C) Expression in yolk extension. (F) Double in situ hybridization for *bcl2l* (blue) and *tg* (red). d, diencephalon; hb, hindbrain; t, telencephalon.

### ***The role of bcl2l on zebrafish thyroid development***

#### **Thyroid-specific transcription factors role on *bcl2l* expression**

*Bcl2l* starts to be expressed in zebrafish thyroid primordium few hours after the transcriptional activation of thyroid transcription factors expression. The role of these proteins on *bcl2l* thyroid regulation was investigated by means of mutant or morphants embryos (embryos in which the level of a specific protein is knocked-down using a gene-specific morpholino).



**Figure 24** Bcl2l expression in *pax2a* mutant embryos. Lateral views with anterior to the top are shown. Stage is indicated bottom left, genotype bottom right. (A-B) *bcl2l* expression in wild-type (A) and in *noi<sup>tu29</sup>* embryo (B). (C-D) *nk2.1a* expression in wild-type (C) and *noi<sup>tu29</sup>* embryo (D). Arrow indicates the thyroid primordium, asterisk the hindbrain-mindbrain boundary.

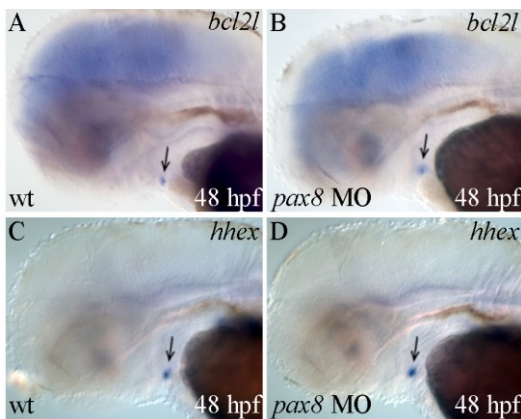


**Figure 25** Bcl2l expression in *pax8* morphant embryos. Lateral views with anterior to the top are shown. Stage is indicated bottom left, genotype bottom right. (A-B) *bcl2l* expression in wild-type (A) and in *pax8* morphant embryo (B). (C-D) *hhhex* expression in wild-type (C) and *pax8* morphant embryo (D). Arrow indicates the thyroid primordium.

To study the role of *pax2a* on *bcl2l* thyroid expression, zebrafish embryos lacking *pax2a* activity, the *noi<sup>tu29</sup>* mutants (Lun and Brand, 1998), were analysed (**Figure 24**). Homozygous mutant embryos have been identified according to characteristic morphological defects, in particular the hindbrain-mindbrain boundary absence (asterisk in **Figure 24**). It was found that *bcl2l* is not expressed in thyroid primordium in absence of *pax2a* (**Figure 24 B**), when the thyroid primordium is known to be still present, as it is confirmed by means of *nk2.1a* expression (**Figure 24 D**). *Bcl2l* expression in other tissue is not impaired in the mutant embryos.

The function of *pax8* on *bcl2l* thyroid expression was investigated injecting the embryos with a combination of two already published morpholinos, able to target all *pax8* splicing isoforms (Mackereth et al., 2005). 2,5 ng of each morpholinos were injected in one-cell stage embryos. The efficacy of morpholino injection was evaluated according to the morphological alteration induced and already described (Mackereth et al., 2005). In *pax8* morphant embryos, *bcl2l* thyroid expression at 48 hpf is comparable to the wild type, indicating that this factor is not involved in *bcl2l* thyroid regulation (**Figure 25 A-B**). To date no published information on *pax8* thyroid function in zebrafish are available; the thyroid phenotype was examined in these embryos checking the expression of thyroid transcription factors, but no anomalies were found (in **Figure 25 C-D** the result for *hhhex* is shown as example), suggesting that *pax8* is not involved in thyroid development in zebrafish.

Some findings obtained in different model systems, have already demonstrated a transcriptional relationship between the Pax family transcription factors and the Bcl2 antiapoptotic proteins: a) *in vitro* experiments, with a mouse kidney cell line, demonstrated that Pax8 can transcriptionally regulate Bcl-2 (Hewitt et al., 1997); b) *in vivo* studies in *C.elegans* demonstrated that the two *Pax2/5/8* genes act as transcriptional regulators of *ced-9*, the *C. elegans bcl-2* gene (Park et al., 2006); c) *in vitro* studies on human rhabdomyosarcoma cell lines have demonstrated that BCL-XL is transcriptionally modulated by PAX3 (Margue et al., 2000). The results exposed here demonstrate that this relationship is conserved also in zebrafish thyroid; the transcriptional regulation of *bcl2l* in zebrafish thyroid primordium, in which two Pax genes are expressed, *pax2a* and *pax8*, is under the control of *pax2a*.

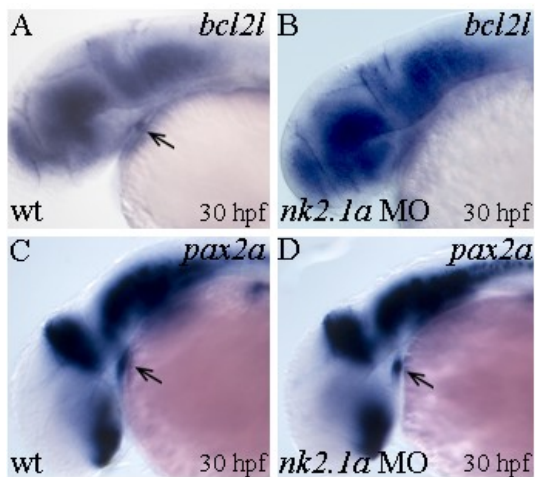


**Figure 26** Bcl2l expression in *nk2.1a* morphant embryos. Lateral views with anterior to the top are shown. Stage is indicated bottom left, genotype bottom right. (A-B) *bcl2l* expression in wild-type (A) and in *nk2.1a* morphant embryo (B). (C-D) *pax2a* expression in wild-type (C) and *nk2.1a* morphant embryo (D). Arrow indicates the thyroid primordium. The *nk2.1a*-MO was injected at a concentration of 2,5 ng per embryo.

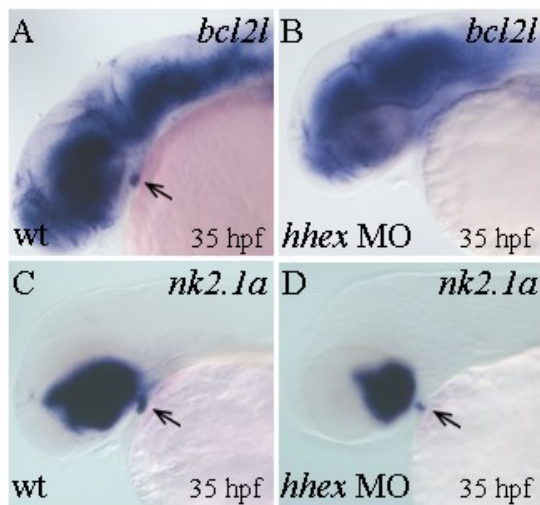


**Figure 27** Bcl2l expression in *hhex* morphant embryos. Lateral views with anterior to the top are shown. Stage is indicated bottom left, genotype bottom right. (A-B) *bcl2l* expression in wild-type (A) and in *hhex* morphant embryo (B). (C-D) *nk2.1a* expression in wild-type (C) and *hhex* morphant embryo (D). Arrow indicates the thyroid primordium. The *hhex*-MO was injected at a concentration of 1,4 ng per embryo

factors, are able to bind and regulate *bcl2l* promoter. A preliminary analysis of *bcl2l* promoter region using TRANSFAC database indicate the presence of binding sites for Pax2 and Nkx2-1 transcription factors: this information should be confirmed by *in vitro* or *in vivo* experiments.

The role of *nk2.1a* and *hhex* on *bcl2l* thyroid regulation was investigated by means of morpholino injection (Elsalini et al., 2003). Down-regulation of *nk2.1a*, obtained injecting 2,5 ng per embryo of the specific morpholino, leads to the loss of *bcl2l* expression in thyroid primordium (**Figure 26**) when this is still present (30 hpf), as it is demonstrated by the persistence of *pax2a* staining (**Figure 26 D**). The expression of *pax2a* in the morphant thyroid primordium allows to exclude also that the effect observed on *bcl2l* transcription is secondary to an effect on *pax2a* transcription.

As for *pax2a* and *nk2.1a*, when *hhex* is down-regulated, injecting 1,4 ng per embryo of the specific morpholino, the thyroid expression of *bcl2l* is lost (**Figure 27**); the staining for *nk2.1a*, at the same stage when *bcl2l* is no more expressed, demonstrates that the loss of *bcl2l* expression is not a consequence of the thyroid primordium disappearance (**Figure 27 D**).

To recapitulate, *bcl2l* is not expressed in thyroid of both *nkx2.1a* and *hhex* morphant embryos as well as of *noi<sup>tu29</sup>* mutants, at the stage when the thyroid primordium is known to be still present (Elsalini et al., 2003; Wendl et al., 2002). In these morphants/mutants, the thyroid primordium forms in its correct position but it subsequently degenerates and eventually disappears (Elsalini et al., 2003; Wendl et al., 2002). So, the obtained results suggest that: a) *bcl2l* transcription is regulated by *pax2a*, *hhex* and *nk2.1a*; c) each of these factors is necessary but not sufficient to ensure *bcl2l* thyroid expression and that c) the loss of the anti-apoptotic gene could have an important role in thyroid degeneration in the manipulated embryos.

The regulation of *bcl2l* by *pax2a*, *nk2.1a* and *hhex* could be direct, if regulatory elements for these transcription factors are present in *bcl2l* promoter, or indirect, if one or more proteins, regulated by thyroid transcription

## Bcl2l functional analysis

### Engineering of zebrafish knockdown embryos for bcl2l

In order to investigate the functional role of zebrafish *bcl2l* in thyroid development, a specific-*bcl2l* morpholino (Kratz et al., 2006), direct against the *bcl2l* ATG upstream sequence (**Figure 28 A**), was injected into one-cell stage embryos, to block mRNA translation, and the phenotype of these embryos was studied by analyzing the expression of thyroid-specific markers.

**Table 2 Optimization of injected amount of *bcl2l* MO.**

MO amount per embryo	Death rate at 48 hpf	
	<i>bcl2l</i> -MO	control-MO
1,5 ng	100%	25%
1 ng	90%	20%
0,83 ng	50%	22%
0,6 ng	30%	22%

Firstly, different concentrations of morpholino were injected into one-cell stage embryos with the aim to select a quantity capable of producing a specific phenotype. Injection of *bcl2l*-MO dramatically increases the mortality rate of zebrafish embryos compared to embryos injected with a control-MO (**Table 2**), as it is expected considering the anti-apoptotic function of *bcl2l*: 1,5 ng of MO leads to 100% death rate at 48 hpf; reducing the amount of injected MO the death rate also decreases. The following functional experiments were done injecting 0,83 ng of MO into one-cell stage embryos; using a lower amount of MO no morphological anomalies are visible. The embryos injected with 0,83 ng of MO show alterations at the level of the expression domains of *bcl2l*: almost all the injected embryos show alteration in the head region with widespread apoptosis in 40% embryos and hypoplastic central nervous system in 43%; another feature of these embryos is the absence of yolk extension occurring in 31% examined embryos (**Figure 28 B;E**). Almost all embryos do not survive after 96-120 hpf; considering that the injection efficiency is not absolute, probably the embryos-living up to 120 hpf are non injected ones.



**Figure 28 Effects of *bcl2l*-MO injection in zebrafish embryo.** (A) *bcl2l*-MO binding site sequence is shown in red, the start codon in green. (B) 30 hpf control-MO injected embryo. (C-D-E) 30 hpf *bcl2l*-MO injected embryos showing widespread head apoptosis (arrow in C), hypoplastic central nervous system (arrow in D) and absence of yolk extension (arrow in E). Genotype is indicated bottom right, percentage bottom left. The injected MO amount was 0,83 ng per embryo.

To confirm that the effect of *bcl2l*-MO injection is specific, rescue experiments were performed through co-injection of MO and corresponding *bcl2l* full-length mRNA at 1-cell stage. mRNA used for rescue should not have a MO-complementary sequence; otherwise, it may rescue the phenotype simply by titrating out the MO. To this purpose *bcl2l* cDNA, without 5'UTR containing the MO-complementary sequence, was cloned in pCS2+ vector

and the corresponding mRNA was produced by *in vitro* transcription. The injection of 200 pg per embryo of modified *bcl2l* mRNA was able to rescue the morphological features induced by *bcl2l* MO (**Figure 29**) and to revert embryo mortality rate to normal level almost completely. These data indicate that *bcl2l* mRNA can compensate for the function impaired by the MO injection and that, therefore, *bcl2l*-MO is able to induce specifically *bcl2l* down-regulation.

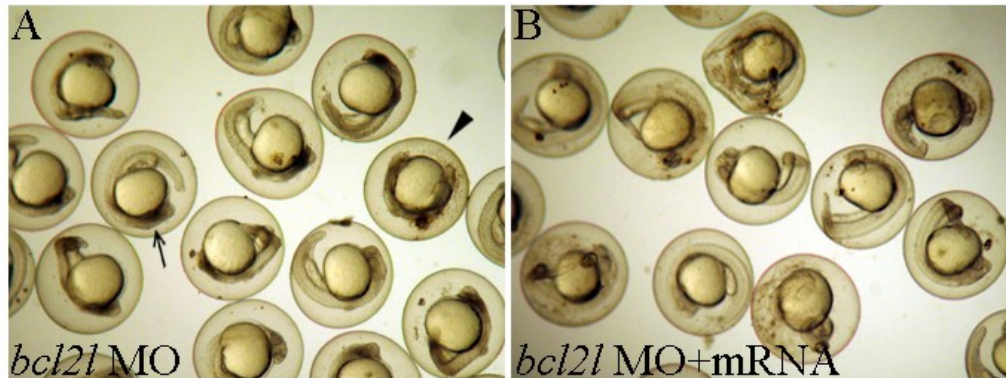


**Figure 29** Co-injection of *bcl2l* MO and *bcl2l* mRNA. The MO was injected at 0,83 ng per embryo and the mRNA at 200 pg per embryo. In (A) representative examples of *bcl2l*-MO injected embryos are shown: arrow indicates an embryos with widespread apoptosis in the head; arrowhead indicates a dead embryo. In (B) representative examples of *bcl2l*-MO and *bcl2l* mRNA co-injected embryos are shown: the widespread apoptosis is almost completely abrogated.

#### Thyroid phenotype analysis of *bcl2l* knocked-down embryos

Embryos injected with *bcl2l*-MO alone or in combination with *bcl2l* mRNA were fixed at around 48 hpf and thyroid phenotype was investigated checking for expression of thyroid transcription factors (**Figure 30**). Embryos injected with 0,83 ng of control-MO were used as control. Thyroid primordium disappears or it is smaller in a high rate of morphant embryos compared to control MO-injected embryos, as it is demonstrated by the absent or reducing staining for all the thyroid markers analyzed. Looking at *pax2a* staining, it is evident that in 29% of morphant embryos thyroid primordium appears smaller than normal (**Figure 30 B**) and it is completely absent in 28% of embryos (**Figure 30 C**), for a total of 57% of *bcl2l* morphant embryos showing thyroid alteration. Similar results are obtained analyzing the embryos for the other thyroid markers.

The thyroid phenotype observed is specifically due to *bcl2l* down-regulation and this is demonstrated by the finding that it is almost completely rescued by *bcl2l* mRNA co-injection: this means that the thyroid *bcl2l* function, lost by means of MO injection, is regained by mRNA injection. Indeed, the majority of rescued embryos shows normal size thyroid primordium (**Figure 30**): in the case of *pax2a* the embryos percentage showing thyroid alteration is decreased to 28%. Statistics of this experiment is shown in **Table 3**.

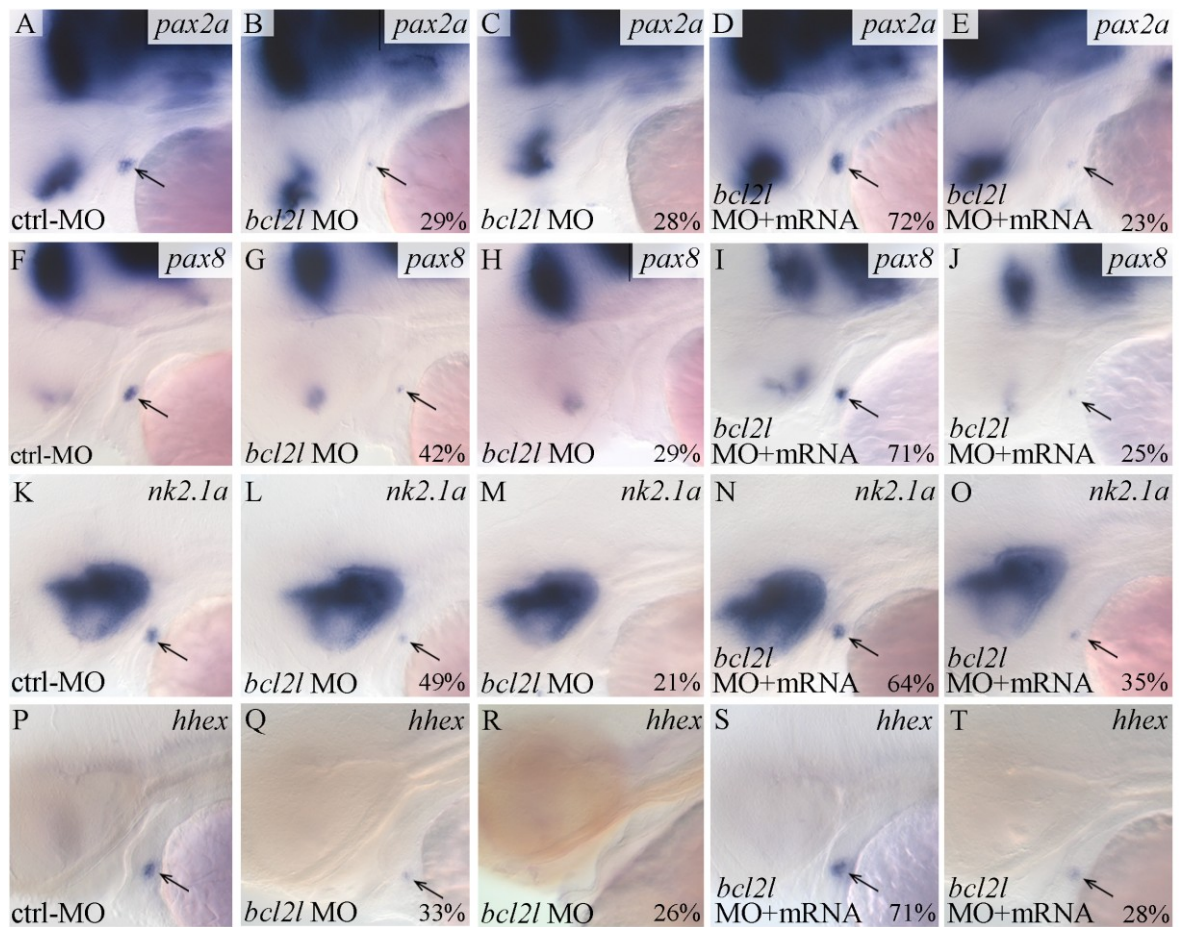


**Figure 30** Thyroid phenotype of *bcl2l* morphant embryos. Lateral views with anterior to the top of 48 hpf embryos are shown. Genotype is indicated bottom left, percentage (indicating the incidence of the described phenotype) bottom right and staining/marker top right. Arrows point to thyroid primordium. The MO was injected at 0,83 ng per embryo and the mRNA at 200 pg per embryo. (A;E) *pax2a* expression in control-MO (A), in *bcl2l*-MO (B-C) injected embryos and in *bcl2l*-MO and *bcl2l*-mRNA co-injected embryos (D-E); (F;J) *pax8* expression in control-MO (F), in *bcl2l*-MO (G-H) injected embryos and in *bcl2l*-MO and *bcl2l*-mRNA co-injected embryos (I-J); (K;O) *nk2.1a* expression in control-MO (K), in *bcl2l*-MO (L-M) injected embryos and in *bcl2l*-MO and *bcl2l*-mRNA co-injected embryos (N-O); (P;T) *hhx* expression in control-MO (P), in *bcl2l*-MO (Q-R) injected embryos and in *bcl2l*-MO and *bcl2l*-mRNA co-injected embryos (S-T).

Considering the morphological alteration induced by *bcl2l*-MO injection in the head region of zebrafish embryos, to verify whether the thyroid phenotype is consequence of a general reduction of foregut endoderm or is a more “specific” and restricted phenotype, the expression of *foxa3*, a ubiquitous marker of endoderm, was checked in *bcl2l* morphants (**Figure 31**). No significant alterations in foregut endoderm were observed in the manipulated embryos, demonstrating the specificity of the thyroid phenotype.

These results indicate that *bcl2l* is indispensable for proper thyroid development and that its missing expression in the morphant embryos for thyroid transcription factors may contribute to the disappearance of the thyroid primordium; the higher incidence of thyroid loss observed in the embryos lacking *nk2.1a* or *hhx* or *pax2a* (Elsalini et al., 2003) compared to that observed in this experiment is explainable with the hypothesis that other proteins regulated by thyroid transcription factors could cooperate with *bcl2l* to ensure the

correct thyroid development. In support of this hypothesis *bcl2l* mRNA was found not able to rescue the thyroid phenotype, when it was injected in combination with *nk2.1a* or *hhex* MO, suggesting that other factors relevant for thyroid development are absent in the morphant embryos. It is important also to keep in mind that *bcl2*-MO injection causes high rate of embryo lethality and so the percentage of embryos showing the thyroid phenotype could be higher than that measured.

The role of *Bcl2* during mouse thyroid development has not been investigated. Studies on knock-out mice for *Bcl2* have been reported from different groups (Kamada et al., 1995; Nakayama et al., 1994; Veis et al., 1993) showing growth retardation, polycystic kidney disease, lymphocytopenia and hypopigmented hair, but no one has reported analysis of thyroid development. From studies on *Pax8* knock-out mice it is known that the absence of thyroid leads to death within three weeks after birth (Friedrichsen et al., 2003; Mansouri et al., 1998). Mice lacking *Bcl2* activity are smaller than the control littermate and a high percentage of them dies in 2-3 weeks (Kamada et al., 1995; Nakayama et al., 1994; Veis et al., 1993), suggesting that thyroid development could be impaired in these mice. The living animals at 3 week survive also longer than 10 weeks. This phenotype is coherent with the heterogeneous thyroid phenotype observed in zebrafish morphant embryos for *bcl2l*.

**Table 3 Statistics of *bcl2l*-MO phenotype**

Genotype/Phenotype	Embryos with normal thyroid signal	Embryos with smaller thyroid signal	Embryos with no thyroid signal	TOT
<b><i>pax2a</i></b>				
<i>bcl2l</i> MO	56 (43%)	38 (29,2%)	36 (27,7%)	130
<i>bcl2l</i> MO + mRNA	76 (72,4%)	24 (22,9%)	5 (4,8%)	105
control MO	100 (80%)	22 (17,6%)	3 (2,4)	125
<b><i>pax8</i></b>				
<i>bcl2l</i> MO	46 (28,9%)	67 (42,1%)	46 (28,9%)	159
<i>bcl2l</i> MO + mRNA	77 (70,6%)	27 (24,8%)	5 (4,6%)	109
control MO	100 (82,6%)	21 (17,4%)	0	121
<b><i>nk2.1a</i></b>				
<i>bcl2l</i> MO	22 (30,5%)	35 (48,6%)	15 (20,8%)	72
<i>bcl2l</i> MO + mRNA	64 (64%)	35 (35%)	1 (1%)	100
control MO	42 (60%)	24 (34,3%)	4 (5,7)	70
<b><i>Hhex</i></b>				
<i>bcl2l</i> MO	34 (41%)	27 (32,9%)	21 (25,6%)	82
<i>bcl2l</i> MO + mRNA	56 (71%)	22 (27,8%)	1 (1,2%)	79
control MO	85 (90,4%)	9 (9%)	0	94

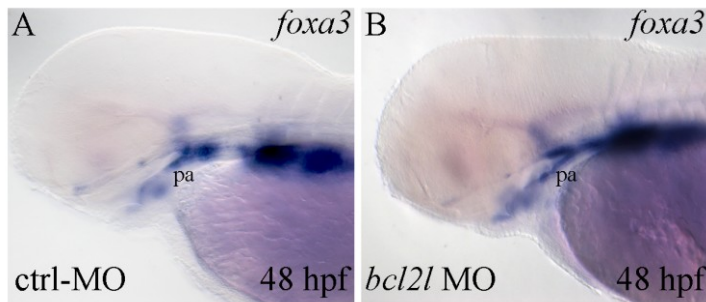


**Figure 31** Foregut endoderm of *bcl2l* morphant embryos. Lateral views with anterior to the top of 48 hpf embryos stained for the endodermal marker *foxa3* are shown. Genotype is indicated bottom left and staining/marker top right. Pa, pharyngeal endoderm.

### Analysis of apoptosis during thyroid degeneration in manipulated embryos

*Bcl2l* is positively regulated by the thyroid transcription factors *hhex*, *nk2.1a* and *pax2a*; down-regulation of these factors leads to loss of *bcl2l* thyroid expression and then to thyroid disappearance. Considering the anti-apoptotic function of *bcl2l*, it could be supposed that thyroid degenerates, in manipulated embryos, by means of apoptotic processes.

To test this hypothesis the activation of caspase-3, an effector caspase that plays a crucial role in the apoptotic cascade, was analyzed in embryos injected with 2,5 ng of *nk2.1a*-MO or with 1,4 ng of *hhex*-MO using a specific antibody for active-caspase-3, by means of WMIHC. The morphant embryos were analyzed at three different developmental stage, 45, 50 and 60 hpf, considering that the thyroid primordium disappears between 48 and 60 hpf. The apoptosis level, measured as caspase-3 activation, was found to be increased in thyroid region of knocked-down embryos compared to embryos injected with 2,5 ng of control-MO (**Table 4**); in particular, the higher number of embryos showing positive active-caspase-3 cells in thyroid region is observed at 50 hpf.

**Table 4** Apoptosis incidence in the region of thyroid primordium in *hhex* and *nk2.1a* morphant embryos

developmental stage / genotype	<i>hhex</i> -MO	<i>nk2.1a</i> -MO	ctrl-MO
45 hpf	25,7% (9/35)	25,8% (8/31)	11,8% (4/34)
50 hpf	49% (25/51)	51,8% (14/27)	5% (1/20)
60 hpf	45,2% (19/42)	27,3% (9/33)	6,9% (2/29)

To verify if the observed apoptotic cells were localized in thyroid primordium, morphant embryos for *nk2.1a*-MO were co-stained for *hhex* via ISH and active-caspase-3 via IHC. Active-caspase-3 positive cells were found in correspondence of *hhex* positive cells in 21 embryos of 129 analyzed (16%) (**Figure 32 B**); in the control-MO injected embryos no active-caspase-3 positive cells were found overlapping with thyroid cells (**Figure 32 A**). The occurrence of active-caspase-3 positive cells in the region of thyroid primordium is indicative that the apoptotic process takes an active role in thyroid degeneration in absence of *nk2.1a* transcription factor.

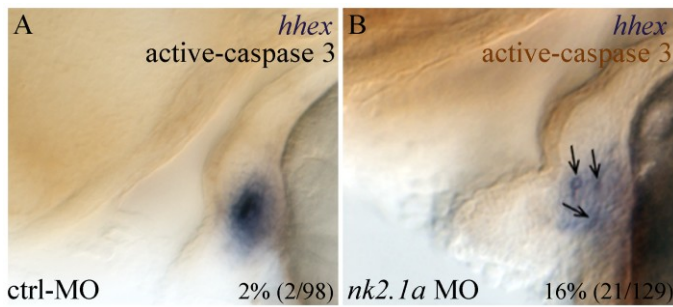


**Figure 32** Detection of apoptotic cells in *nk2.1a* morphant embryos. Lateral views with anterior to the top of 50 hpf embryos are shown. Genotype is indicated bottom left, percentage (indicating the incidence of apoptotic cells overlapping with thyroid cells) bottom right and staining/markers top right. Thyroid cells are stained with *hhx*-probe via ISH and apoptotic cells are stained with active-caspase-3-antibody via IHC. Arrow points to active-caspase-3 positive cells in thyroid primordium.

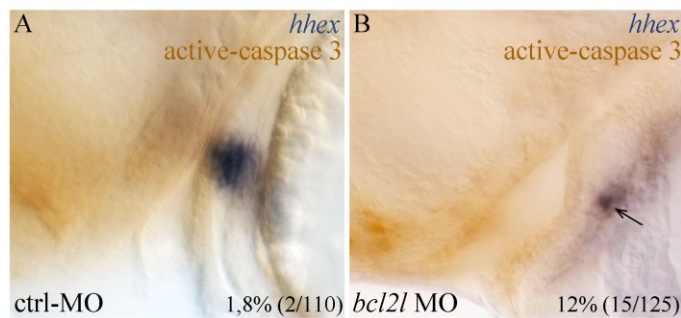


**Figure 33** Detection of apoptotic cells in *bcl2l* morphant embryos. Lateral views with anterior to the top of 42 hpf embryos are shown. Genotype is indicated bottom left, percentage (indicating the incidence of apoptotic cells overlapping with thyroid cells) bottom right and staining/markers top right. Thyroid cells are stained with *hhx*-probe via ISH and apoptotic cells are stained with active-caspase-3-antibody via IHC. Arrow points to active-caspase-3 positive cells in thyroid primordium.

the classical caspase-mediated apoptosis. Indeed, it has been documented by *in vitro* and *in vivo* experiment that programmed cell death can occur also in absence of caspase activation and that this mechanism, called caspase-independent cell death, is really diffuse (Constantinou et al., 2009). The stimuli inducing caspase-independent cell death are not necessarily different from those inducing caspase-dependent cell death and the two pathways may be activated simultaneously. Furthermore, many events that take place in caspase-dependent cell death are also involved in caspase-independent cell death; this is the case of Bcl2 that is able to prevent also the caspase-independent cell death (Okuno et al., 1998). The possibility that, in our experimental model, thyroid degeneration occurs via both cell death mechanisms and that *bcl2l* is involved in regulating both mechanism remains still open. Furthermore, simultaneously persistence of both mechanisms could explain why the incidence of active-caspase-3-positive cells observed in thyroid primordium is lower than the incidence of thyroid disappearance in morphant embryos. Another still open question is whether *bcl2l* is able to impact on thyroid development using a mechanism different from apoptosis. Indeed, in a variety of experimental models it has been demonstrated that antiapoptotic Bcl2 family genes have a role in regulating processes

The same experiment was performed on *bcl2l* morphant embryos; active-caspase-3-positive cells overlapping with *hhx*-positive cells were observed in 15 of 125 (12%) morphant embryos (**Figure 33 B**) compared to 2 of 110 of control-MO injected embryos (**Figure 33 A**). The presence of active-caspase-3 signal in thyroid primordium of *bcl2l* morphant embryos suggests that this factor performs its antiapoptotic function during thyroid development.

The finding that active-caspase-3 positive cells are increased in number in thyroid region of embryos lacking *nk2.1a* or *hhx* and/or the antiapoptotic factor *bcl2l* is the first direct index that caspase-dependent apoptosis plays a role in thyroid degeneration in the embryos deprived of thyroid transcription factors and that apoptotic processes are prevented during normal thyroid development by the antiapoptotic factor *bcl2l*.

These result do not permit to exclude the possibility that *bcl2l* functions during thyroid development also by mechanisms other than the only prevention of

beyond their function as antiapoptotic molecules: mouse Bcl2 promotes differentiation and activity beyond that survival of both osteoblasts and osteoclasts (Nagase et al., 2009); it is involved in determining chondrocytes phenotype, probably by regulating SOX9, a transcription factor necessary for expressing the major cartilage matrix proteins (Kinkel and Horton, 2003); Bcl2 plays also a role in regulating axonal growth rate and regeneration in mouse embryonic neurons (Chen et al., 1997; Hilton et al., 1997); the zebrafish *bcl-2* homologue *nrz* contributes to cell movements during gastrulation by negatively regulating the expression of Snail-1, a transcription factor that controls cell adhesion (Arnaud et al., 2006). Our data indicate that *bcl2l* down-regulation causes impairment in thyroid development but do not permit to exclude that this could happen also via a mechanism independent from the apoptotic one.

## 5. Conclusions

The experimental work presented in this thesis has led to the acquisition of new information on thyroid evolution and development.

Conservation of the known mechanisms underlying thyroid development and function in mouse and zebrafish prompted to perform a comparative analysis in zebrafish of new data on mouse thyroid bud transcriptome. The low correspondence in thyroid expression profile observed in the two experimental models strongly suggests that molecular changes in thyroid morphogenesis occurred during the transition from lower to higher vertebrates, but after that the biochemistry of thyroid function was conquered in evolution. In particular, the high number of genes expressed in mouse thyroid bud and not found in zebrafish thyroid bud could represent newly acquired functions by the thyroid tissue during the vertebrates lineage. Hence, from an evolutionary point of view, the scattered thyroid follicles in zebrafish could be considered, morphologically and molecularly, one step in the progressive rearrangement of the pharyngeal area that, starting from the invertebrate endostyle precursor has conducted to the mammalian gland.

Even if molecular changes have modified the capacity of thyroid cells to shape the mammalian gland, the key molecular factors relevant for thyroid cells identity and maintenance are clearly conserved. This is the case of the thyroid transcription factors and of the new function identified in thyroid in both mouse and zebrafish. The work presented here demonstrates that an antiapoptotic function present in mouse thyroid primordium was already present in fish, suggesting its essential role for thyroid development independently from the molecular divergence occurred during thyroid evolution. In zebrafish, *bcl2l* is expressed in thyroid bud since early steps of development; its thyroid transcription is finely regulated by the transcription factors *nk2.1a*, *pax2a* and *hhex*, each one necessary but not sufficient to achieve normal *bcl2l* thyroid expression. This tight synergic regulation is index that *bcl2l* transcription is essential for thyroid development; in fact, down-regulation of *bcl2l* leads to severe impairments in normal thyroid development probably due to the loss of its antiapoptotic function. Considering that an antiapoptotic factor of Bcl2 gene family is expressed also in mouse thyroid bud, it is likely that also in human, thyroid development requires this function and that its impairment leads to congenital hypothyroidism.

## 6. Acknowledgements

At the end of this PhD experience I can assert that it was a significant period for my personal and scientific growth. Many people and many events have contributed to make this experience really formative. Therefore, I would like to acknowledge all the persons that, in different ways, helped me during this pleasant, important but also hard period of my life.

Starting from the beginning, I would like to acknowledge Prof. Roberto Di Lauro who believed in me and gave me the opportunity to perform the PhD program under his supervision. Then, I have to thank Dr. Paolo Sordino who hosted me in his laboratory at the Stazione Zoologica Anton Dohrn and supported me with scientific and human advises, daily, over the last three years. I would also like to acknowledge Henrik Fagman who carried out the mouse work and contributed to my work with helpful comments and suggestions. Many thanks to all people working at the Stazione and in particular to all members of Cellular and Developmental Biology Department. Many thanks to my past and present lab colleagues, Nada Langellotto, Antonio Emidio Fortunato, Ornella Affinito, Bruna Facello and Francesco Toscano, for their friendship and moral support. Special thanks to Elena De Felice for her contribution to this work and, above all, for her affection.

I have also to thank my housemate friends in Napoli, Emanuela, Roberta and Annarita for their friendship, support and cheerful evenings during the last years. Special thanks to my family; every progress in my personal life and in my work is especially due to their support and encouragement. In the end, I thank my boyfriend Michele for giving me serenity and joy also in the most stressful moments of these three years.

## 7. References

- Abe, M., Tamamura, Y., Yamagishi, H., Maeda, T., Kato, J., Tabata, M. J., Srivastava, D., Wakisaka, S. and Kurisu, K. (2002). Tooth-type specific expression of dHAND/Hand2: possible involvement in murine lower incisor morphogenesis. *Cell Tissue Res* **310**, 201-12.
- Abramowicz, M. J., Targovnik, H. M., Varela, V., Cochaux, P., Krawiec, L., Pisarev, M. A., Propato, F. V., Juvenal, G., Chester, H. A. and Vassart, G. (1992). Identification of a mutation in the coding sequence of the human thyroid peroxidase gene causing congenital goiter. *J Clin Invest* **90**, 1200-4.
- Alberti, L., Proverbio, M. C., Costagliola, S., Romoli, R., Boldrighini, B., Vigone, M. C., Weber, G., Chiumello, G., Beck-Peccoz, P. and Persani, L. (2002). Germline mutations of TSH receptor gene as cause of nonautoimmune subclinical hypothyroidism. *J Clin Endocrinol Metab* **87**, 2549-55.
- Alt, B., Elsalini, O. A., Schrupf, P., Haufs, N., Lawson, N. D., Schwabe, G. C., Mundlos, S., Gruters, A., Krude, H. and Rohr, K. B. (2006a). Arteries define the position of the thyroid gland during its developmental localisation. *Development* **133**, 3797-804.
- Alt, B., Reibe, S., Feitosa, N. M., Elsalini, O. A., Wendl, T. and Rohr, K. B. (2006b). Analysis of origin and growth of the thyroid gland in zebrafish. *Dev Dyn* **235**, 1872-83.
- Amendola, E., De Luca, P., Macchia, P. E., Terracciano, D., Rosica, A., Chiappetta, G., Kimura, S., Mansouri, A., Affuso, A., Arra, C. et al. (2005). A mouse model demonstrates a multigenic origin of congenital hypothyroidism. *Endocrinology* **146**, 5038-47.
- Arnaud, E., Ferri, K. F., Thibaut, J., Haftek-Terreau, Z., Aouacheria, A., Le Guellec, D., Lorca, T. and Gillet, G. (2006). The zebrafish bcl-2 homologue Nr2 controls development during somitogenesis and gastrulation via apoptosis-dependent and -independent mechanisms. *Cell Death Differ* **13**, 1128-37.
- Bamforth, J. S., Hughes, I. A., Lazarus, J. H., Weaver, C. M. and Harper, P. S. (1989). Congenital hypothyroidism, spiky hair, and cleft palate. *J Med Genet* **26**, 49-51.
- Bedford, F. K., Ashworth, A., Enver, T. and Wiedemann, L. M. (1993). HEX: a novel homeobox gene expressed during haematopoiesis and conserved between mouse and human. *Nucleic Acids Res* **21**, 1245-9.
- Bernal, J. (2007). Thyroid hormone receptors in brain development and function. *Nat Clin Pract Endocrinol Metab* **3**, 249-59.
- Bernasconi, M., Remppis, A., Fredericks, W. J., Rauscher, F. J., 3rd and Schafer, B. W. (1996). Induction of apoptosis in rhabdomyosarcoma cells through down-regulation of PAX proteins. *Proc Natl Acad Sci U S A* **93**, 13164-9.
- Bogue, C. W., Ganea, G. R., Sturm, E., Ianucci, R. and Jacobs, H. C. (2000). Hex expression suggests a role in the development and function of organs derived from foregut endoderm. *Dev Dyn* **219**, 84-9.
- Brickman, J. M., Jones, C. M., Clements, M., Smith, J. C. and Beddington, R. S. (2000). Hex is a transcriptional repressor that contributes to anterior identity and suppresses Spemann organiser function. *Development* **127**, 2303-15.
- Canfield, A. E., Hadfield, K. D., Rock, C. F., Wylie, E. C. and Wilkinson, F. L. (2007). HtrA1: a novel regulator of physiological and pathological matrix mineralization? *Biochem Soc Trans* **35**, 669-71.
- Cangul, H., Morgan, N. V., Forman, J. R., Saglam, H., Aycan, Z., Yakut, T., Gulten, T., Tarim, O., Bober, E., Cesur, Y. et al. Novel TSHR mutations in consanguineous families with congenital non-goitrous hypothyroidism. *Clin Endocrinol (Oxf)*.
- Carre, A., Szinnai, G., Castanet, M., Sura-Trueba, S., Tron, E., Broutin-L'Hermite, I., Barat, P., Goizet, C., Lacombe, D., Moutard, M. L. et al. (2009). Five new TTF1/NKX2.1 mutations in brain-lung-thyroid syndrome: rescue by PAX8 synergism in one case. *Hum Mol Genet* **18**, 2266-76.

**Castanet, M., Park, S. M., Smith, A., Bost, M., Leger, J., Lyonnet, S., Pelet, A., Czernichow, P., Chatterjee, K. and Polak, M.** (2002). A novel loss-of-function mutation in TTF-2 is associated with congenital hypothyroidism, thyroid agenesis and cleft palate. *Hum Mol Genet* **11**, 2051-9.

**Castanet, M., Polak, M., Bonaiti-Pellie, C., Lyonnet, S., Czernichow, P. and Leger, J.** (2001). Nineteen years of national screening for congenital hypothyroidism: familial cases with thyroid dysgenesis suggest the involvement of genetic factors. *J Clin Endocrinol Metab* **86**, 2009-14.

**Chen, D. F., Schneider, G. E., Martinou, J. C. and Tonegawa, S.** (1997). Bcl-2 promotes regeneration of severed axons in mammalian CNS. *Nature* **385**, 434-9.

**Chen, Y., Dabovic, B., Colarossi, C., Santori, F. R., Lilic, M., Vukmanovic, S. and Rifkin, D. B.** (2003). Growth retardation as well as spleen and thymus involution in latent TGF-beta binding protein (Ltbp)-3 null mice. *J Cell Physiol* **196**, 319-25.

**Civitareale, D., Castelli, M. P., Falasca, P. and Saiardi, A.** (1993). Thyroid transcription factor 1 activates the promoter of the thyrotropin receptor gene. *Mol Endocrinol* **7**, 1589-95.

**Clifton-Bligh, R. J., Wentworth, J. M., Heinz, P., Crisp, M. S., John, R., Lazarus, J. H., Ludgate, M. and Chatterjee, V. K.** (1998). Mutation of the gene encoding human TTF-2 associated with thyroid agenesis, cleft palate and choanal atresia. *Nat Genet* **19**, 399-401.

**Congdon, T., Nguyen, L. Q., Nogueira, C. R., Habiby, R. L., Medeiros-Neto, G. and Kopp, P.** (2001). A novel mutation (Q40P) in PAX8 associated with congenital hypothyroidism and thyroid hypoplasia: evidence for phenotypic variability in mother and child. *J Clin Endocrinol Metab* **86**, 3962-7.

**Constantinou, C., Papas, K. A. and Constantinou, A. I.** (2009). Caspase-independent pathways of programmed cell death: the unraveling of new targets of cancer therapy? *Curr Cancer Drug Targets* **9**, 717-28.

**Cordier, A. C. and Haumont, S. M.** (1980). Development of thymus, parathyroids, and ultimobranchial bodies in NMRI and nude mice. *Am J Anat* **157**, 227-63.

**Crompton, M. R., Bartlett, T. J., MacGregor, A. D., Manfioletti, G., Buratti, E., Giancotti, V. and Goodwin, G. H.** (1992). Identification of a novel vertebrate homeobox gene expressed in haematopoietic cells. *Nucleic Acids Res* **20**, 5661-7.

**D'Andrea, B., Iacone, R., Di Palma, T., Nitsch, R., Baratta, M. G., Nitsch, L., Di Lauro, R. and Zannini, M.** (2006). Functional inactivation of the transcription factor Pax8 through oligomerization chain reaction. *Mol Endocrinol* **20**, 1810-24.

**Damante, G. and Di Lauro, R.** (1994). Thyroid-specific gene expression. *Biochim Biophys Acta* **1218**, 255-66.

**Damante, G., Tell, G. and Di Lauro, R.** (2001). A unique combination of transcription factors controls differentiation of thyroid cells. *Prog Nucleic Acid Res Mol Biol* **66**, 307-56.

**Dathan, N., Parlato, R., Rosica, A., De Felice, M. and Di Lauro, R.** (2002). Distribution of the *tif2/foxe1* gene product is consistent with an important role in the development of foregut endoderm, palate, and hair. *Dev Dyn* **224**, 450-6.

**David, N. B. and Rosa, F. M.** (2001). Cell autonomous commitment to an endodermal fate and behaviour by activation of Nodal signalling. *Development* **128**, 3937-47.

**Davies, T. F., Ando, T., Lin, R. Y., Tomer, Y. and Latif, R.** (2005). Thyrotropin receptor-associated diseases: from adenomata to Graves disease. *J Clin Invest* **115**, 1972-83.

**De Felice, M., Damante, G., Zannini, M., Francis-Lang, H. and Di Lauro, R.** (1995). Redundant domains contribute to the transcriptional activity of the thyroid transcription factor 1. *J Biol Chem* **270**, 26649-56.

**De Felice, M. and Di Lauro, R.** (2004). Thyroid development and its disorders: genetics and molecular mechanisms. *Endocr Rev* **25**, 722-46.

- De Felice, M., Ovitt, C., Biffali, E., Rodriguez-Mallon, A., Arra, C., Anastassiadis, K., Macchia, P. E., Mattei, M. G., Mariano, A., Scholer, H. et al.** (1998). A mouse model for hereditary thyroid dysgenesis and cleft palate. *Nat Genet* **19**, 395-8.
- de Sanctis, L., Corrias, A., Romagnolo, D., Di Palma, T., Biava, A., Borgarello, G., Gianino, P., Silvestro, L., Zannini, M. and Dianzani, I.** (2004). Familial PAX8 small deletion (c.989\_992delACCC) associated with extreme phenotype variability. *J Clin Endocrinol Metab* **89**, 5669-74.
- Dentice, M., Cordeddu, V., Rosica, A., Ferrara, A. M., Santarpia, L., Salvatore, D., Chiovato, L., Perri, A., Moschini, L., Fazzini, C. et al.** (2006). Missense mutation in the transcription factor NKX2-5: a novel molecular event in the pathogenesis of thyroid dysgenesis. *J Clin Endocrinol Metab* **91**, 1428-33.
- Di Palma, T., Nitsch, R., Mascia, A., Nitsch, L., Di Lauro, R. and Zannini, M.** (2003). The paired domain-containing factor Pax8 and the homeodomain-containing factor TTF-1 directly interact and synergistically activate transcription. *J Biol Chem* **278**, 3395-402.
- Dow, C. J., Dumont, J. E. and Ketelbant, P.** (1986). [Percentage of epithelial cells, fibroblasts and endothelial cells in the dog thyroid]. *C R Seances Soc Biol Fil* **180**, 629-32.
- Doyle, D. A., Gonzalez, I., Thomas, B. and Scavina, M.** (2004). Autosomal dominant transmission of congenital hypothyroidism, neonatal respiratory distress, and ataxia caused by a mutation of NKX2-1. *J Pediatr* **145**, 190-3.
- Elsalini, O. A., von Gartzten, J., Cramer, M. and Rohr, K. B.** (2003). Zebrafish *hhex*, *nk2.1a*, and *pax2.1* regulate thyroid growth and differentiation downstream of Nodal-dependent transcription factors. *Dev Biol* **263**, 67-80.
- Endo, T., Kaneshige, M., Nakazato, M., Ohmori, M., Harii, N. and Onaya, T.** (1997). Thyroid transcription factor-1 activates the promoter activity of rat thyroid Na<sup>+</sup>/I<sup>-</sup> symporter gene. *Mol Endocrinol* **11**, 1747-55.
- Everett, L. A., Glaser, B., Beck, J. C., Idol, J. R., Buchs, A., Heyman, M., Adawi, F., Hazani, E., Nassir, E., Baxevanis, A. D. et al.** (1997). Pendred syndrome is caused by mutations in a putative sulphate transporter gene (PDS). *Nat Genet* **17**, 411-22.
- Fagman, H., Andersson, L. and Nilsson, M.** (2006). The developing mouse thyroid: embryonic vessel contacts and parenchymal growth pattern during specification, budding, migration, and lobulation. *Dev Dyn* **235**, 444-55.
- Fagman, H., Grande, M., Edsbacke, J., Semb, H. and Nilsson, M.** (2003). Expression of classical cadherins in thyroid development: maintenance of an epithelial phenotype throughout organogenesis. *Endocrinology* **144**, 3618-24.
- Fagman, H., Grande, M., Gritli-Linde, A. and Nilsson, M.** (2004). Genetic deletion of sonic hedgehog causes hemiagenesis and ectopic development of the thyroid in mouse. *Am J Pathol* **164**, 1865-72.
- Fagman, H., Liao, J., Westerlund, J., Andersson, L., Morrow, B. E. and Nilsson, M.** (2007). The 22q11 deletion syndrome candidate gene *Tbx1* determines thyroid size and positioning. *Hum Mol Genet* **16**, 276-85.
- Fagman, H. and Nilsson, M.** Morphogenesis of the thyroid gland. *Mol Cell Endocrinol* **323**, 35-54.
- Filion, G. J., Zhenilo, S., Salozhin, S., Yamada, D., Prokhortchouk, E. and Defossez, P. A.** (2006). A family of human zinc finger proteins that bind methylated DNA and repress transcription. *Mol Cell Biol* **26**, 169-81.
- Friedl, P. and Gilmour, D.** (2009). Collective cell migration in morphogenesis, regeneration and cancer. *Nat Rev Mol Cell Biol* **10**, 445-57.
- Friedrichsen, S., Christ, S., Heuer, H., Schafer, M. K., Mansouri, A., Bauer, K. and Visser, T. J.** (2003). Regulation of iodothyronine deiodinases in the Pax8<sup>-/-</sup> mouse model of congenital hypothyroidism. *Endocrinology* **144**, 777-84.
- Gorbman, A. and Bern, H.** (1962). Textbook of comparative endocrinology. New York: Wiley.

- Grant, D. B., Smith, I., Fuggle, P. W., Tokar, S. and Chapple, J.** (1992). Congenital hypothyroidism detected by neonatal screening: relationship between biochemical severity and early clinical features. *Arch Dis Child* **67**, 87-90.
- Grasberger, H., Ringkanant, U., Lefrancois, P., Abramowicz, M., Vassart, G. and Refetoff, S.** (2005). Thyroid transcription factor 1 rescues PAX8/p300 synergism impaired by a natural PAX8 paired domain mutation with dominant negative activity. *Mol Endocrinol* **19**, 1779-91.
- Guazzi, S., Price, M., De Felice, M., Damante, G., Mattei, M. G. and Di Lauro, R.** (1990). Thyroid nuclear factor 1 (TTF-1) contains a homeodomain and displays a novel DNA binding specificity. *Embo J* **9**, 3631-9.
- Hewitt, S. M., Hamada, S., Monarres, A., Kottical, L. V., Saunders, G. F. and McDonnell, T. J.** (1997). Transcriptional activation of the bcl-2 apoptosis suppressor gene by the paired box transcription factor PAX8. *Anticancer Res* **17**, 3211-5.
- Hilton, M., Middleton, G. and Davies, A. M.** (1997). Bcl-2 influences axonal growth rate in embryonic sensory neurons. *Curr Biol* **7**, 798-800.
- Ho, C. Y., Houart, C., Wilson, S. W. and Stainier, D. Y.** (1999). A role for the extraembryonic yolk syncytial layer in patterning the zebrafish embryo suggested by properties of the hex gene. *Curr Biol* **9**, 1131-4.
- Hubner, A., Cavanagh-Kyros, J., Rincon, M., Flavell, R. A. and Davis, R. J.** Functional cooperation of the proapoptotic Bcl2 family proteins Bmf and Bim in vivo. *Mol Cell Biol* **30**, 98-105.
- Jezirowska, A., Pniewska-Siark, B., Brzezianska, E., Pastuszek-Lewandoska, D. and Lewinski, A.** (2006). A novel mutation in the thyrotropin (thyroid-stimulating hormone) receptor gene in a case of congenital hypothyroidism. *Thyroid* **16**, 1303-9.
- Kamada, S., Shimono, A., Shinto, Y., Tsujimura, T., Takahashi, T., Noda, T., Kitamura, Y., Kondoh, H. and Tsujimoto, Y.** (1995). bcl-2 deficiency in mice leads to pleiotropic abnormalities: accelerated lymphoid cell death in thymus and spleen, polycystic kidney, hair hypopigmentation, and distorted small intestine. *Cancer Res* **55**, 354-9.
- Kameda, Y., Ito, M., Nishimaki, T. and Gotoh, N.** (2009). FRS2alpha is required for the separation, migration, and survival of pharyngeal-endoderm derived organs including thyroid, ultimobranchial body, parathyroid, and thymus. *Dev Dyn* **238**, 503-13.
- Kaufman, M. H. and Bard, J.** (1999). The thyroid. In: The anatomic basis of mouse development. San Diego: Academic Press.
- Keijzer, R., van Tuyl, M., Meijers, C., Post, M., Tibboel, D., Grosveld, F. and Koutsourakis, M.** (2001). The transcription factor GATA6 is essential for branching morphogenesis and epithelial cell differentiation during fetal pulmonary development. *Development* **128**, 503-11.
- Kimmel, C. B., Ballard, W. W., Kimmel, S. R., Ullmann, B. and Schilling, T. F.** (1995). Stages of embryonic development of the zebrafish. *Dev Dyn* **203**, 253-310.
- Kimura, J. and Deutsch, G. H.** (2007). Key mechanisms of early lung development. *Pediatr Dev Pathol* **10**, 335-47.
- Kimura, S., Hara, Y., Pineau, T., Fernandez-Salguero, P., Fox, C. H., Ward, J. M. and Gonzalez, F. J.** (1996). The T/ebp null mouse: thyroid-specific enhancer-binding protein is essential for the organogenesis of the thyroid, lung, ventral forebrain, and pituitary. *Genes Dev* **10**, 60-9.
- Kimura, S., Ward, J. M. and Minoo, P.** (1999). Thyroid-specific enhancer-binding protein/thyroid transcription factor 1 is not required for the initial specification of the thyroid and lung primordia. *Biochimie* **81**, 321-7.
- Kinkel, M. D. and Horton, W. E., Jr.** (2003). Coordinate down-regulation of cartilage matrix gene expression in Bcl-2 deficient chondrocytes is associated with decreased SOX9 expression and decreased mRNA stability. *J Cell Biochem* **88**, 941-53.
- Kirsten, D.** (2000). The thyroid gland: physiology and pathophysiology. *Neonatal Netw* **19**, 11-26.

- Kratz, E., Eimon, P. M., Mukhyala, K., Stern, H., Zha, J., Strasser, A., Hart, R. and Ashkenazi, A.** (2006). Functional characterization of the Bcl-2 gene family in the zebrafish. *Cell Death Differ* **13**, 1631-40.
- Krude, H., Schutz, B., Biebermann, H., von Moers, A., Schnabel, D., Neitzel, H., Tonnies, H., Weise, D., Lafferty, A., Schwarz, S. et al.** (2002). Choreoathetosis, hypothyroidism, and pulmonary alterations due to human NKX2-1 haploinsufficiency. *J Clin Invest* **109**, 475-80.
- Kuramoto, K., Negishi, M. and Katoh, H.** (2009). Regulation of dendrite growth by the Cdc42 activator Zizimin1/Dock9 in hippocampal neurons. *J Neurosci Res* **87**, 1794-805.
- Kusakabe, T., Hoshi, N. and Kimura, S.** (2006). Origin of the ultimobranchial body cyst: T/ebp/Nkx2.1 expression is required for development and fusion of the ultimobranchial body to the thyroid. *Dev Dyn* **235**, 1300-9.
- Lania, G., Zhang, Z., Huynh, T., Caprio, C., Moon, A. M., Vitelli, F. and Baldini, A.** (2009). Early thyroid development requires a Tbx1-Fgf8 pathway. *Dev Biol* **328**, 109-17.
- Lazzaro, D., Price, M., de Felice, M. and Di Lauro, R.** (1991). The transcription factor TTF-1 is expressed at the onset of thyroid and lung morphogenesis and in restricted regions of the foetal brain. *Development* **113**, 1093-104.
- Lu, J., Izvolzky, K. I., Qian, J. and Cardoso, W. V.** (2005). Identification of FGF10 targets in the embryonic lung epithelium during bud morphogenesis. *J Biol Chem* **280**, 4834-41.
- Lun, K. and Brand, M.** (1998). A series of no isthmus (noi) alleles of the zebrafish pax2.1 gene reveals multiple signaling events in development of the midbrain-hindbrain boundary. *Development* **125**, 3049-62.
- Macchia, P. E., Lapi, P., Krude, H., Pirro, M. T., Missero, C., Chiovato, L., Souabni, A., Baserga, M., Tassi, V., Pinchera, A. et al.** (1998). PAX8 mutations associated with congenital hypothyroidism caused by thyroid dysgenesis. *Nat Genet* **19**, 83-6.
- Mackereth, M. D., Kwak, S. J., Fritz, A. and Riley, B. B.** (2005). Zebrafish pax8 is required for otic placode induction and plays a redundant role with Pax2 genes in the maintenance of the otic placode. *Development* **132**, 371-82.
- Maiorana, R., Carta, A., Floriddia, G., Leonardi, D., Buscema, M., Sava, L., Calaciura, F. and Vigneri, R.** (2003). Thyroid hemiagenesis: prevalence in normal children and effect on thyroid function. *J Clin Endocrinol Metab* **88**, 1534-6.
- Mansouri, A., Chowdhury, K. and Gruss, P.** (1998). Follicular cells of the thyroid gland require Pax8 gene function. *Nat Genet* **19**, 87-90.
- Margue, C. M., Bernasconi, M., Barr, F. G. and Schafer, B. W.** (2000). Transcriptional modulation of the anti-apoptotic protein BCL-XL by the paired box transcription factors PAX3 and PAX3/FKHR. *Oncogene* **19**, 2921-9.
- Marians, R. C., Ng, L., Blair, H. C., Unger, P., Graves, P. N. and Davies, T. F.** (2002). Defining thyrotropin-dependent and -independent steps of thyroid hormone synthesis by using thyrotropin receptor-null mice. *Proc Natl Acad Sci U S A* **99**, 15776-81.
- Martinez Barbera, J. P., Clements, M., Thomas, P., Rodriguez, T., Meloy, D., Kioussis, D. and Beddington, R. S.** (2000). The homeobox gene Hex is required in definitive endodermal tissues for normal forebrain, liver and thyroid formation. *Development* **127**, 2433-45.
- Mazet, F.** (2002). The Fox and the thyroid: the amphioxus perspective. *Bioessays* **24**, 696-9.
- Medeiros-Neto, G., Targovnik, H. M. and Vassart, G.** (1993). Defective thyroglobulin synthesis and secretion causing goiter and hypothyroidism. *Endocr Rev* **14**, 165-83.
- Michael, L. and Davies, J. A.** (2004). Pattern and regulation of cell proliferation during murine ureteric bud development. *J Anat* **204**, 241-55.
- Minoo, P., Su, G., Drum, H., Bringas, P. and Kimura, S.** (1999). Defects in tracheoesophageal and lung morphogenesis in Nkx2.1(-/-) mouse embryos. *Dev Biol* **209**, 60-71.

**Moreno, J. C., Bikker, H., Kempers, M. J., van Trotsenburg, A. S., Baas, F., de Vijlder, J. J., Vulmsa, T. and Ris-Stalpers, C.** (2002). Inactivating mutations in the gene for thyroid oxidase 2 (THOX2) and congenital hypothyroidism. *N Engl J Med* **347**, 95-102.

**Moreno, J. C., Klootwijk, W., van Toor, H., Pinto, G., D'Alessandro, M., Leger, A., Goudie, D., Polak, M., Gruters, A. and Visser, T. J.** (2008). Mutations in the iodotyrosine deiodinase gene and hypothyroidism. *N Engl J Med* **358**, 1811-8.

**Mostowska, A., Hozyasz, K. K., Biedziak, B., Misiak, J. and Jagodzinski, P. P.** Polymorphisms located in the region containing BHMT and BHMT2 genes as maternal protective factors for orofacial clefts. *Eur J Oral Sci* **118**, 325-32.

**Moya, C. M., Perez de Nanclares, G., Castano, L., Potau, N., Bilbao, J. R., Carrascosa, A., Bargada, M., Coya, R., Martul, P., Vicens-Calvet, E. et al.** (2006). Functional study of a novel single deletion in the TITF1/NKX2.1 homeobox gene that produces congenital hypothyroidism and benign chorea but not pulmonary distress. *J Clin Endocrinol Metab* **91**, 1832-41.

**Muratovska, A., Zhou, C., He, S., Goodyer, P. and Eccles, M. R.** (2003). Paired-Box genes are frequently expressed in cancer and often required for cancer cell survival. *Oncogene* **22**, 7989-97.

**Nagasaki, K., Narumi, S., Asami, T., Kikuchi, T., Hasegawa, T. and Uchiyama, M.** (2008). Mutation of a gene for thyroid transcription factor-1 (TITF1) in a patient with clinical features of resistance to thyrotropin. *Endocr J* **55**, 875-8.

**Nagase, Y., Iwasawa, M., Akiyama, T., Kadono, Y., Nakamura, M., Oshima, Y., Yasui, T., Matsumoto, T., Hirose, J., Nakamura, H. et al.** (2009). Anti-apoptotic molecule Bcl-2 regulates the differentiation, activation, and survival of both osteoblasts and osteoclasts. *J Biol Chem* **284**, 36659-69.

**Nagashima, T., Murakami, M., Onigata, K., Morimura, T., Nagashima, K., Mori, M. and Morikawa, A.** (2001). Novel inactivating missense mutations in the thyrotropin receptor gene in Japanese children with resistance to thyrotropin. *Thyroid* **11**, 551-9.

**Nakada, C., Iida, A., Tabata, Y. and Watanabe, S.** (2009). Forkhead transcription factor foxe1 regulates chondrogenesis in zebrafish. *J Exp Zool B Mol Dev Evol* **312**, 827-40.

**Nakayama, K., Nakayama, K., Negishi, I., Kuida, K., Sawa, H. and Loh, D. Y.** (1994). Targeted disruption of Bcl-2 alpha beta in mice: occurrence of gray hair, polycystic kidney disease, and lymphocytopenia. *Proc Natl Acad Sci U S A* **91**, 3700-4.

**Nitsch, R., Di Dato, V., di Gennaro, A., de Cristofaro, T., Abbondante, S., De Felice, M., Zannini, M. and Di Lauro, R.** Comparative genomics reveals a functional thyroid-specific element in the far upstream region of the PAX8 gene. *BMC Genomics* **11**, 306.

**Noy, P., Williams, H., Sawasdichai, A., Gaston, K. and Jayaraman, P. S.** PRH/Hex controls cell survival through coordinate transcriptional regulation of vascular endothelial growth factor signaling. *Mol Cell Biol* **30**, 2120-34.

**Ogasawara, M. and Satou, Y.** (2003). Expression of FoxE and FoxQ genes in the endostyle of *Ciona intestinalis*. *Dev Genes Evol* **213**, 416-9.

**Ohno, M., Zannini, M., Levy, O., Carrasco, N. and di Lauro, R.** (1999). The paired-domain transcription factor Pax8 binds to the upstream enhancer of the rat sodium/iodide symporter gene and participates in both thyroid-specific and cyclic-AMP-dependent transcription. *Mol Cell Biol* **19**, 2051-60.

**Ohuchi, H., Hori, Y., Yamasaki, M., Harada, H., Sekine, K., Kato, S. and Itoh, N.** (2000). FGF10 acts as a major ligand for FGF receptor 2 IIIb in mouse multi-organ development. *Biochem Biophys Res Commun* **277**, 643-9.

**Okuno, S., Shimizu, S., Ito, T., Nomura, M., Hamada, E., Tsujimoto, Y. and Matsuda, H.** (1998). Bcl-2 prevents caspase-independent cell death. *J Biol Chem* **273**, 34272-7.

**Olivieri, A., Stazi, M. A., Mastroiacovo, P., Fazzini, C., Medda, E., Spagnolo, A., De Angelis, S., Grandolfo, M. E., Taruscio, D., Cordeddu, V. et al.** (2002). A population-based study on the

frequency of additional congenital malformations in infants with congenital hypothyroidism: data from the Italian Registry for Congenital Hypothyroidism (1991-1998). *J Clin Endocrinol Metab* **87**, 557-62.

**Pabst, O., Herbrand, H., Takuma, N. and Arnold, H. H.** (2000). NKX2 gene expression in neuroectoderm but not in mesendodermally derived structures depends on sonic hedgehog in mouse embryos. *Dev Genes Evol* **210**, 47-50.

**Park, D., Jia, H., Rajakumar, V. and Chamberlin, H. M.** (2006). Pax2/5/8 proteins promote cell survival in *C. elegans*. *Development* **133**, 4193-202.

**Park, S. M., Clifton-Bligh, R. J., Betts, P. and Chatterjee, V. K.** (2004). Congenital hypothyroidism and apparent athyreosis with compound heterozygosity or compensated hypothyroidism with probable hemizyosity for inactivating mutations of the TSH receptor. *Clin Endocrinol (Oxf)* **60**, 220-7.

**Parlato, R., Avantaggiato, V. and De Felice, M.** (1999). 26th Annual meeting of the European Thyroid Association. Milano, Italy, August 28-September 1, 1999. Abstracts. *J Endocrinol Invest* **22**, 1-140.

**Parlato, R., Rosica, A., Rodriguez-Mallon, A., Affuso, A., Postiglione, M. P., Arra, C., Mansouri, A., Kimura, S., Di Lauro, R. and De Felice, M.** (2004). An integrated regulatory network controlling survival and migration in thyroid organogenesis. *Dev Biol* **276**, 464-75.

**Pasca di Magliano, M., Di Lauro, R. and Zannini, M.** (2000). Pax8 has a key role in thyroid cell differentiation. *Proc Natl Acad Sci U S A* **97**, 13144-9.

**Pellizzari, L., D'Elia, A., Rustighi, A., Manfioletti, G., Tell, G. and Damante, G.** (2000). Expression and function of the homeodomain-containing protein Hex in thyroid cells. *Nucleic Acids Res* **28**, 2503-11.

**Pera, E. M. and Kessel, M.** (1998). Demarcation of ventral territories by the homeobox gene NKX2.1 during early chick development. *Dev Genes Evol* **208**, 168-71.

**Perrone, L., Pasca di Magliano, M., Zannini, M. and Di Lauro, R.** (2000). The thyroid transcription factor 2 (TTF-2) is a promoter-specific DNA-binding independent transcriptional repressor. *Biochem Biophys Res Commun* **275**, 203-8.

**Perry, R., Heinrichs, C., Bourdoux, P., Khoury, K., Szots, F., Dussault, J. H., Vassart, G. and Van Vliet, G.** (2002). Discordance of monozygotic twins for thyroid dysgenesis: implications for screening and for molecular pathophysiology. *J Clin Endocrinol Metab* **87**, 4072-7.

**Plachov, D., Chowdhury, K., Walther, C., Simon, D., Guenet, J. L. and Gruss, P.** (1990). Pax8, a murine paired box gene expressed in the developing excretory system and thyroid gland. *Development* **110**, 643-51.

**Pohlenz, J., Medeiros-Neto, G., Gross, J. L., Silveiro, S. P., Knobel, M. and Refetoff, S.** (1997). Hypothyroidism in a Brazilian kindred due to iodide trapping defect caused by a homozygous mutation in the sodium/iodide symporter gene. *Biochem Biophys Res Commun* **240**, 488-91.

**Postiglione, M. P., Parlato, R., Rodriguez-Mallon, A., Rosica, A., Mithbaokar, P., Maresca, M., Marians, R. C., Davies, T. F., Zannini, M. S., De Felice, M. et al.** (2002). Role of the thyroid-stimulating hormone receptor signaling in development and differentiation of the thyroid gland. *Proc Natl Acad Sci U S A* **99**, 15462-7.

**Postlethwait, J. H., Woods, I. G., Ngo-Hazelett, P., Yan, Y. L., Kelly, P. D., Chu, F., Huang, H., Hill-Force, A. and Talbot, W. S.** (2000). Zebrafish comparative genomics and the origins of vertebrate chromosomes. *Genome Res* **10**, 1890-902.

**Presta, I., Arturi, F., Ferretti, E., Mattei, T., Scarpelli, D., Tosi, E., Scipioni, A., Celano, M., Gulino, A., Filetti, S. et al.** (2005). Recovery of NIS expression in thyroid cancer cells by overexpression of Pax8 gene. *BMC Cancer* **5**, 80.

- Puppin, C., D'Elia, A. V., Pellizzari, L., Russo, D., Arturi, F., Presta, I., Filetti, S., Bogue, C. W., Denson, L. A. and Damante, G.** (2003). Thyroid-specific transcription factors control Hex promoter activity. *Nucleic Acids Res* **31**, 1845-52.
- Puppin, C., Presta, I., D'Elia, A. V., Tell, G., Arturi, F., Russo, D., Filetti, S. and Damante, G.** (2004). Functional interaction among thyroid-specific transcription factors: Pax8 regulates the activity of Hex promoter. *Mol Cell Endocrinol* **214**, 117-25.
- Rastogi, M. V. and LaFranchi, S. H.** Congenital hypothyroidism. *Orphanet J Rare Dis* **5**, 17.
- Reiter, J. F., Kikuchi, Y. and Stainier, D. Y.** (2001). Multiple roles for Gata5 in zebrafish endoderm formation. *Development* **128**, 125-35.
- Ristoratore, F., Spagnuolo, A., Aniello, F., Branno, M., Fabbrini, F. and Di Lauro, R.** (1999). Expression and functional analysis of Citif1, an ascidian NK-2 class gene, suggest its role in endoderm development. *Development* **126**, 5149-59.
- Rohr, K. B. and Concha, M. L.** (2000). Expression of nk2.1a during early development of the thyroid gland in zebrafish. *Mech Dev* **95**, 267-70.
- Romert, P. and Gauguin, J.** (1973). The early development of the median thyroid gland of the mouse. A light-, electron-microscopic and histochemical study. *Z Anat Entwicklungsgesch* **139**, 319-36.
- Royaux, I. E., Suzuki, K., Mori, A., Katoh, R., Everett, L. A., Kohn, L. D. and Green, E. D.** (2000). Pendrin, the protein encoded by the Pendred syndrome gene (PDS), is an apical porter of iodide in the thyroid and is regulated by thyroglobulin in FRTL-5 cells. *Endocrinology* **141**, 839-45.
- Shaw-White, J. R., Bruno, M. D. and Whitsett, J. A.** (1999). GATA-6 activates transcription of thyroid transcription factor-1. *J Biol Chem* **274**, 2658-64.
- Shaw, G. M., Carmichael, S. L., Laurent, C. and Rasmussen, S. A.** (2006). Maternal nutrient intakes and risk of orofacial clefts. *Epidemiology* **17**, 285-91.
- Shivdasani, R. A.** (2002). Molecular regulation of vertebrate early endoderm development. *Dev Biol* **249**, 191-203.
- Small, E. M., Vokes, S. A., Garriock, R. J., Li, D. and Krieg, P. A.** (2000). Developmental expression of the *Xenopus* Nkx2-1 and Nkx2-4 genes. *Mech Dev* **96**, 259-62.
- Sunthornthepvarakui, T., Gottschalk, M. E., Hayashi, Y. and Refetoff, S.** (1995). Brief report: resistance to thyrotropin caused by mutations in the thyrotropin-receptor gene. *N Engl J Med* **332**, 155-60.
- Suzuki, K., Kobayashi, Y., Katoh, R., Kohn, L. D. and Kawaoi, A.** (1998). Identification of thyroid transcription factor-1 in C cells and parathyroid cells. *Endocrinology* **139**, 3014-7.
- Takuma, N., Sheng, H. Z., Furuta, Y., Ward, J. M., Sharma, K., Hogan, B. L., Pfaff, S. L., Westphal, H., Kimura, S. and Mahon, K. A.** (1998). Formation of Rathke's pouch requires dual induction from the diencephalon. *Development* **125**, 4835-40.
- Taylor, J. S., Van de Peer, Y., Braasch, I. and Meyer, A.** (2001). Comparative genomics provides evidence for an ancient genome duplication event in fish. *Philos Trans R Soc Lond B Biol Sci* **356**, 1661-79.
- Thiery, J. P. and Sleeman, J. P.** (2006). Complex networks orchestrate epithelial-mesenchymal transitions. *Nat Rev Mol Cell Biol* **7**, 131-42.
- Thomas, P. Q., Brown, A. and Beddington, R. S.** (1998). Hex: a homeobox gene revealing peri-implantation asymmetry in the mouse embryo and an early transient marker of endothelial cell precursors. *Development* **125**, 85-94.
- Tonacchera, M., Agretti, P., De Marco, G., Perri, A., Pinchera, A., Vitti, P. and Chiovato, L.** (2001). Thyroid resistance to TSH complicated by autoimmune thyroiditis. *J Clin Endocrinol Metab* **86**, 4543-6.
- Toublanc, J. E.** (1992). Comparison of epidemiological data on congenital hypothyroidism in Europe with those of other parts in the world. *Horm Res* **38**, 230-5.

- Veis, D. J., Sorenson, C. M., Shutter, J. R. and Korsmeyer, S. J.** (1993). Bcl-2-deficient mice demonstrate fulminant lymphoid apoptosis, polycystic kidneys, and hypopigmented hair. *Cell* **75**, 229-40.
- Wagner, A.** (1998). The fate of duplicated genes: loss or new function? *Bioessays* **20**, 785-8.
- Weber, A., Marquardt, J., Elzi, D., Forster, N., Starke, S., Glaum, A., Yamada, D., Defossez, P. A., Delrow, J., Eisenman, R. N. et al.** (2008). Zbtb4 represses transcription of P21CIP1 and controls the cellular response to p53 activation. *Embo J* **27**, 1563-74.
- Wendl, T., Adzic, D., Schoenebeck, J. J., Scholpp, S., Brand, M., Yelon, D. and Rohr, K. B.** (2007). Early developmental specification of the thyroid gland depends on hox-expressing surrounding tissue and on FGF signals. *Development* **134**, 2871-9.
- Wendl, T., Lun, K., Mione, M., Favor, J., Brand, M., Wilson, S. W. and Rohr, K. B.** (2002). Pax2.1 is required for the development of thyroid follicles in zebrafish. *Development* **129**, 3751-60.
- Westerlund, J., Andersson, L., Carlsson, T., Zoppoli, P., Fagman, H. and Nilsson, M.** (2008). Expression of Islet1 in thyroid development related to budding, migration, and fusion of primordia. *Dev Dyn* **237**, 3820-9.
- Wolfe, H. J., Voelkel, E. F. and Tashjian, A. H., Jr.** (1974). Distribution of calcitonin-containing cells in the normal adult human thyroid gland: a correlation of morphology with peptide content. *J Clin Endocrinol Metab* **38**, 688-94.
- Woods, I. G., Wilson, C., Friedlander, B., Chang, P., Reyes, D. K., Nix, R., Kelly, P. D., Chu, F., Postlethwait, J. H. and Talbot, W. S.** (2005). The zebrafish gene map defines ancestral vertebrate chromosomes. *Genome Res* **15**, 1307-14.
- Xu, P. X., Zheng, W., Laclef, C., Maire, P., Maas, R. L., Peters, H. and Xu, X.** (2002). Eya1 is required for the morphogenesis of mammalian thymus, parathyroid and thyroid. *Development* **129**, 3033-44.
- Yu, J. K., Holland, L. Z., Jamrich, M., Blitz, I. L. and Hollan, N. D.** (2002). Amphioxus winged helix/forkhead gene encoding a protein closely related to vertebrate thyroid transcription factor-2: expression during pharyngeal development. *Evol Dev* **4**, 9-15.
- Zannini, M., Avantaggiato, V., Biffali, E., Arnone, M. I., Sato, K., Pischetola, M., Taylor, B. A., Phillips, S. J., Simeone, A. and Di Lauro, R.** (1997). TTF-2, a new forkhead protein, shows a temporal expression in the developing thyroid which is consistent with a role in controlling the onset of differentiation. *Embo J* **16**, 3185-97.
- Zannini, M., Francis-Lang, H., Plachov, D. and Di Lauro, R.** (1992). Pax-8, a paired domain-containing protein, binds to a sequence overlapping the recognition site of a homeodomain and activates transcription from two thyroid-specific promoters. *Mol Cell Biol* **12**, 4230-41.
- Zorn, A. M. and Wells, J. M.** (2009). Vertebrate endoderm development and organ formation. *Annu Rev Cell Dev Biol* **25**, 221-51.

## 8. Appendix

**Table 5 Gene enriched in mouse thyroid bud (E10) with a fold change  $\geq 10$ .**

Mouse Gene symbol	Gene title	Gene symbol Zebrafish ortholog	Ensembl gene ID Zebrafish ortholog	Clone availability	24 - 28 hpf	42 -48 hpf	72 hpf	96 hpf
4930426D05Rik	RIKEN cDNA 4930426D05 gene	---						
ligp1-LOC100044196	interferon inducible GTPase 1	irgf3 - LOC797731	ENSDARG0000062820	Cloned	Ubiquitous (high level)	Ubiquitous (low level) - CNS (central nervous system) (high level)	Ubiquitous (low level)	Ubiquitous (low level)
		LOC563833	ENSDARG0000062828	---	---	---	---	---
		A3QJW3_DANRE	ENSDARG0000070772	---	---	---	---	---
		irgf1	ENSDARG0000070774	---	---	---	---	---
		IRGC (4 of 10)	ENSDARG0000078453	---	---	---	---	---
		LOC565002	ENSDARG0000014975	Cloned	Ubiquitous (high level)	Ubiquitous (low level) - CNS (high level)	Ubiquitous (low level)	Ubiquitous (low level)
		LOC100007513	ENSDARG0000060910	Cloned		Ubiquitous (low level) - CNS (high level)	Ubiquitous (low level)	Ubiquitous (low level)
		IRGC (9 of 10) - LOC571560	ENSDARG0000067617	---	---	---	---	---

		irgq2	ENSDARG0000068657	---	---	---	---	---
		irge4	ENSDARG0000070317	IRBOp991D0896D	CNS (rhombencephalon, cerebellum, tegmentum)	CNS (rhombencephalon, cerebellum, tegmentum)	No expression	No expression
Bcl2	B-cell leukemia/lymphoma 2	bcl2	ENSDARG0000025613	IRAKp961L09304Q	Pronephric ducts - CNS - otic placode	Pronephric ducts - CNS - otic placode	No expression	No expression
Prlr	prolactin receptor	prlra	ENSDARG0000016570	Cloned	Pronephric ducts - pancreatic bud	Pronephric ducts - pancreatic bud	Pronephric ducts - pancreatic bud	Pronephric ducts - pancreatic bud
		prlrb	ENSDARG0000045955	Cloned	Pronephric ducts	Pronephric ducts	Pronephric ducts	Pronephric ducts
Cpne4	copine IV	si:dkey-5n4.1	ENSDARG0000062754	Cloned	Olfactory placodes	Olfactory placodes	Olfactory placodes	Olfactory placodes
		Q1LYM2_DANRE	ENSDARG0000040069	---	---	---	---	---
Ptpre	protein tyrosine phosphatase, receptor type, E	NP_001038642.1	ENSDARG0000021151	Cloned	CNS - ventral somites	CNS - heart	CNS	No expression
		LOC567443	ENSDARG0000015891	Cloned	No expression	CNS - eyes - liver	CNS	No expression
	Transcribed locus							
Hivep3	human immunodeficiency virus type 1 enhancer binding protein 3	HIVEP3 (1 of 2)	ENSDARG0000037154	IMAGp998G0819851Q	No expression	No expression	No expression	CNS
		A5PMB4_DANRE	ENSDARG0000075928	---	---	---	---	---
Nptx1	neuronal pentraxin 1	zgc:85889	ENSDARG00	IRAKp961F08239Q	otic vesicles	CNS - heart - otic vesicles	CNS - pharynx	CNS - pharynx

			000030735 - ENSDARG00 000074671					
		si:dkey-14o18.2	ENSDARG00 000062995	---	---	---	---	---
Irs4	insulin receptor substrate 4	IRS4	ENSDARG00 000052065	---	---	---	---	---
2310010M24Rik	RIKEN cDNA 2310010M24 gene	lypd6b	ENSDARG00 000057226	Cloned	CNS - otic vesicles - pronephric ducts - tail - olfactory placodes	CNS - otic vesicles - olfactory placodes - heart	CNS - otic vesicles - olfactory placodes - heart	CNS - otic vesicles - olfactory placodes - heart
1600029D21Rik	RIKEN cDNA 1600029D21 gene	---						
Matn2	matrilin 2	matn4	ENSDARG00 000015947	IRALp962J02 64Q	pharyngeal arches - posterior blood island - primitive hematopoietic cells - otic vesicles - pronephric duct - retina	caudal fin - dorsal fin - pectoral fin - posterior blood island - otic vesicles - retina	somites - retina - pharynx - pectoral fin	pectoral fin - gut- neuromast
Bcl11b	B-cell leukemia/lymphoma 11B	A2CE94_DANRE	ENSDARG00 000062510	Cloned	CNS (optic tectum - tegmentum - cerebellum - rhombencephalon)	CNS (optic tectum - tegmentum - cerebellum - rhombencephalon) - heart region	CNS (optic tectum - tegmentum - cerebellum - rhombencephalon) - heart region	CNS
		LOC100000503	ENSDARG00 000067727	Cloned	CNS (optic tectum - diencephalon - cerebellum - rhombencephalon)	CNS (optic tectum - diencephalon - cerebellum - rhombencephalon)	CNS (optic tectum - diencephalon - cerebellum - rhombencephalon)	CNS

Klhl14	kelch-like 14 (Drosophila)	LOC794722	ENSDARG0000045275	Cloned	CNS (cerebellum ) - optic nerve	CNS (cerebellum - rhombencephalon) - optic nerve	CNS	CNS
Clstn2	calsyntenin 2	clstn2	ENSDARG0000060637	Cloned	CNS - epithelial cells	CNS	CNS - gut	CNS
		LOC569664	ENSDARG0000060638	Cloned	CNS (telencephalon)	CNS - olfactory placodes - heart	Olfactory placodes - heart	Olfactory placodes
Stc2	stanniocalcin 2	stc2	ENSDARG0000056680	IMAGp998E1314597Q	Pituitary gland	Pituitary gland - pectoral fin	Pituitary gland - pectoral fin	Pituitary gland - pectoral fin
		LOC558195		IMAGp998E0315213Q	Pharyngeal arches	Pharyngeal arches	Pharyngeal arches	Pharyngeal arches
Cpxm2	carboxypeptidase X 2 (M14 family)	LOC797452	ENSDARG0000078792	---	---	---	---	---
Slc4a5	solute carrier family 4, sodium bicarbonate cotransporter, member 5	A2BIJ8_DANRE	ENSDARG0000002771	---	---	---	---	---
		SLC4A5 (2 of 2)	ENSDARG0000005966	---	---	---	---	---
Chdh	choline dehydrogenase	CHDH	ENSDARG0000075162	Cloned	Somites - pronephric ducts	Liver - gut - thyroid region - pronephric ducts	Liver - gut	Live - gut
Ctxn3	cortexin 3	CTXN3	ENSDARG0000033508	---	---	---	---	---
		wu:fj35c01	ENSDARG0000075413	---	---	---	---	---
5730414M22Rik	RIKEN cDNA 5730414M22 gene / Kcnma1	NP_001139072.1	ENSDARG0000079840	---	---	---	---	---
Cd44	CD44 antigen							
Hexb	hexosaminidase B	zgc:112084	ENSDARG0000052113	IRBOP991F1111D	No expression	No expression	No expression	No expression

		hexa	ENSDARG0000034368	IRBVp5006B1013D	Eyes	ubiquitous (in particular pronephric ducts - hematopoietic cells - CNS -pharynx)	Eyes	Gut
Htra1	HtrA serine peptidase 1	zgc:172061	ENSDARG0000014907z	---	---	---	---	---
		htra1	ENSDARG0000032831	IRBOP991C0443D	Lens - tail	Heart	Bulbus arteriosus - thyroid region	Bulbus arteriosus
Gcgr	glucagon receptor	LOC565237	ENSDARG0000036272	---	---	---	---	---
		LOC562973	ENSDARG0000070973	Cloned	Pancreatic bud	No expression	Gut - liver	No expression
Elfn1	leucine rich repeat and fibronectin type III, extracellular 1	ENSDARG0000073889	ENSDARG0000073889	Cloned	CNS	CNS	CNS	CNS
		sc:d0369	ENSDARG0000074372	---	---	---	---	---
		LOC562570	ENSDARG0000078141	Cloned	CNS	CNS	CNS	CNS
Scara5	scavenger receptor class A, member 5	si:ch211-200p13.4	ENSDARG0000010425	---	---	---	---	---
Zbtb20	zinc finger and BTB domain containing 20	zgc:158317	ENSDARG0000005586	IRBOP991C1178D	No expression	CNS	CNS (low level)	CNS (low level)
5033414K04Rik	RIKEN cDNA 5033414K04 gene	pid1	ENSDARG0000040315	IRBVp5006D118D	CNS	CNS	CNS - thyroid region	CNS (low level)
Moxd1	monooxygenase, DBH-like 1	moxd1	ENSDARG0000031136	---	---	---	---	---
		moxd1l	ENSDARG0000069296	IMAGp998M0615143Q	Ubiquitous (low level)	Olfactory placodes	Ubiquitous (low level) - olfactory	No expression

							placodes (high level)	
Vldlr	very low density lipoprotein receptor	vldlr	ENSDARG0000006257	IRBOP991F0216D	CNS	CNS	CNS	CNS
Afap1l2	actin filament associated protein 1-like 2	AFAP1L2	ENSDARG0000074806	---	---	---	---	---
Tcfcp2l1	transcription factor CP2-like 1	tfc21	ENSDARG0000029497	IMAGp998L1014682Q	Pituitary gland	Pituitary gland	Gut	Liver - gut
		si:ch211-207c15.3	ENSDARG0000018000	IRBOP991D07105D	CNS	CNS	CNS	CNS
		sich211-210c8.8	ENSDARG0000060306	Cloned	CNS	CNS	Pharynx, swimming bladder	No expression
	Transcribed locus	---						
Socs2	suppressor of cytokine signaling 2	socs2	ENSDARG0000045557	Cloned	Ubiquitous (low level)	Ubiquitous (low level)	Ubiquitous (low level)	CNS - eyes
Ryr3	ryanodine receptor 3	ryr3	ENSDARG0000042531	IMAGp998H1219257Q	Somites	Somites	Somites	Somites
Corin	Corin	BOV3M2_DANRE	ENSDARG0000063640	---	---	---	---	---
	Transcribed locus	---						
Calm3	calmodulin-like 3	Calm3a	ENSDARG0000037014	IRBOP991G0338D	Eyes - CNS - pronephric ducts - cloaca - somites	Eyes - CNS - pronephric ducts - cloaca - somites	CNS	CNS - gut - eyes
Galns	galactosamine (N-acetyl)-6-sulfate sulfatase	galns	ENSDARG0000051853	IRBOP991E0878D	Ubiquitous (high level)	Epidermal cells	CNS	Pharyngeal arches - olfactory placodes

**Table 6 Gene enriched in thyroid and in lung buds (E10) with a fold change  $\geq 10$ .**

Mouse Gene symbol	Gene title	Gene symbol Zebrafish ortholog	Ensembl gene ID Zebrafish ortholog	Clone availability	24 - 28 hpf	42 -48 hpf	72 hpf	96 hpf
Sorl1	sortilin-related receptor	SORL1	ENSDARG0000013892	Cloned	No expression	No expression	No expression	No expression
Rassf10	Ras association (RalGDS/AF-6) domain family (N-terminal) member 10	RASSF10 (1 of 2)	ENSDARG0000074159	---	---	---	---	---
Prss8	protease, serine, 8 (prostasin)	zgc:92313	ENSDARG0000040513	---	---	---	---	---
		LOC100001520	ENSDARG0000027196	---	---	---	---	---
		zgc:101788	ENSDARG0000055644	Cloned	Olfactory placodes	Olfactory placodes	Olfactory placodes	Olfactory placodes
Adrbk2	adrenergic receptor kinase, beta 2	adrbk2	ENSDARG0000013007	IMAGp998N0614836Q	CNS	CNS - heart	CNS	CNS - gut
1810019J16Rik	RIKEN cDNA 1810019J16 gene	LOC797923	ENSDARG0000079834	IMAGp998M2115687Q	No expression	Pharynx (low level)	Ubiquitous	Ubiquitous
		LOC100150862	ENSDARG0000069522	IMAGp958O243308Q	Posterior region of CNS	Posterior region of CNS	Eyes	Gut
Spint1	serine protease inhibitor, Kunitz type 1	spint1b	ENSDARG0000012467	IRAKp961D12311Q	No expression	No expression	No expression	No expression
		spint1a/spint1l	ENSDARG0000023673	IRBOp991A044D	Pectoral fins - epidermal cells - otic	Pectoral fins - epidermal cells - otic	pharyngeal region	pharyngeal region - liver

					vesicles	vesicles -pharynx		
Ltbp3	latent transforming growth factor beta binding protein 3	A2BFE2_DANRE	ENSDARG0000035682	IMAGp998E0914796Q	Heart - thyroid region	Heart - thyroid region	Heart - thyroid region	no expression
Sorbs2	sorbin and SH3 domain containing 2	B8JIG0_DANRE	ENSDARG0000003046	---	---	---	---	---
		B8A438_DANRE	ENSDARG0000061603	Cloned	Somites - rombomers - heart	CNS - heart - eyes - somites	Eyes - heart	Eyes - heart - CNS
Pla2g7	phospholipase A2, group VII (platelet-activating factor acetylhydrolase, plasma)	zgc:77563	ENSDARG0000003584	IRBOp991A0137D	Lens	Lens	No expression	No expression
		zgc:153597	ENSDARG0000002981	IRBOp991A0285D	No expression	Epidermal cells	No expression	CNS
Slc16a2	solute carrier family 16 (monocarboxylic acid transporters), member 2	si:ch211-241j12.1	ENSDARG0000020984	IRBOp991D1178D	Blood cells	Caudal fin - liver - pectoral fin - pharyngeal region - blood island	Heart - liver - pectoral fin	Heart - liver - pectoral fin
Dsg2	desmoglein 2	ENSDARG0000039665	ENSDARG0000039665	---	---	---	---	---
		ENSDARG0000062750	ENSDARG0000062750	---	---	---	---	---
		LOC571042	ENSDARG0000076426	IMAGp998M0714816Q	heart region - thyroid region	heart region - thyroid region	Heart - gut	CNS - gut
		ENSDARG0000076945	ENSDARG0000076945	IMAGp958O023217Q	Pectoral fins - olfactory placodes - pharyngeal endoderm	Pectoral fins - pharynx - ventral caudal fin	Pharynx	Pharynx
Grina	glutamate receptor, ionotropic, N-methyl D-aspartate-associated protein 1	zgc:64102	ENSDARG0000052746	IMAGp998J1614304Q	CNS	Ubiquitous (low level) - CNS (high level)	CNS	CNS

		zgc:136572	ENSDARG0000023262	IMAGp998B0215589Q	CNS	No expression	Ubiquitous (low level)	CNS
Marveld2	MARVEL (membrane-associating) domain containing 2	Q32PL4_DANRE	ENSDARG0000025076	Cloned	Ubiquitous	Ubiquitous	Ubiquitous	Ubiquitous
		marveld2b	ENSDARG0000061651	IRALp962I0964Q	Ubiquitous	Heart	Pharynx	Pharynx - CNS
		BOUXTO_DANRE	ENSDARG0000061800	---	---	---	---	---
Egfl6	EGF-like-domain, multiple 6	EGFL6	ENSDARG0000045958	IRBOP991D0675D	Somites - pharyngeal endoderm - hindbrain - caudal fin	Pharynx - pectoral fins - caudal fin	Pharynx	Ubiquitous (low level)
		NP_001139052.1	ENSDARG0000018721	---	---	---	---	---
Zbtb4	zinc finger and BTB domain containing 4	Q06Z31_DANRE	ENSDARG0000061827	IMAGp998J1210761Q	Diencephalon - hindbrain midbrain boundary - thyroid region	Thyroid region - CNS	CNS - heart - region of thyroid follicles	CNS
EG432995	predicted gene, EG432995	---						
Atp10a	ATPase, class V, type 10A	LOC567172	ENSDARG0000061039	IMAGp998O1712421Q	No expression	No expression	No expression	No expression
		NP_001139079.1	ENSDARG0000078887		---	---	---	---
Cdh1	cadherin 1	cdh1	ENSDARG0000024371	Cloned	Epidermis - pronephric ducts - olfactory placodes	Pharynx	Pharynx	Pharynx
		LOC567602	ENSDARG0000035796	IMAGp998P2015688Q	Heart	Heart	No expression	Pharynx
		si:busm1-71b9.2	ENSDARG0000068142	---	---	---	---	---

		si:busm1-180o5.1	ENSDARG0000068137	---	---	---	---	---
Prkar1b	protein kinase, cAMP dependent regulatory, type I beta	zgc:153624	ENSDARG0000062926	IRBOp991D0586D	Hindbrain	Hindbrain	Hindbrain	Hindbrain
St14	suppression of tumorigenicity 14	st14b/zgc:152947	ENSDARG0000044655	IRBOp991C0583D	No expression	No expression	No expression	No expression
		st14a	ENSDARG0000061173	IRBOp991G0283D	Cloaca -olfactory placodes - otic vesicles - epidermis pharyngeal pouches	CNS - pharynx	Pharynx	Pharynx
		LOC557248	ENSDARG0000060754	IMAGp998E0919186Q	Pharynx - epidermis	Pharynx - pectoral fins - caudal fins	Posterior pharynx	Pharynx - gut
Tmem176a	transmembrane protein 176A	ENSDARG0000074390	ENSDARG0000074390	---	---	---	---	---
		LOC100007221	ENSDARG0000018671	---	---	---	---	---
		NP_001139082.1	ENSDARG0000078659	---	---	---	---	---
BC034069	cDNA sequence BC034069	---						
Lonrf3	LON peptidase N-terminal domain and ring finger 3	---						
H6pd	hexose-6-phosphate dehydrogenase	LOC569348	ENSDARG0000060153	IMAGp998P228992Q	No expression	No expression	No expression	No expression
D630039A03Rik	RIKEN cDNA D630039A03 gene	zgc:171750	ENSDARG0000078638	---	---	---	---	---
	Transcribed locus							
Kcnk1	potassium channel,	NP_0011390	ENSDARG0000017254	IMAGp998F	No expression	No expression	CNS (low level)	CNS (low level)

	subfamily K, member 1	47.1		0911846Q				
		zgc:165664	ENSDARG0000045067	IRBOP991A05104D	Hindbrain	No expression	CNS (low level)	CNS (low level)
Slco2a1	solute carrier organic anion transporter family, member 2a1	slco2a1	ENSDARG0000061896	IRBOP991H1097D	No expression	No expression	No expression	CNS
		zgc:123236	ENSDARG0000054609	IRBOP991C0372D	Pharyngeal arches	Pharyngeal arches	Pharyngeal arches	No expression
Eppk1	epiplakin 1	eppk1		IMAGp998O1710281Q	pharyngeal endoderm - heart - first pair of branching arteries	Pharynx	Pharynx - pharyngeal arches - pronephric ducts - gut	Pharynx - gut
Rnf128	ring finger protein 128	rnf128	ENSDARG0000016867	IMAGp998G0414808Q	Olfactory placodes - pectoral fins - pharynx	posterior pharynx - liver	Gut	No expression
		ENSDARG0000029890	ENSDARG0000029890	---	---	---	---	---
Cldn7	claudin 7	cldn7	ENSDARG0000014047	IRBOP991C1217D	Epidermis - pronephric ducts - olfactory placodes - lateral line primordium - otic vesicles	Epidermis - pronephric ducts - olfactory placodes - lateral line primordium - otic vesicles - pharyngeal endoderm	Lateral line - pharynx - ear - nose - pectoral fin - pronephric ducts	Lateral line - pharynx - ear - nose - pectoral fin - pronephric ducts
		zgc:92192	ENSDARG0000036376	---	---	---	---	---
Nbeal2	neurobeachin-like 2	NBEAL2 (1 of 2)	ENSDARG0000032436	---	---	---	---	---
		NBEAL2 (2 of 2)	ENSDARG0000044955	---	---	---	---	---
Spint2	serine protease	zgc:153795	ENSDARG00	IRBOP991C0	otic vesicle -	Pharynx - cloaca -	Pharynx	Pharynx

	inhibitor, Kunitz type 2		000069476	692D	pronephric ducts	olfactory placodes - pronephric ducts		
		si:dkey-61p9.9	ENSDARG0000068873	---	---	---	---	---
Tle2	transducin-like enhancer of split 2, homolog of Drosophila E(spl)	Q1MT48_DA NRE	ENSDARG0000008767	---	---	---	---	---
		si:ch211-81i17.1	ENSDARG0000042484	Cloned	CNS	CNS	CNS	CNS
Marveld3	MARVEL (membrane-associating) domain containing 3	si:ch211-191a24.4	ENSDARG0000037528	IRBVp5006C1213D	No expression	Pharynx - cloaca	Pharynx	Pharynx
		zgc:66450	ENSDARG0000026011	IRBOp991C019D	No expression	No expression	No expression	No expression
Tbx3	T-box 3	Tbx3b	ENSDARG0000002216	IRBOp991D0491D	otic vesicles - eyes	Otic vesicles - eyes - pectoral fin	Eyes	No expression
		LOC568479 similat to Txb 3b	ENSDARG0000061509	---	---	---	---	---
Slc44a3	solute carrier family 44, member 3	B8A445_DA NRE	ENSDARG0000015946	IMAGp998J1815677Q	Ubiquitous	ubiquitous (high level)	ubiquitous	CNS
		LOC571619		---	---	---	---	---
Epb4.1l4b	erythrocyte protein band 4.1-like 4b	LOC407635	ENSDARG0000061398	---	---	---	---	---
		epb4.114	ENSDARG0000040087	IRAKp961M14136Q	CNS (hindbrain)	CNS - lens	CNS (low level)	No expression
		epb41l5	ENSDARG0000032324	IRBOp991H0237D	CNS (low level) - eyes - olfactory placodes	No expression	CNS (low level)	No expression
Map3k5	mitogen-activated protein kinase	map3k5	ENSDARG0000005416	IMAGp998C208948Q	CNS - somites	CNS - somites	CNS - pharynx	Pharynx

	kinase kinase 5							
Cldn3	claudin 3	LOC792492	ENSDARG0000041504	---	---	---	---	---
		cldnh	ENSDARG0000069503	IRBOp991E034D	Pituitary gland - pronephric ducts - olfactory placodes	Pituitary gland - olfactory placodes	Olfactory placodes	Olfactory placodes
Cdh16	cadherin 16	CDH16	ENSDARG0000077570	Cloned	Corpuscles of Stannius	Corpuscles of Stannius	Corpuscles of Stannius	Corpuscles of Stannius
		si:busm1-71b9.3	ENSDARG0000051843	---	---	---	---	---
Arhgef16	Rho guanine nucleotide exchange factor (GEF) 16	NP_001116755.1	ENSDARG0000077114	---	---	---	---	---
Rbm35b	RNA binding motif protein 35b	rbm35b	ENSDARG0000018814	IRBOp991E0315D	olfactory placodes - pronephric ducts - otic placodes - pharynx - liver	otic placodes - pharynx - liver	pharynx	Gut
Capg	capping protein (actin filament), gelsolin-like	capg	ENSDARG0000021318	---	---	---	---	---
		BOROM1_DANRE	ENSDARG0000035560	---	---	---	---	---
Hpn	hepsin	si:dkey-33i11.3	ENSDARG0000027609	IRBOp991C0393D	ubiquitous (low level)	ubiquitous (low level)	ubiquitous (low level)	Gut
BC031353	cDNA sequence BC031353	si:dkey-266j9.3	ENSDARG0000040452	IRAKp961O16284Q	CNS - somites	CNS - pectoral fin - thyroid region	CNS	CNS - gut - pharynx
		A2CEB6_DANRE	ENSDARG0000068650	---	---	---	---	---
Cckar	cholecystokinin A receptor	LOC569038	ENSDARG0000052089	IMAGp998M1117138Q	Somites	Somites - pectoral fins	Somites - heart - pectoral fin - pharyngeal arches	Somites - pectoral fins - CNS - pharyngeal

								arches
Meg3	maternally expressed 3	---						
Tapbp	TAP binding protein	tpsn	ENSDARG0000036803	IRBOp991A08107D	No expression	No expression	No expression	No expression
		tpsn (si:ch211-51f10.1)	ENSDARG0000045011	---	---	---	---	---
Rgs17	regulator of G-protein signaling 17	rgs17	ENSDARG0000039435	IRBOp991C0248D	CNS - eyes	CNS - eyes	CNS - eyes	CNS
Centb1 /// Tnk1	tyrosine kinase, non-receptor, 1 /// centaurin, beta 1	zgc:153917	ENSDARG0000056346	IRBOp991C0380D	No expression	No expression	No expression	No expression
Nrxn3	neurexin III	nrxn3a	ENSDARG0000043746	IRBVp5006G0715D	Ubiquitous	Ubiquitous	Ubiquitous	Ubiquitous
		nrxn3b	ENSDARG0000062693	---	---	---	---	---

**Table 7 Selected genes enriched in mouse thyroid bud with FC<10.**

Gene symbol	Gene title	Gene symbol Zebrafish ortholog	Ensembl gene ID Zebrafish ortholog	Clone availability	24 - 28 hpf	42 -48 hpf	72 hpf	96 hpf
Odz4	odd Oz/ten-m homolog 4 (Drosophila)	odz4	ENSDARG0000034264	IMAGp998D139545Q	CNS	CNS	CNS	CNS
		ENSDARG0000037122	ENSDARG0000037122	---	---	---	---	---

		A8E7B2_DANRE	ENSDARG0000011171	---	---	---	---	---
		ENSDARG0000078358	ENSDARG0000078358	---	---	---	---	---
Zfp612	zinc finger protein 612							
Bmf	Bcl2 modifying factor	bmf2	ENSDARG0000041414	---	---	---	---	---
		bmf1	GeneID: 571949	Cloned	Somites - heart- CNS	pectoral fins - heart-thyroid region	pectoral fins	pectoral fins
Dock9	dedicator of cytokinesis 9	LOC100151488	ENSDARG0000016311	IMAGp998G2414303Q	pharyngeal arches - ventral somites - pronephric ducts - eyes - CNS-pancreas	otic vesicles - thyroid region - pancreas	CNS - eyes - heart	Pharynx
		DOCK9 (2 of 2)	ENSDARG0000079069	IMAGp998N0515229Q	liver - notochord - pharyngeal arches - lens - heart	Heart	liver - gut - pharyngeal arches - heart - lens	Pharynx
Zfp467	zinc finger protein 467							
Hhip	Hedgehog-interacting protein	hhip	ENSDARG0000060397	IRBOp991C1183D	olfactory placodes - lens - CNS - tail - pectoral fins	pectoral fins - pharyngeal arch	Pharynx - pectoral fins	Pharynx - pectoral fins
Cxcl12	chemokine (C-X-C motif) ligand 12	cxcl12a	ENSDARG0000037116	IRBOp991G0372D	pharyngeal arches - notochord - CNS	pharyngeal region	pharyngeal region	pharyngeal region
		cxcl12b	ENSDARG0000055100	IRBOp991H0176D	pharyngeal arches - thyroid region - tail somites	CNS - pharyngeal region	pharyngeal region	pharyngeal region
Sall1	sal-like 1 (Drosophila)	sall1b	dxzENSDARG00000022145	---	---	---	---	---
		sall1a	ENSDARG00	IMAGp998P	Stamnum corpuscles -	Stamnum corpuscles	Stamnum	CNS - eyes

			000074144	0815678Q	CNS - rombomers - neural tube - pectoral fin	- CNS - rombomers - neural tube - pectoral fin - pronephric duct - heart - thyroid region	corpuscles - CNS - heart - pharyngeal arch - eyes	
		LOC100149526	ENSDARG0000075891	---	---	---	---	---
Odz2	odd Oz/ten-m homolog 2 (Drosophila)	A8E7B2_DANRE	ENSDARG0000011171	---	---	---	---	---
		ENSDARG0000037122	ENSDARG0000037122	---	---	---	---	---
Id4 /// LOC100045546	inhibitor of DNA binding 4 /// similar to Id4	zgc:123214	ENSDARG0000045131	IRBOP991A0872D	CNS (hindbrain) - heart	CNS	CNS	CNS
Gli2	GLI-Kruppel family member GLI2	gli 2 a	ENSDARG0000025641	IMAGp998I068975Q	Ubiquitous (high levels)	CNS (nose, commissure) pharyngeal region	Pharyngeal region	Pharyngeal region
		gli 2 b	ENSDARG0000020884	IMAGp998P0119328Q	Posterior CNS - blood island	CNS - pharyngeal arches	Pharyngeal arches	Pharyngeal arches